Entwicklung und Automatisierung
3D-gedruckter mikrofluidischer Systeme zur
Integration und Kultivierung adhärenter Zellkulturen

Von der Naturwissenschaftlichen Fakultät der
Gottfried Wilhelm Leibniz Universität Hannover

zur Erlangung des Grades

Doktor der Naturwissenschaften (Dr. rer. nat.)

genehmigte Dissertation

von

Steffen Nils Winkler, M. Sc.

(2022)

„Fantasie ist wichtiger als Wissen, denn Wissen ist begrenzt.“

Albert Einstein (1879 – 1955)

Kurzfassung

Mikrofluidische Systeme werden zur Manipulation von Flüssigkeiten auf Mikroebene eingesetzt. Von ihnen profitieren insbesondere Biowissenschaften durch die Reduktion von Reagenzien und die Automatisierung ganzer Arbeitsabläufe. Die Mikrostrukturierung erlaubt zudem die Entwicklung neuartiger mikrofluidischer Zellkultursysteme wie den *organ-on-a-chip* Systemen. Diese Systeme zeichnen sich durch eine höhere physiologische Relevanz gegenüber klassischen *in vitro* Systemen aus und können zur Rekonstruktion einzelner Organfunktionen genutzt werden.

Aufgrund ihrer komplizierten Fertigung wird jedoch der Zugang zu diesen Systemen für Biowissenschaftler:innen erschwert, sodass ihr Potential noch kaum in kommerziellen Produkten realisiert werden konnte. Eine Lösung bietet die additive Fertigung (3D-Druck) mikrofluidischer Systeme, durch die die unkomplizierte Herstellung eigener Prototypen an Ort und Stelle ermöglicht wird. Um den 3D-Druck jedoch auch für die Herstellung mikrofluidischer Zellkultursysteme nutzen zu können, benötigt es deutlich mehr Biokompatibilitätsstudien zu neuen 3D-Druckmaterialien.

In diesem Sinne wurde in dem ersten Teil dieser Arbeit die *in vitro* Biokompatibilität eines aus Polyacrylat bestehenden, hitzebeständigen 3D-Druckmaterials sowie dessen Eignung für die Heißdampfsterilisation untersucht. Dabei konnte eine Biokompatibilität gegenüber adhärenten Mausfibroblasten und Hefezellen nachgewiesen werden. Diese Ergebnisse ermöglichen somit den Einsatz des Materials für die Zellkultur. Die Biokompatibilität blieb auch nach Heißdampfsterilisation unbeeinträchtigt, sodass mit diesem Material gedruckte Zellkultursysteme unkompliziert sterilisiert werden können. Im Gegensatz dazu erwies sich das Material für menschliche embryonale Nierenzellen in Suspension als schädlich, was die Bedeutung einer auf den Organismus und die Anwendung zugeschnittenen Biokompatibilitätsprüfung verdeutlicht.

Im zweiten Teil dieser Arbeit wurde das evaluierte 3D-Druckmaterial zur Herstellung eines vollautomatischen mikrofluidischen Ventilsystems eingesetzt, dessen Nutzen anschließend durch die Automatisierung eines Zellkulturassays als Machbarkeitsstudie demonstriert wurde. Alle mikrofluidischen Komponenten inklusive Anschlüsse, Mikromischer, Mikroventile und Auslässe wurden dabei in einem Stück gefertigt. Die kostengünstige und leicht zu steuernde Aktuation der 3D-gedruckten Ventilmembranen durch Servomotoren ist ein komplett neuer Ansatz. Die Automatisierung des Systems erfolgte durch einen Raspberry Pi Computer sowie selbst entwickelter Python Skripte. Durch den kompakten Computer wird die portable und ferngesteuerte Verwendung des Ventilsystems ermöglicht. Nachdem eine zuverlässige Mischgenauigkeit sowie die hohe Robustheit der Ventile gezeigt werden konnte, wurde das mikrofluidische Ventilsystem zur Automatisierung eines Zytotoxizitätsassays als Machbarkeitsstudie verwendet. Das von der Konzentration des Toxins abhängige Zellwachstum wurde dabei mittels Lebendzellmikroskopie und Bildverarbeitung automatisiert ausgewertet. Die Ergebnisse wurden anschließend mit denen eines pipettierten Assays verglichen. Beide Assays zeigten ein fast identisches Wachstumsverhalten, das die Eignung des Systems für die Zellkultur beweist.

Letztendlich konnte durch den 3D-Druck in Kombination mit der Biokompatibilitätsbestimmung eines 3D-Druckmaterials die Automatisierung von Zellkulturassays durch ein neu entwickeltes, 3D-gedrucktes mikrofluidisches Ventilsystem ermöglicht werden. Mit der Veröffentlichung der 3D-Modelle und Skripte ist es Wissenschaftler:innen nun möglich, das System an ihre eigenen Anwendungen anzupassen.

Stichworte: 3D-Druck, Biokompatibilität, Mikrofluidik, Zellkultur, Automatisierung, Mikroventil, lab-on-a-chip

Abstract

Microfluidic systems have the ability to handle liquids on microscale. Especially in life sciences, they are used for the reduction of reagents, automation of full workflows or the manipulation of cells. Advanced microfluidic valve systems have been developed for spatiotemporal reagent control of cell culture assays. While they show great potential to even automate novel 3D cell culture systems like sophisticated *organ-on-a-chip* systems, their complex fabrication and operation strongly limits the access for life sciences. In turn, additive manufacturing, also known as 3D printing, circumvents these barriers by enabling the one-step fabrication of customized devices. In the present doctoral thesis, the full process from the evaluation of the biocompatibility of a 3D printing material to the development of a 3D-printed microfluidic valve system to the full automatization of a proof-of-concept cell culture assay is presented.

In the first part of this work, the *in vitro* biocompatibility as well as its compatibility to heat steam sterilization of a 3D printing material for high resolution 3D printing of microfluidic devices was evaluated. With the proven biocompatibility to adherent mouse fibroblasts and yeast cells, that remained unaffected after heat steam sterilization, the use of the material for automation in cell culture had been enabled. In contrast, the material was found to be harmful to human embryonal kidney suspension cells, demonstrating the importance of biocompatibility testing tailored to the organism and the application.

In the second part of this thesis, the evaluated 3D printing material was applied to the fabrication of a fully-automated microfluidic valve system. Thereby the 3D-printed chip includes inlets, micromixer, microvalves and outlets as a single part. The actuation of the 3D-printed valve membranes by miniature servomotors is a low-cost, easily to control and – to the best knowledge of the author – a complete new approach. The automatization using a Raspberry Pi computer and customized Python scripts created a portable and remotely controllable device. After accurate mixing and valve robustness was proven, the whole microfluidic valve system was applied to a proof-of-concept cytotoxicity assay. Automated analysis of cell growth by live-cell-imaging and image processing revealed highly similar results compared to a pipetted assay as the standard liquid handling technique in cell culture.

In conclusion, the advantages of 3D printing in combination with the biocompatibility evaluation of a 3D-printed material realized the fully automated control of cell culture assays by a newly developed microfluidic valve system. The publication of the 3D-models and automatization scripts empowers scientists its customization to their own applications.

Keywords: 3D printing, biocompatibility, microfluidics, cell culture, automatization, microvalve, lab-on-a-chip

Inhaltsverzeichnis

Abbildungsverzeichnis

Abkürzungsverzeichnis

µTAS	Mikrototalanalysensystem
	(engl.: *micro-total-analysis-system*)
2D	zweidimensional
2PP	Zweiphotonenpolymerisation
	(engl.: *two-photon polymerization*)
3D	dreidimensional
ADME	Absorption, Distribution, Metabolismus, Elimination
bzw.	beziehungsweise
CAD	Computergestütztes Design
	(engl.: *computer-aided design*)
CPT	Camptothecin
CTB	Cell-Titer-Blue
DLP	Dynamische Lichtprozessierung
	(engl.: *digital light processing*)
FACS	Fluoreszenz-aktivierte Zellsortierung
	(engl.: *fluorescence-activated cell sorting*)
FDM	Schmelzschichtung
	(engl.: *fused depostion modelling*)
HEK	Menschliche embryonale Nierenzellen
	(engl.: *human embryonal kidney cells*)
i.d.R.	in der Regel
IC50	Inhibitorische Konzentration bei 50 % Inhibition
	(engl.: *inhibitory concentration at 50 % inhibition*)
ISO	Internationale Organisation für Normung
	(engl.: *International Standard Organization*, ISO)
LOC	„Labor auf einem Chip"
	(engl.: *lab-on-a-chip*)

MEMS	Mikro-Elektronisch-Mechanische Systeme
MJP	Mehrstrahldruck (engl.: *multi-jet printing*)
MTT	3-(4,5-Dimethylthiazol-2-yl)-2,5-diphenyltetrazoliumbromid
n.c.	normalerweise geschlossen (engl.: *normally closed*)
n.o.	normalerweise geöffnet (engl.: *normally open*)
OOC	„Organ auf einem Chip" (engl.: *organ-on-a-chip*)
OWZE	Organisation für wirtschaftliche Zusammenarbeit und Entwicklung
PµSL	Projektionsmikro-Stereolithografie (engl.: *projection micro stereolithography*)
PDMS	Polydimethylsiloxan
SLA	Stereolithografie
SLS	Selektives Lasersintern
USP	United States Pharmacopeia
z.B.	zum Beispiel

1 Einleitung

Mit der rasanten Entwicklung eines neuartigen mRNA-Impfstoffes gegen das Virus SARS-CoV-2 im Jahr 2020 haben sich das enorme Innovationspotential der modernen Biotechnologie und ihr Einfluss auf zentrale Aspekte der gesamten Gesellschaft eindrucksvoll gezeigt. Es scheint nur folgerichtig anzunehmen, dass sich die Aufmerksamkeit und damit die Investitionsbereitschaft in Anbetracht der Entwicklung neuer, immer vielversprechender Technologien in den kommenden Jahren und Jahrzehnten weiter erhöhen werden.

Eine dieser Technologien ist die Mikrofluidik. Durch die Handhabung von Flüssigkeiten auf Mikroebene ermöglicht sie der Biotechnologie die Automatisierung und Digitalisierung komplexer Laborarbeiten in Form von sogenannten *„lab-on-a-chip"* (LOC, dt.: Labor auf einem Chip) Systemen. So konnten beispielsweise *point-of-care* Analysesysteme für Blutdiagnosen direkt beim Arzt [1] oder *on-chip* Mikrobioreaktoren für Bioprozessoptimierungen im Hochdurchsatz entwickelt werden [2]. In der adhärenten Zellkultur ermöglicht die Mikrostrukturierung der Zellumgebung die Nachbildung physiologischer Prozesse, welche mit einer größeren Verlässlichkeit und Relevanz experimenteller Ergebnisse verbunden ist. Dieser Vorteil wird beispielsweise in sogenannten *organ-on-a-chip* Zellkultursystemen genutzt, die als Alternative für Tierversuche in der Pharmaindustrie eingesetzt werden sollen [3].

Solche fortgeschrittenen Zellkultursysteme sind im Gegensatz zu klassischen 2D Zellkulturen räumlich strukturiert und werden i.d.R. über mikrofluidische Kanäle versorgt. Die Automatisierung des Mediumzuflusses für Screenings kann folglich nicht durch Pipettierroboter erreicht werden. Hierbei sind integrierte Mikroventilsysteme überlegen, da sie die räumlich-, zeitlich- und konzentrationsaufgelöste Kontrolle von Reagenzien in verschiedenen Mikrokanälen gleichzeitig ermöglichen. Eine Kombination dieser Ventilsysteme mit mikrofluidischen Zellkultursystemen eröffnet somit komplexe Zellexperimente über längere Zeiträume mit nur geringfügigen Eingriffen des Menschen.

Die vielversprechenden Möglichkeiten, die die Mikrofluidik für weite Teile der Lebenswissenschaften bringt, wurden längst erkannt. Es ist nur eine Frage der Zeit, bis sich die Synergien aus Mikrofluidik und Biotechnologie in wegweisenden Technologien und Produkten niederschlagen. Doch genau dort liegt die Herausforderung: Obwohl schon lange an vielversprechenden mikrofluidischen Systemen für die Biotechnologie geforscht wird, finden nur wenige auch Anwendung in marktreifen Produkten [4]. Aufgrund kostspieliger Fertigung und geringer Anwenderfreundlichkeit sind sie vielfach zu komplex. Da Prototypen oft nicht den Weg aus dem Labor zur eigentlichen Anwendung schaffen, werden sie daher sogar als *„chip-in-a-lab"* parodiert [5].

Ein zentrales Problem stellt dabei die komplexe und kostspielige Fertigung mikrofluidischer Systeme dar, welche Biowissenschaftler:innen den Zugang zur Technologie erschwert [6]. Eine Lösung bietet die additive Fertigung (3D-Druck), bei der Wissenschaftler:innen mikrofluidische Systeme selbstständig entwickeln und

in ihrem eigenen Labor fertigen können. Sie wird unter anderem auch als „die kommende 3D-Druck-Revolution der Mikrofluidik" bezeichnet [7]. Im Gegensatz zu klassischen Herstellungsverfahren sind geeignete 3D-Drucker mit Kosten von wenigen tausend Euro bis hin zu hochauflösenden Druckern mit mehreren zehntausend Euro durchaus finanzierbar. Die Freiheit im Design der 3D-Bauteile erleichtert die Automatisierung durch vereinfachte Integration externer Elemente für Sensorik oder Mechanik. Um den Einsatz im direkten Kontakt mit lebenden Organismen, wie beispielsweise in der Zellkultur, zu erlauben, werden zunächst biokompatible 3D-Druckmaterialien benötigt. Beim 3D-Druck können neben der Wahl des 3D-Baumaterials und des Organismus zusätzlich auch die Bedingungen des Druckprozesses, die anschließende Aufarbeitung der Bauteile oder Sterilisationsprozesse Einfluss auf die Biokompatibilität nehmen.

Neben der Biokombatibilitätstestung von 3D-Druckmaterialien, erleichtert insbesondere auch eine stetige Entwicklung neuer, 3D-gedruckter mikrofluidischer Systeme die Verwendung der Mikrofluidik in der Zellkultur. Dabei erlaubt die Bereitstellung digitaler CAD-Modelle (engl.: computer-aided-design) Biowissenschaftler:innen einen sofortigen Einstieg in die Mikrofluidik. Einzelne Funktionselemente wie Mikromischer oder Mikroventile können somit als separate Module verwendet und beispielsweise zur Automatisierung individualisierter Zellkultursysteme genutzt werden. Diese durch den 3D-Druck ermöglichte Modularität bietet Biowissenschaftler:innen die Chance, die Vorteile der Mikrofluidik deutlich intensiver zu nutzen.

2 Zielsetzung

Ziel dieser Doktorarbeit ist die Evaluation der Biokompatibilität und Sterilisierbarkeit eines bislang noch nicht untersuchten 3D-Druckmaterials sowie dessen Verwendung zur Entwicklung 3D-gedruckter mikrofluidischer Systeme zur Automatisierung adhärenter Zellkulturassays.

Dazu soll zunächst die Biokompatibilität des für den hochauflösenden 3D-Druck einsetzbare 3D-Druckmaterials VisiJet M2S-HT90 getestet werden, um dessen Einsatz in der Zellkultur zu ermöglichen. Da die Biokompatibilität 3D-gedruckter Materialien stark von den gewählten Sterilisationsverfahren sowie der Wahl des Organismus abhängt, sollen Biokompatibilitätsbestimmungen mit verschiedenen Sterilisationsverfahren und Organismen erfolgen. Aufgrund der Hitzebeständigkeit des Materials sollen dabei die Auswirkungen der Heißdampfsterilisation als gängigste Form der Sterilisation getestet werden. Zudem sollen Organismen gewählt werden, die häufig in Forschung und Industrie eingesetzt werden, sodass bei bewiesener Biokompatibilität ein hoher Nutzen für die Biowissenschaften entsteht.

Darauf aufbauend sollen 3D-gedruckte mikrofluidische Systeme entwickelt werden, die zur Automatisierung in der Zellkultur genutzt werden können. Grundlegendes Ziel ist dabei die Automatisierung eines vielfach verwendeten Zellkulturassays als Machbarkeitsstudie. Um die für Assays notwendige Parallelisierung über ein mikrofluidisches System zu ermöglichen, sollen zunächst digital steuerbare, 3D-gedruckte Mikroventile entwickelt werden. Anschließend soll die Integration der Ventile in ein vollständig automatisiertes, 3D-gedrucktes mikrofluidisches Ventilsystem erfolgen. Im Vergleich zu klassisch gefertigten Ventilsystemen soll ein kompaktes und kostengünstiges System entstehen, dass auch die Anwendung außerhalb steriler Umgebungen ermöglicht. Dieses soll zunächst durch verschiedene Tests zur Mischgenauigkeit und Robustheit charakterisiert und final zur Automatisierung eines Zellkulturassays angewendet werden.

Letztlich soll diese Arbeit den Nutzen des 3D-Drucks zur Fertigung mikrofluidischer Systeme zur automatisierte Zellkulturassays demonstrieren. Das zu entwickelnde System sowie die daraus gewonnenen Erkenntnisse sollen in nachfolgenden Arbeiten zur Automatisierung von mikrofluidischen Zellkultursystemen wie *organ-on-a-chip* Systemen dienen können. Ziel ist dabei auch die Veröffentlichung der entwickelten 3D-gedruckten Systeme inklusive aller 3D-Modelle, um die Verwendung und Anpassung der Systeme durch andere Wissenschaftler:innen zu ermöglichen und damit die Popularität 3D-gedruckter Mikrofluidik in der Zellkultur zu erhöhen.

3 Theoretische Grundlagen

3.1 Mikrofluidik

Die Mikrofluidik ist eine Technologie, bei der Fluide, also Flüssigkeiten und Gase, in Größenordnungen von Mikrometern kontrolliert und manipuliert werden. Angetrieben durch Fortschritte der Mikrosystemtechnik mit der Etablierung des Photolithographieverfahrens und der Einführung Mikro-Elektronisch-Mechanischer Systeme (MEMS) wurden Ende der 70er Jahre bis Anfang der 90er erstmals sogenannte *micro-total-ana-lysis-systems* (µTAS, dt.: Mikrototalanalysensystem) oder auch *lab-on-a-chip* (LOC, dt.: Labor auf einem Chip) genannte Systeme entwickelt, dessen Bezeichnungen oftmals synonym verwendet werden [8, 9]. Ziel dieser Systeme ist es, verschiedene Arbeitsschritte im Labor, wie beispielsweise das Mischen, Verdünnen, Inkubieren, Analysieren und Trennen von Flüssigkeiten und Stoffen, in einem einzigen System zu vereinen und somit neben der Miniaturisierung auch einen hohen Grad an Automatisierung zu erreichen. Diese zwei Eigenschaften sind mitunter die wichtigsten Vorteile von LOCs und ermöglichen insbesondere in den Bereichen der Chemie und Lebenswissenschaften enormes Innovationspotential. Zu nennen sind einerseits die Verwendung von kleinsten Probenmengen im unteren Mikroliterbereich, die Einsparung teurer Reagenzien sowie die Manipulation von komplexeren Bestandteilen wie Proteinen und Zellen auf Mikroebene. Andererseits reduziert die durch Pumpen und Ventile erreichte Automatisierung und Parallelisierung den menschlichen Faktor und führt somit zu einer höheren Reproduzierbarkeit und Zeitersparnis [10].

Mit der Mikrosystemtechnik als Muttertechnologie ist die Mikrofluidik jedoch primär eine Ingenieurswissenschaft. Diese Tatsache verhinderte lange Zeit einen Zugang zu den Biowissenschaften, sodass das Potential bis heute keineswegs vollständig ausgeschöpft ist und – wie weiter in Kapitel 3.1.1 diskutiert – die Ergebnisse vielversprechender Forschungsprojekte noch nicht als kommerzielle Produkte realisiert werden konnten [6].

Einen großen Durchbruch für die Mikrofluidik brachte um die Jahrtausendwende die Softlithographie, bei der das Silikon Polydimethylsiloxan (PDMS) zur Fertigung mikrofluidischer Systeme genutzt wird und welche auch heute noch breite Anwendung findet [11, 12]. Dabei wird im klassischen Lithographie-Verfahren eine Gussform (engl. *mold*) hergestellt, welche die Strukturen der Kanäle als Negativ enthält. Anschließend wird die Gussform mit flüssigem PDMS übergossen, welches nach Polymerisation abgelöst und in einem Plasmaofen an einen Objektträger gebunden wird. Neben zahlreichen weiteren Herstellungsverfahren sind insbesondere auch die maschinelle Mikrobearbeitung (engl.: *micromachining*) durch Fräsen, das Ätzen der Kanalstrukturen in Glas (engl.: *edging*), der Spritzguss und das Thermoformen von Polymeren oder auch additive Fertigungstechnologien wie der 3D-Druck, welcher in Kapitel 3.2 explizit behandelt wird, zu nennen [13].

Das besondere Strömungsverhalten der Mikrofluidik zeichnet sich durch eine in den Mikrokanälen dominierende laminare Strömung aus. Diese resultiert entsprechend der Gleichung nach Reynolds mit

$$Re = \frac{\rho \cdot v \cdot d}{\eta} \tag{1}$$

Re: Reynoldszahl; ρ: Fluiddichte; v: Flussgeschwindigkeit; d: Kapillardurschmesser; η: Dynamische Viskosität

aus dem geringen Kapillardurchmesser im Mikrometerbereich, sodass sehr niedrige Reynoldszahlen (<1) mit anteilig wirkenden hohen Reibungskräften vorliegen [14]. Dabei wird eine Strömung bis zu der kritischen Reynoldszahl von 2300 noch als laminar betrachtet. Laminare Strömung charakterisiert sich durch parallel verlaufende Fluidschichten und eine diffusionsgetriebene Durchmischung. In der Praxis bedeutet dies, dass sich zwei zusammenlaufende Flüssigkeiten in einem Kapillarsystem nicht wie bei großen Rohrdurchmessern durch Turbulenz, sondern vor allem zeit- und grenzflächenabhängig vermischen. Folglich stellt die schnelle effektive Durchmischung zweier Flüssigkeiten in der Mikrofluidik eine große Herausforderung dar, welche nur durch passiv wirkende, komplexe Kanalgeometrien oder aktiver Durchmischung erreicht werden kann. Der beispielsweise in dieser Arbeit verwendete 3D-gedruckte HC-Mikromischer nach Enders *et al.* nutzt komplexe 3D-gedruckte Strukturen und kombiniert somit die *split-and-recombine* (dt.: Teilen und Zusammenführen) Methodik, bei der die Flüssigkeitsgrenzfläche erhöht wird, mit chaotischen Strömungen [15]. Nichtsdestotrotz bietet die laminare Strömung in bestimmten Anwendungen auch Vorteile. So lassen sich z.B. die Verschiebungen der Fluidschichten in spiralförmig verlaufenden Kanälen (in sogenannten Spiralseparatoren) zur Abtrennung von Zellen nutzen [16].

Neben der laminaren Strömung bewirkt die Miniaturisierung auch eine starke Vergrößerung des Oberflächen-zu-Volumen-Verhältnisses, welche den Stoff- und Wärmeaustausch beschleunigt [10]. Dies ist insbesondere in Zellkultursystemen von Vorteil, da somit ein schneller und effektiver Austausch von Sauerstoff, Medium und Wärme für verbessertes Zellwachstum sorgen kann [17, 18].

3.1.1 Mikrofluidik in der Biotechnologie

Die Mikrofluidik bietet insbesondere im Bereich der Biotechnologie, wo die automatisierte, parallelisierte und reproduzierbare Manipulation von Flüssigkeiten essentiell ist, eine Vielzahl neuer Entwicklungsmöglichkeiten. Hier zu nennen sind insbesondere mikrofluidische, analytische Systeme für die schnelle *point-of-care* Diagnostik [19], Mikrobioreaktoren zur effizienten Optimierung von Bioprozessen [2] und die Rekonstruktion einzelner Organfunktionen durch *organ-on-a-chip* Systeme (s. Kapitel 3.3) für ein physiologisch relevanteres Wirkstoffscreening in der Pharmaindustrie [20]. Seit der Einführung des PDMS-Herstellungsverfahrens wurden zahlreiche neue mikrofluidische Systeme mit Fokus auf biotechnologische Anwendungen hervorgebracht. Allerdings kommen viele vielsprechende Ansätze mikrofluidischer Systeme bisher kaum über die Entwicklung im Labor hinaus. Die Bewertung der Mikrofluidik mit einem Technologie-Reifegrad (engl.: *technoloy readiness level*) der Stufe 3-4 (von insgesamt 12 Stufen) bestätigt, dass die Technologie noch in das Stadium des *proof-of-concept* (dt.: Machbarkeitsstudie) bzw. des „Versuchsaufbaus im

Labor" eingeordnet wird [21]. Für den Einsatz der Mikrofluidik in der Biotechnologie wurden schon früh der schlechte Zugang für Biowissenschaftler:innen zur Mikrofluidik als Ursache ausgemacht [6]. Zudem sind Eintrittshürden in der Biotechnologie aufgrund der hohen Investitions- und Entwicklungskosten i.d.R. sehr hoch. Daher ist die Identifikation und Einschätzung der vielversprechendsten Anwendungsgebiete mikrofluidischer Systeme in der Biotechnologie umso wichtiger, um Forschung und Entwicklung frühzeitig ausrichten zu können.

Im folgenden Übersichtsartikel „*Microfluidics in Biotechnology: Quo Vadis*", der in dem Textbuch „*Microfluidics in Biotechnology*" der Buchserie „*Advances in Biochemical Engineering/Biotechnology*" erschienen ist, wird die Rolle der Mikrofluidik in der Biotechnologie diskutiert. Dabei wird zunächst der Status Quo der Mikrofluidik in Hinblick auf eine kommerzielle Nutzung in Form biotechnologischer Unternehmen erörtert, anschließend potentielle Lösungen zur Überwindung vorliegender Herausforderungen der Technologie diskutiert sowie neue, besonders vielversprechende Trends identifiziert.

Microfluidics in Biotechnology: Quo Vadis

Steffen Winkler, Alexander Grünberger, and Janina Bahnemann

Contents

Abstract The emerging technique of microfluidics offers new approaches for precisely controlling fluidic conditions on a small scale, while simultaneously facilitating data collection in both high-throughput and quantitative manners. As such, the so-called lab-on-a-chip (LOC) systems have the potential to revolutionize the field of biotechnology. But what needs to happen in order to truly integrate them

S. Winkler and J. Bahnemann (✉)
Institute of Technical Chemistry, Leibniz University Hannover, Hannover, Germany
e-mail: jbahnemann@iftc.uni-hannover.de

A. Grünberger (✉)
Multiscale Bioengineering, Technical Faculty, Bielefeld University, Bielefeld, Germany
e-mail: alexander.gruenberger@uni-bielefeld.de

into routine biotechnological applications? In this chapter, some of the most promising applications of microfluidic technology within the field of biotechnology are surveyed, and a few strategies for overcoming current challenges posed by microfluidic LOC systems are examined. In addition, we also discuss the intensifying trend (across all biotechnology fields) of using point-of-use applications which is being facilitated by new technological achievements.

Graphical Abstract
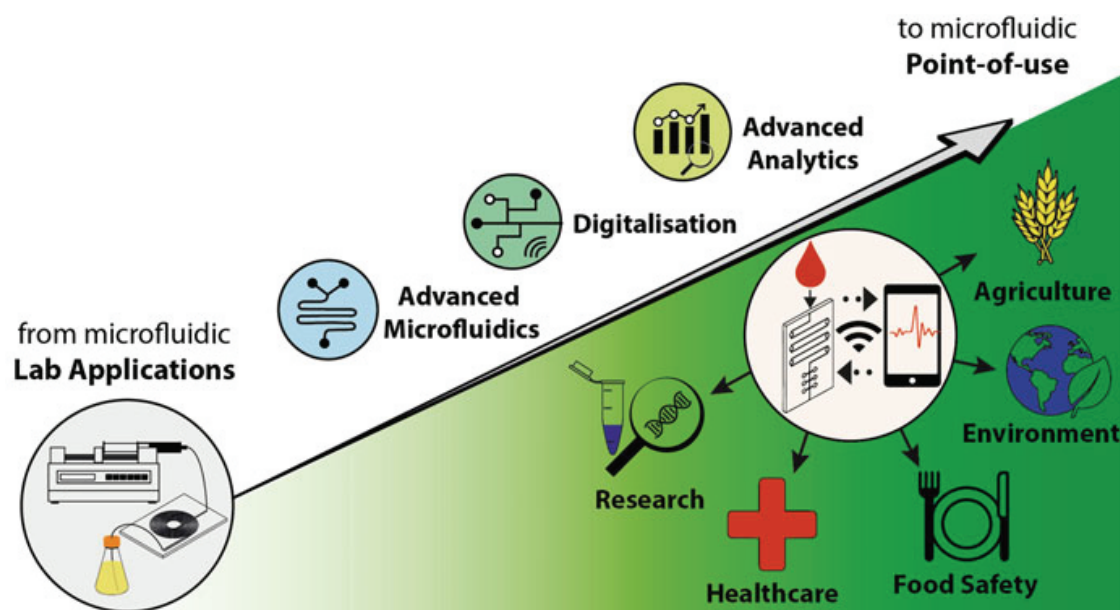
Keywords Biochemical engineering, Industrial biotechnology, Lab-on-a-chip, Medical biotechnology, Microfluidic screening, Microfluidics, Nanofluidics, Organ-on-a-chip, Point-of-care, Point-of-use

1 Introduction

The application of microfluidic systems in biotechnology has recently become a subject of intense research interest [1, 2]. Emerging research and industrial applications include point-of-care medical diagnostics [3], organ-on-a-chip [4], and multiresistant bacteria testing [5] via microbioreactors [6] in red biotechnology. In white biotechnology, current approaches include catalysis, single-cell culture [7, 8], and droplet-based screening [9] through integrated biosensors and other analytics in miniaturized devices. Nevertheless, many microfluidic applications still depend on proof-of-concept systems, which have not yet realized their full potential. Accordingly, one of the most pressing challenges that will need to be addressed over the next few years is how to efficiently and effectively transform these systems into

routine applications that can actually be advanced into the market and, ideally, exceed the "gold standards" that currently exist in the field.

But how does this process look like? What, exactly, does it entail? In this review, the current state of the art of microfluidic systems is surveyed, with the aim of highlighting some of the most promising applications that have been developed to date. Furthermore, we identify and consider a number of pressing challenges that must be addressed before the full potential of this emerging technology can be realized within the field of biotechnology – and a few emerging applications and technologies are also highlighted to illustrate how (taken together) they might be leveraged to create superior microfluidic devices in the near future. Finally, we offer a few cautious predictions regarding how microfluidic systems might shape biotechnology in the future.

2 Main Fields of Microfluidics in Biotechnology and Their Realized Potential

There is an enormous variety of microfluidic systems currently being deployed in the field of biotechnology research – although lab-on-a-chip (LOC) is frequently employed as an umbrella term to broadly describe all of these microfluidic-based biotechnologies. By way of example, some of these systems include PCR-, genomics-, proteomics-, diagnosis-, catalysis-, transfection-, organ-, human-, tumor-, electrophoresis-, differentiation-, microscopy-, and bioreactors-on-a-chip. While most LOCs remain locked in the proof-of-concept phase, over the last decade a few have made advancements into the broader market. The commercial potential of LOCs has thus already been partially realized, in the form of aspiring start-ups and commercially available devices – although the present state of affairs only hits at the tremendous future potential for deploying LOCs within routine biotechnological applications. In this review, we have identified 350 companies that have begun to explore incorporating microfluidics into biotechnological applications (Fig. 1), with the particular focus on microfluidic devices in the following application areas in biotechnology: clinical applications, including point-of-care (POC) devices and other devices for clinical diagnosis; screening techniques; cell manipulation and analysis, such as single-cell sorting; genetics and genomics, with established technologies like PCR-on-a-chip; bioanalytics and biosensors; and organ-on-a-chip (OOC), among others.

The number of companies developing microfluidic systems for biotechnological application is now growing significantly. The first companies in this field primarily focused on diagnostic devices and gene analysis systems (see Fig. 1, "Clinical Applications (POC/Diagnosis)" and "Genetics and Genomics"). This is not surprising, taking into account that the first microfluidic breakthroughs in the world of biotechnology were achieved in these fields. Driven by the human genome project, capillary electrophoresis technology (a predecessor to the electrophoresis-on-a-chip)

9
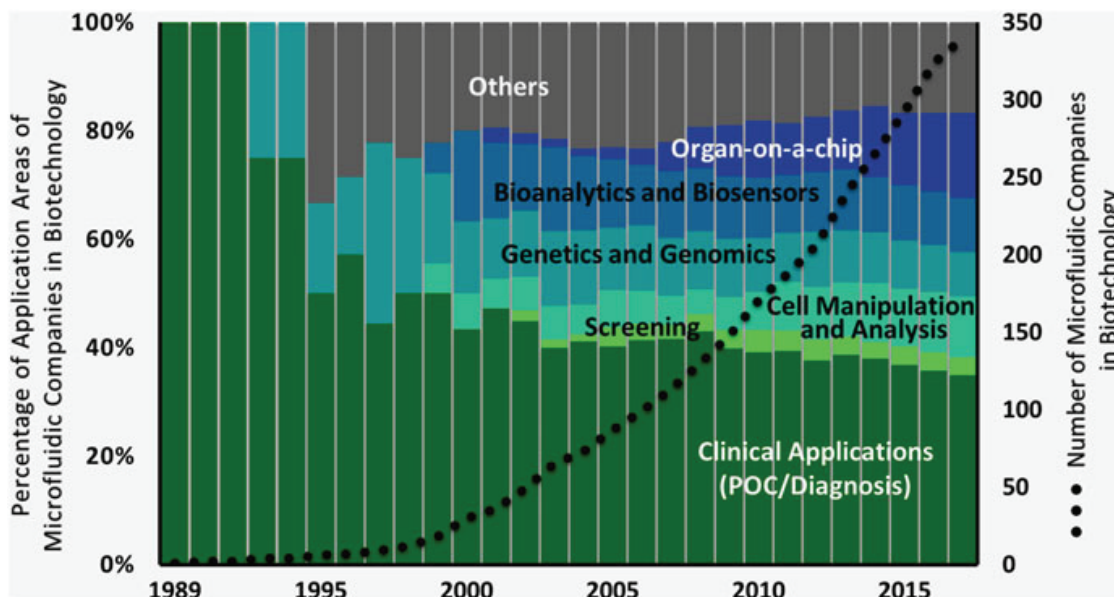
Fig. 1 Overview of the development of companies offering microfluidics for application in biotechnology over the past 20 years. This figure is based on an extensive market research, which the authors have carried out consistently (based on the references [10–12]) in 2020 and reflects only a trend in company development. The authors provide no guarantee for the exact number of existing companies focusing on microfluidics for biotechnological applications
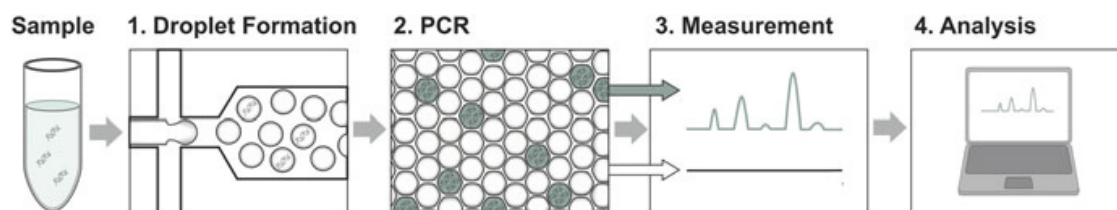
Fig. 2 The principle of digital PCR. In the first step, droplet microfluidics is used to distribute the DNA molecules in independent droplets. After the PCR, only droplets containing DNA are detected by fluorescence measurements. The distribution of DNA in the droplets follows a Poisson's distribution that is finally used to calculate the DNA quantity. Translated with permission from J. Bahnemann and A. Grünberger [15], Copyright (2021), Zukunftsforum Biotechnologie (Hrsg.), DECHEMA e.V. Frankfurt/M. (2021)

was invented to increase DNA sequencing speed and throughput [13]. Not only the sequencing, but also the powerful technology of PCR has been successfully miniaturized [14]. PCR-on-a-chip technology has developed rapidly in recent years, and these days more advanced technologies that build on this foundation – such as the digital PCR (dPCR) (Fig. 2) [16, 17] – are actually beginning to replace longstanding non-microfluidic "gold standards" such as quantitative PCR (qPCR).

Companies have also increasingly started to deploy these technologies in more commercially profitable endeavors, that is the development of POC diagnostics (Fig. 3). The potent combination of advanced liquid handling features – such as pumping, mixing, and separation – with gene analysis techniques, and the potential
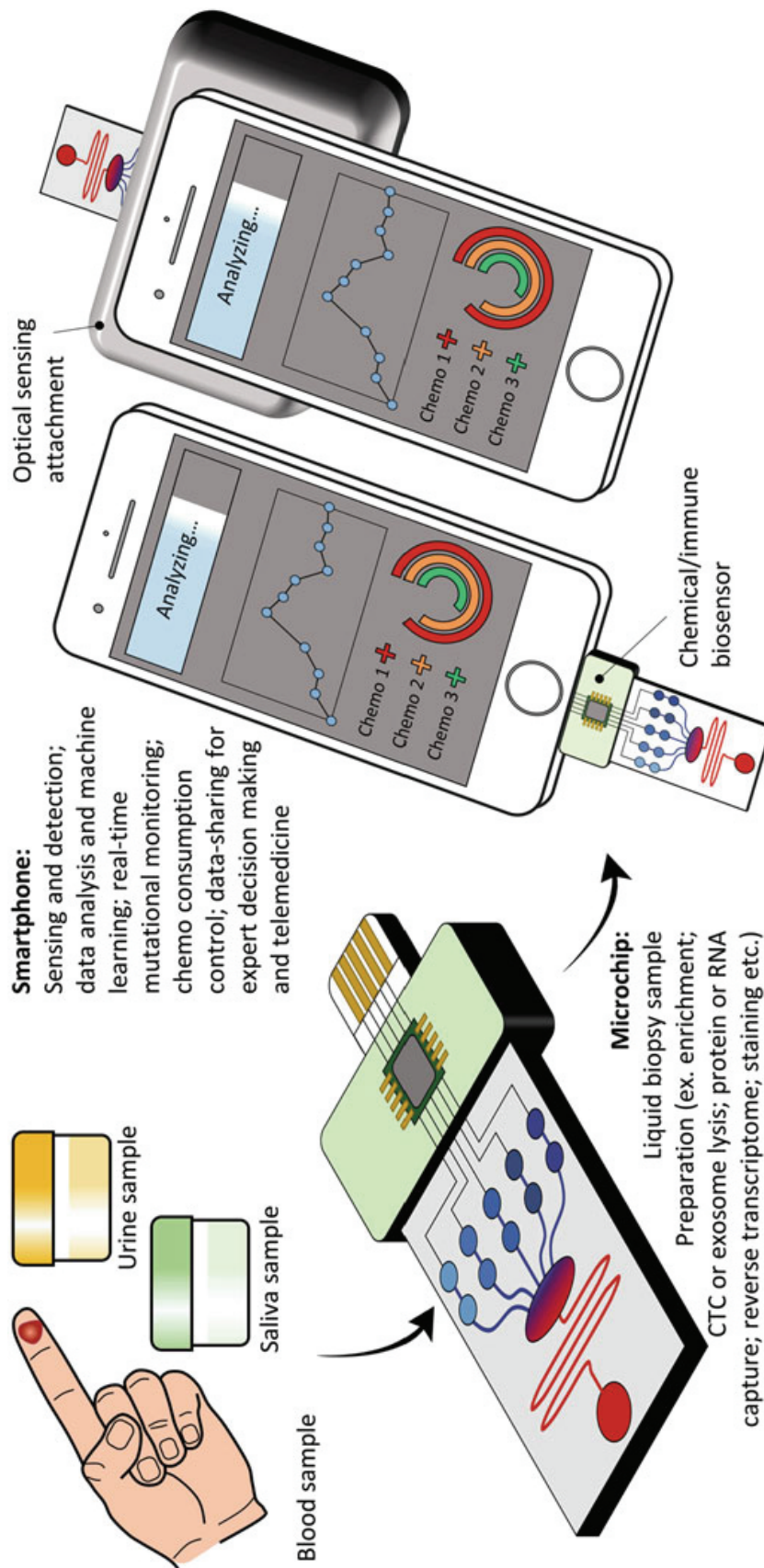
Fig. 3 Example of a microfluidic point-of-care device. A patient sample, such as blood, saliva, or urine, is processed and analyzed using a microfluidic chip. The chip contains a biosensor for detection of biologic markers and is read out and analyzed by a connected smartphone. Reprinted from Samandari et al. [18] (Copyright (2018), with permission from Elsevier)
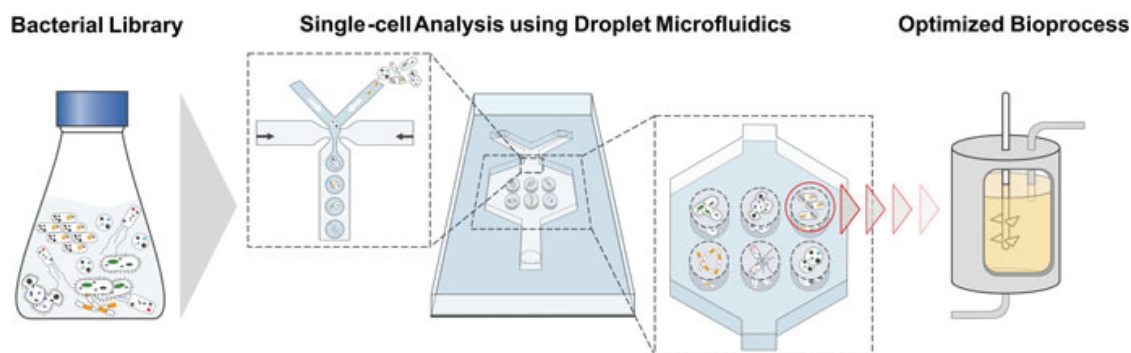
Fig. 4 Principle of single-cell analysis using droplet microfluidics. Herein, droplet microfluidics is used to singularize different types or strains of bacteria of a library in droplets followed by single-cell analysis and identification of potent cells for optimization of a specific bioprocess. Translated with permission from J. Bahnemann and A. Grünberger [15], Copyright (2021), Zukunftsforum Biotechnologie (Hrsg.), DECHEMA e.V. Frankfurt/M. (2021)

for usage in highly rentable clinical studies, has led to a veritable explosion of microfluidic POC start-up companies. Indeed, POC devices (see chapter: "Lab-on-a-Chip Devices for Point-of-Care Medical Diagnostics" [3]) currently constitute the single largest market for LOCs in biotechnologies.

The discovery of droplet microfluidics has facilitated the emerging field of single-cell analytics (Fig. 4). In the last years, droplet microfluidics has been applied to cell sorting [19], mammalian cell analysis [20, 21], microorganism analysis [22], and single-cell drug screening [23]. In addition, developments in the field of droplet microfluidics have also led to advancements in microfluidic ultra-high-throughput screening [24]. One major push on this front is to replace the current well-plate drug screening process commonly used in the pharmaceutical industry by droplet microfluidics.

As illustrated in the chart shown in Fig. 1, there are also companies working in the field of bioanalytics and biosensors. These companies offer an ever-increasing set of diverse analytical tools – from biosensors for environmental or animal applications to novel microfluidic modulation spectrometers [25], microfluidic resistive pulse sensing [26], sub-terahertz (THz) vibrational spectroscopy [27], optical microcavity technologies [28], to name but a few.

OOC applications represent perhaps the latest – and certainly the most advanced – application of this technology. OOCs combine tissue engineering with microfluidics to achieve complex 2D or 3D cellular systems [4]. Due to their exciting potential to revolutionize drug testing protocols and minimize costs associated with drug failure in the clinical stages (which is unfortunately extremely common), multiple start-ups have charged into the market in this area [29]. Furthermore, these systems can also be further refined into disease-on-a-chip (DOC) systems, which may be able to provide researchers entirely new insights into pathological processes. Even human-on-a-chip systems are now being developed. In principle, these systems combine several OOCs containing different human cells in a single chip to simulate even the most complex human physiological processes (Fig. 5).
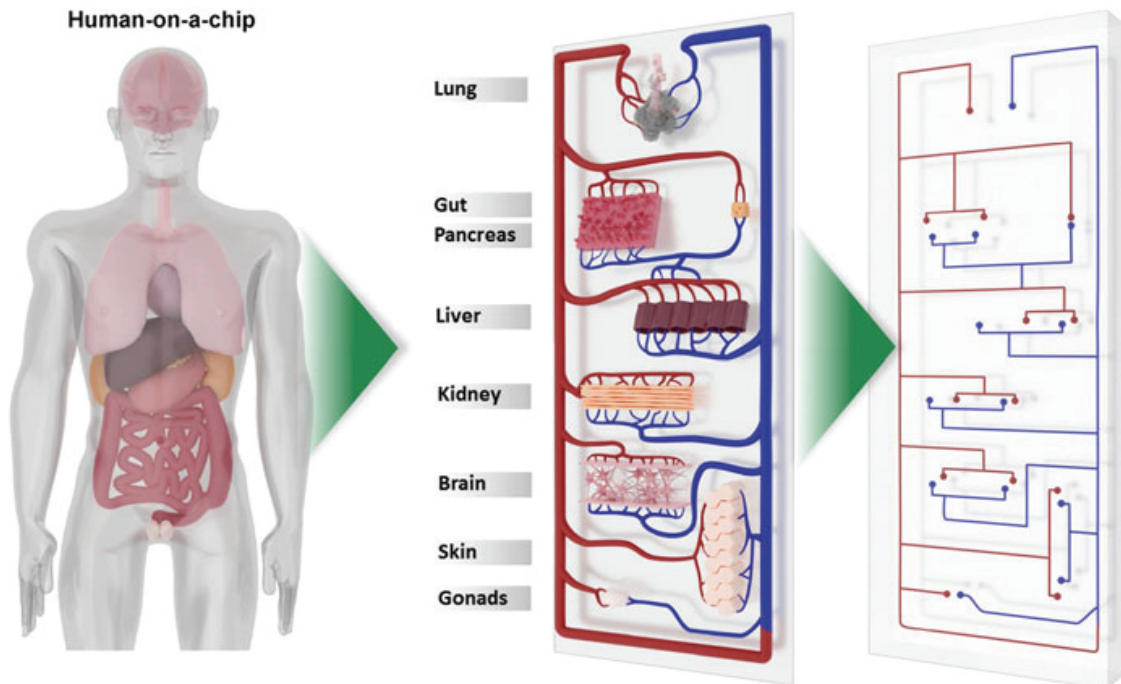
Fig. 5 Principle of the human-on-a-chip. The human-on-a-chip mimics human physiological processes by connecting and maintaining several different organ-on-a-chip systems in a single microfluidic chip. With permission *from Springer International Publishing: Bahnemann et al.* [30], *Copyright (2021)*

As the illustrated examples demonstrate, microfluidics is currently experiencing a significant breakthrough period within the field of biotechnology. The sheer scope and diversity of the adoption of this technology in this field is perhaps most starkly underlined by the fact that the fraction of "unassignable" companies (see Fig. 1, "Others") is increasing rapidly. At the same time, however, microfluidics unquestionably still remains in its infancy – indeed, many LOCs exist only in the form of proof-of-concept systems [31]. With inconvenient handling requirements, comparatively low robustness, complex standards, and bulky hardware, LOCs are often derided as complicated "chip-in-a-lab" systems [32]. Accordingly, beyond the few commercially available systems, most published microfluidic devices still suffer from a low technological readiness level (TRL) of just 3–4 points out of a 12-point scale [32]. Even comparatively established technologies in this area – such as POC testing – have a long way to go before their full potential will be realized. Critical challenges continue to plague researchers and developers, and must be adequately addressed before microfluidic routine applications can truly replace the current "gold standards" in biotechnology.

3 Challenges and Solutions for Microfluidic Proof-of-Concept Systems in Biotechnology

In the last 20–30 years, the applications of microfluidic technologies have been pioneered in research areas such as microsystems engineering, physics, chemistry, and biology. This has led to the development of a wide array of promising proof-of-concept systems, which primarily seek to miniaturize and automatize existing lab procedures in a LOC format. But the central question now faced by this maturing industry is whether these systems actually confer any true advantage over the "gold standards" that are currently being used in these areas. Three major challenges – summarized in Fig. 6 – that continue to plague microfluidic proof-of-concept systems and early commercialized devices are identified and discussed below.

3.1 Design and Fabrication

The first key obstacle for the development and deployment of microfluidic devices for biotechnological applications has been the relatively limited access that researchers actually have to microfluidic fabrication facilities [33–35]. As reported by Kotz et al. [36], a number of fabrication techniques have been developed for manufacturing microfluidic devices. Perhaps the most widely used are molding
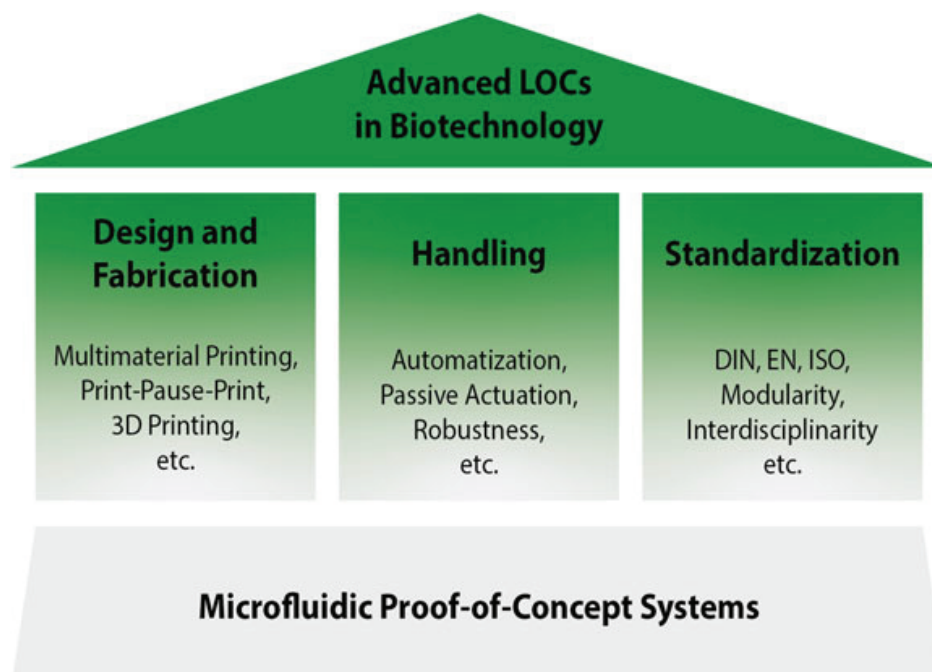
Fig. 6 Towards advanced microfluidic devices in biotechnology. Microfluidic proof-of-concept systems are currently facing great challenges, such as the design and fabrication, handling and standardization of microfluidic devices, to become advanced LOCs for real-world applications in biotechnology

techniques – including, for example, hot embossing, injection molding, and soft lithography – and laminates. While these techniques represent a solid foundation for the production of three-dimensional microfluidic structures, they are also extremely laborious and costly [31]. As a result, only engineers and microsystems technicians who are already experts in the field of microfluidics tend to be comfortable deploying them, whereas experts in the fields of their intended substantive application – such as biologists and biochemists – can generally contribute little to their development. In addition, the complicated and time-consuming developmental process of these fabrication techniques creates an understandable reluctance to implement many small, but often useful, improvements. One potential solution is showcased in the latest advances in additive manufacturing [31, 37–40].

Design and fabrication through these methods are comparatively much simpler, and 3D printers are far more affordable than classic clean room facilities. Furthermore, one early concern with respect to this method – that the printing resolution would be too low – has effectively been mitigated through recent advancements in multijet printing [41], stereolithography, and two-photon laser techniques (which are now reaching the micrometer and even nanometer scale). As the number of 3D printers is increasing, so are the number of different 3D printing materials that can be used.

Especially for biological applications, materials (such as acrylates or silicones) that are biocompatible are increasingly being brought onto the market [42–44]. Although many high-resolution 3D printers remain limited for fabrications employing just a single material, in the last few years, tremendous efforts have been made to achieve multimaterial 3D printing [45] or multiprocess 3D printing (as well as print-pause-print (PPP) 3D printing) [46]. The successful integration of sealing connections (e.g., elastic silicones), movable functional units (e.g., microvalves or micropumps [47]), porous barriers (e.g., porous membranes [48]), electronic components (e.g., electrochemical sensors [49, 50], heating/cooling elements [51], magnetic elements [52], and cupper fibers for dielectrophoresis [53]) – and even the implementation of chemical reagents [54, 55] solely by 3D printing – has already been well demonstrated in the literature. Because multimaterial 3D printing is of significant interest for many other industries, we will likely see further advances within this field in the years to come.

3.2   Handling

As one might expect, realizing the vision of miniaturizing very complex multi-step lab procedures into a simple LOC has also turned out to be a very challenging endeavor. At the micro- or nano-scale, even the smallest disturbances – such as dust particles, air bubbles, vibrations, leaking interconnections, leachables, etc. – can lead to dysfunction of the whole chip, necessitating time-consuming and expensive repair (or even replacement) efforts. The robustness of any LOC is thus a crucial component of consideration [56], and this is only all the more true when the system in
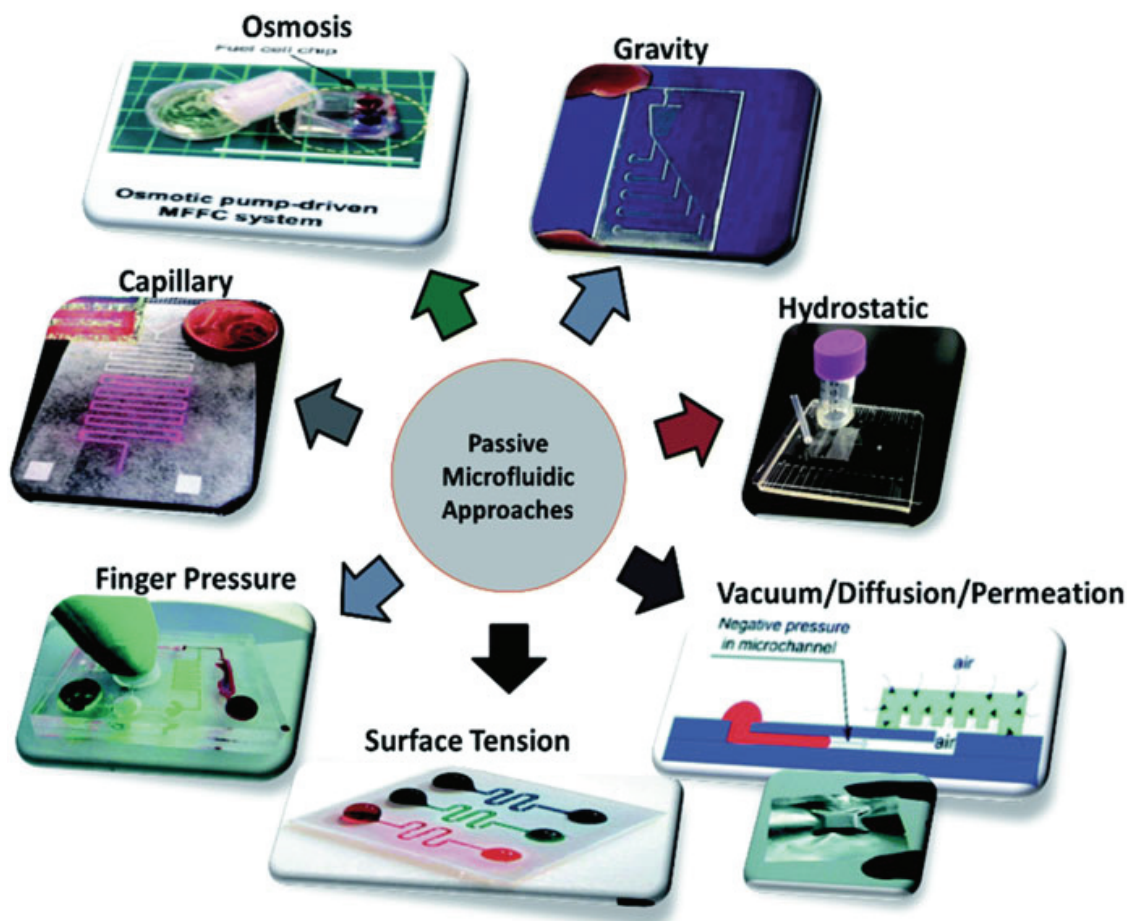
Fig. 7 Different approaches employed in passively driven microfluidics and LOC devices. All techniques are actuated by a single driving force that is controlled by specific structural elements for precise control of flow, mixing events, and other LOC operations. Reproduced from Ref. [57] with permission from The Royal Society of Chemistry

question will be used not by a trained scientist, but rather by untrained people (such as students or even patients) as in the so-called easy-to-use POC devices.

Improving the robustness of future LOC devices can be best achieved by replacing actively controlled units, such as pumps and valves, with passively controlled elements that are incorporated directly into the design of the chip itself (Fig. 7). Paper-based POC devices have already illustrated how this can be realized by using microcapillary forces that induce a passively controlled flow [58]. These flow speeds depend on the kind of adsorption material used, which can be determined during the design process. Similarly, centrifugal POC devices use predefined channel sizes to convert centrifugal forces into well-defined liquid flow. The so-called passive check and burst valves allow a more complex design of the fluid circuit. And complex processes can also be completely controlled by either the chip design or by a few external actuators. The concept of passive control can be transferred into any application where easy handling and automatization is needed –

and since many protocols for preparative or analytical applications in biotechnology follow predictable steps that are always the same, this is a logical fit.

Adoption of this principle is currently a prime focus of the so-called microfluidic circuits or microfluidic networks [59]. These networks seek to transfer Ohm's law ($U = I \cdot R$) of electric resistance into the field of microfluidics, where the resistance R corresponds to the microfluidic channel resistance, the intensity I to the flow-rate, and the potential U to the pressure [60]. In theory, this means that the flow can be controlled by the channel resistance, the channel resistance in turn by the channel geometry, and the channel geometry by the chip design and fabrication. Using these built-in control features, a manufacturer can theoretically exert maximum control of the process – to the point where, at least ideally, an unexperienced end user may only need to push a start-button. This principle can also be further extended to achieve time-dependent LOC control (e.g., where a specific valve only opens when an increasing pressure gradient reaches a critical value, etc.). Duncan et al. have already used a constant and single vacuum source in combination with microvalves and resistors to achieve oscillating microvalves, which, in principle, could function as a membrane-based micropump [61]. Furthermore, slower or faster oscillations could certainly be achieved by adaptation of the resistors, leading to different pump speeds. Just like in electronic chips, these oscillators could theoretically be further used to induce rhythms that activate several LOC procedures after a specific time or after a single externally controlled event (such as a simple valve opening).

None of the above-mentioned methods can currently control complete LOC procedures. However, although they are still in their infancy, these methods already demonstrate the high potential of passively controlled microfluidics for easy-to-use but fully automated LOCs – as illustrated by the possibility that a sophisticated design of a microfluidic chip could (for example) be harnessed to upgrade a microvalve to a micropump without losing robustness. In contrast, classic pneumatic micropumps are controlled by at least two pressure or vacuum sources [62], which are in turn controlled by external valves constituting a serious additional risk for device dysfunctionalities.

3.3   Standardization

In principle, the primary purpose of LOC technologies is to transfer research in the fields of biology and chemistry into our modern world of machines, computers, and data. This requires tremendous interdisciplinary input from scientists across a wide range of fields, all leveraging and combining their specific areas of substantive knowledge to design, manufacture, functionalize, automize, and deploy sophisticated LOCs. On the one hand, this interdisciplinarity push has led to a huge variety in LOC devices while, on the other hand, it has also led to veritable confusion in the form of a seemingly endless number of different fabrication techniques, design concepts, ways of flow control, integration techniques, etc. Successful mass-market incorporation of microfluidics technology into biotechnological applications will

ultimately require the adoption of *standardization concepts* (e.g., ISO standards, protocols and guidelines to organize the pioneered knowledge into a common microfluidic language, etc.) in order to allow researchers from all fields to meaningfully understand and contribute to future LOC development by adopting high level good manufacturing practice (GMP) standards in most fields of biotechnology. This standardization will also allow biologists to consider fabrication and design rules (such as material properties and microchannel characteristics), and engineers to consider biological demands (such as maximal shear flow, biocompatibility and more), and to allow both groups to effectively communicate their own needs using a common language of sorts [63].

For very basic operations (such as pumping, mixing, and separation), microfluidic solutions have already been developed that can be further characterized and classified to develop a database of microfluidic operators. This modularity is crucial to facilitate faster design and configuration via plug-and-play processes [31]. Once again, drawing on analogies to the field of mechanics, these modules could be saved as 3D computer-aided design (CAD) files – although, of course, new software must still be developed to enable the proper and efficient use of these files. 3D printing of microfluidic devices, in particular, could further push the standardization of LOC modules. Additionally, there is a need for standardization efforts regarding the chip-to-world interface [64]. Currently, many proof-of-concept systems use diverse kinds of tube connections, pumps, control units, and more. For industrial applications (such as drug screening), however, LOCs must be easily implementable into existing processes and standards.

4 Emerging LOCs: From the Lab to the Chip

One focus of current microfluidics development aims to miniaturize biotechnological workflows "to the chip," in order to take advantage of greatly improved workflows that are realizable via miniaturization and/or automatization. In principle, this holds true not just for classical LOCs procedures (such as the PCR), but also for newer biotechnological methods (see following subchapters). The huge variety of possible LOCs cannot be summed up in a single book chapter; therefore, in this section, we focus only on a subset of novel LOCs that show a high potential for further revolutionizing biotechnologies.

4.1 Directed Evolution and Adapted Laboratory Evolution

In 2018, the Nobel Prize in Chemistry was awarded to Frances H. Arnold for her pioneering achievements in directed evolution. The techniques that she spearheaded have helped to optimize reactions by developing faster, more specific, more stable, and/or more sensitive enzymes [65]. These advances are of particular interest for

large industries focused on improving or streamlining the performance of bioprocesses. Using the phenomenon of mutagenesis, enzymes can be either specifically or randomly modified to create mutant libraries, which can then be subsequently screened to identify improved enzyme abilities. The last step remains a challenging task – and LOC platforms that make use of droplet screening, in combination with advanced droplet sorting systems, are ideal tools for efficiently screening mutant libraries to identify enzymes with enantio-selectivity or high catalytic activity in ultrahigh-throughput [66]. Organisms (such as *Escherichia coli*) that express the mutant enzymes may also be singularized in droplets, lysed, analyzed, and sorted. Such systems could even be further extended by LOC-based transformation or transfection, to re-cultivate promising mutants. It also bears noting that the high-throughput and automatization properties of directed evolution on-chip would contribute to a greater understanding of enzyme mechanisms and evolution processes in general.

4.2 "CRISPR-on-a-Chip" (COC)

Emmanuelle Charpentier and Jennifer A. Doudna were honored with the Nobel Prize for Chemistry in 2020 for their outstanding scientific achievement in developing the CRISPR-Cas (*C*lustered *R*egularly *I*nterspaced *S*hort *P*alindromic *R*epeats) method for gene editing. The discovery of the so-called gene scissor represents a fundamental breakthrough in the field of molecular biology, and is expected to tremendously change life sciences in the years to come [67, 68] – just like DNA sequencing and PCR have done in previous decades. Indeed, researchers have already started to use this technique in microfluidic platforms [69], predominantly for on-chip point-of-care gene detection with CRISPR-based gene biosensors or automated gene editing in LOCs.

One recently developed chip uses a graphene field-effect transistor, in combination with a deactivated CRISPR-Cas9 protein complexed with a specific single-guide RNA, to achieve the unmediated detection of a specific gene on-chip (Fig. 8a) [70]. In contrast to PCR, this system can abstain from gene amplification and leverage CRISPR technology to create gene biosensors. By implementing biosensors into future COCs, this technique could potentially be used to screen large numbers of mutations for detecting diseases in a microarray – and the quantification of gene expression could also be applied to clusters of genes for a completely new molecular understanding of gene regulation and other basic mechanisms (such as cell differentiation), which in turn might be used for the development of novel drugs.

In combination with microfluidics, the CRISPR-Cas9 system may also be used to automatize gene editing. A recent approach combines digital microfluidics with the CRISPR-Cas9 technique for on-chip gene editing of cell cultures (Fig. 8b) [71]. Similar platforms could enable multiplexing and high-throughput gene editing in future, opening up theoretically endless application possibilities across many diverse subfields in the biotechnology sphere.
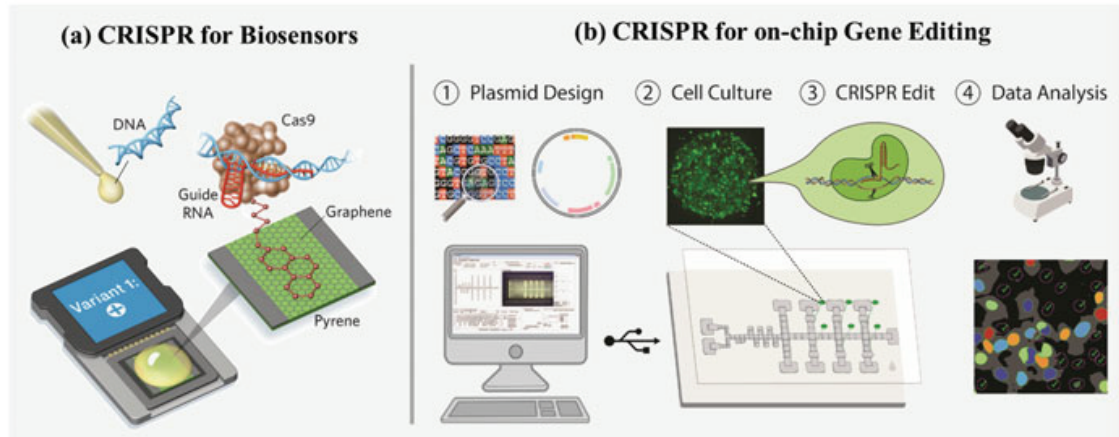
Fig. 8 CRISPR-on-a-chip. (**a**) CRISPR-Cas9 for unamplified gene detection in biosensors. The Cas9 complexed with a target-specific guide RNA is immobilized on the surface of the graphene within a graphene field-effect transistor. The complex identifies and binds to the target gene, resulting in an electrical signal output. Adapted by permission from Springer Nature: Nature Biomedical Engineering, Hajian et al. [70], copyright, 2020. (**b**) An automated CRISPR-based gene editing platform. Designed plasmids (1) are used for gene editing of cell cultures inside a microfluidic chip (2, 3) and results are analyzed by microscopy (4). The computer-controlled chip is based on digital microfluidics for dispersion, merging, mixing, and splitting of droplets. Reproduced from Ref. [71] with permission from The Royal Society of Chemistry

4.3 Organisms-on-a-Chip

After single-cell analysis and organs-on-a-chip, the "next level of life" is represented in the emerging "organisms-on-a-chip" technology. Similar to organs-on-a-chip, organisms-on-a-chip can be used for drug testing, diagnosis, or simply to understand biochemical and physiological processes. Prominent examples thereof are the nematode *Caenorhabditis elegans* [72], the malaria parasite *Plasmodium falciparum* [73], and the zebrafish [74]. Plants-on-a-chip [75] and roots-on-a-chip [76] have also been developed in the field of green biotechnology, while for blue biotechnology corals-on-a-chip are being developed [77]. It can simply be stated that the opportunities for future organisms-on-a-chip systems are essentially endless – although to date, few avenues have truly been explored in this emerging field. One challenge is the difficulty of adequately emulating natural as well as defined artificial environments [78, 79] to enable detailed fundamental insights regarding an organism's overall behavioral pattern.

5 Future LOC Technologies: From Lab Applications to Point-of-Use Solutions

The dawning of the twenty-first century has ushered in the so-called information age, and the immediate access to comprehensive information enabled by this incredible technological revolution in computing will only become increasingly important in the years to come. Industrial applications are already promoting on-demand and easy-to-use technologies. Smartphones, for example, have demonstrated the enormous benefit of immediate information exchange. POC devices remain perhaps the best examples, to date, of similar efforts to leverage microfluidic biotechnologies for rapid extraction of information via implemented analytics – however, in the future, this trend will not be limited to POC and other red biotechnological analytic devices, but will instead almost certainly expand to all biotechnology fields in the form of point-of-use applications (Fig. 9). Accordingly, in the following we will discuss three central LOC technologies representing advancements of current microfluidic lab applications to point-of-use analytics in all aspects of biotechnology.

5.1 Advanced Microfluidic Technologies

Point-of-use applications require robust LOCs based on easy-to-use working principles. As described above, passively actuated LOCs (such as paper, centrifugal, and
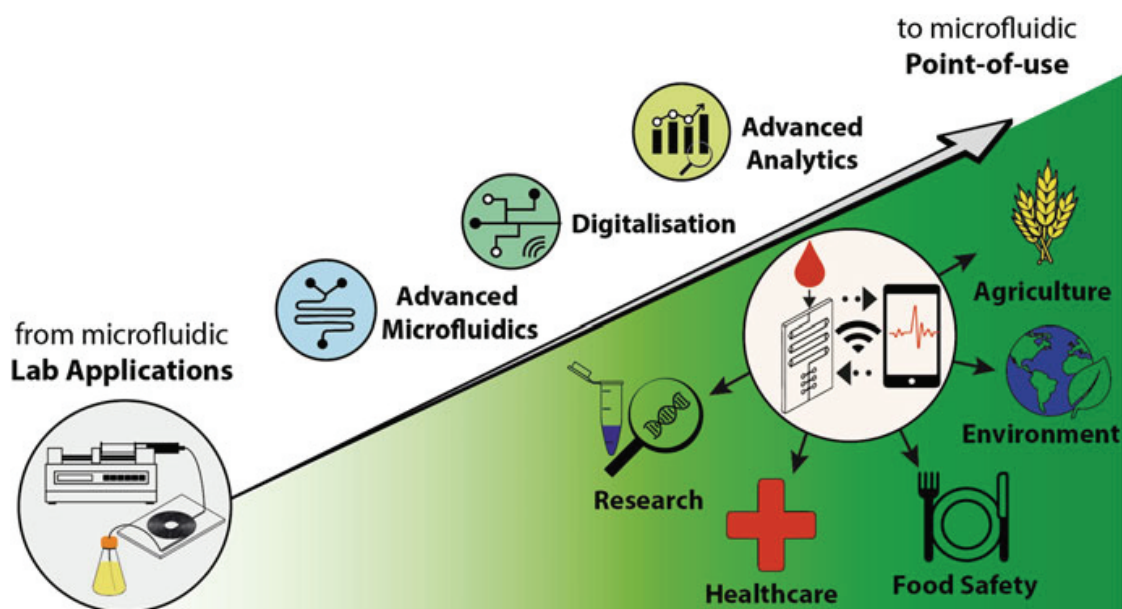
Fig. 9 Microfluidic devices in biotechnology: From microfluidic lab applications to microfluidic point-of-use. Advances in microfluidics, analytics, and digitalization will accelerate the trend to advanced microfluidic devices – available at the point-of-use. These point-of-use systems will rapidly expand to large biotechnological application fields, such as research, healthcare, food safety, environment protection, and agriculture

capillary microfluidics) further these goals by increasing the level of automatization within the system. Another emerging technology that also exhibits great potential to automate actively controlled LOCs is digital microfluidics based on the concept of electrowetting. Electrowetting – originally developed for displays and lenses – uses electrodes that, when activated, increase hydrophilicity. Consequently, droplets of liquids can be freely controlled in two dimensions and mixed, incubated, or divided using digital commands [80]. These very basic operations in turn facilitate greater automatization of lab procedures. In addition, the electronic (i.e., digital) control of droplets also makes it easier to connect and control electrowetting-based LOCs with smartphones. Because LOCs always benefit from advances in liquid handling within the system, this technique is increasingly being leveraged within new microfluidic applications [80].

LOCs must also offer as many functionalities as possible to meet the complex demands of endless possible point-of-use applications – and the nascent field of nanofluidics offers even greater promise for further expansion of microfluidic functions [81, 82]. Due to substantial recent improvements in device fabrication, LOCs have now reached the nanometer and even sub-nanometer scale. This does not simply result in advantages such as the further increase in throughput; it also introduces both molecular and quantum effects, as well as special fluid phenomena not seen in macroscale systems [82]. These effects include (for example) faster flow of water in nanotubes and faster ion transport, both of which can be used for biological or biotechnological purposes. For example, nanochannels have already been designed to mimic the high water permeability and selectivity of aquaporins [83], and artificial carbon nanotube molecular transport systems have been designed that mimic the process seen in proteins transported across cell membranes [84].

5.2 Advanced Miniaturized Analytics

Aside from microfluidic technologies, implementable analytics are also essential for advancing to omnifarious point-of-use systems. Biosensors are currently the analytical tools of choice in this regard [44, 85]. They typically contain biological catalytic recognition elements (such as enzymes, antibodies, aptamers [86], peptides, cells, or molecularly imprinted polymers) and a transducer (which is typically electrochemical, optical, acoustic, or gravimetric in nature) [87, 88]. Transducer technology in particular has been rapidly advancing, to the point where nanoresonators, localized surface plasmon resonance (LSPR) [89], surface acoustic waves (SAW) [90], optical fibers [91], photonic crystals [92], and quartz crystal microbalances (QCM) [93] are now all being miniaturized into an on-chip format. But biosensors may not be the tool of choice in the future – emerging analytics such as microscopy-on-a-chip [94, 95], terahertz spectroscopy [96], and field asymmetric ion mobility spectrometry (FAIMS) all show tremendous promise on this front [97]. As soon as it comes to identification and quantification of analytes in complex samples, however, state-of-the-art analytics such as mass spectrometry, Raman-, NMR-, or IR-spectroscopy

remain indispensable. Although attempts have been made to miniaturize mass spectrometers [98], NMR- [99], IR- [100], and Raman spectrometers [99], miniaturized building components are often not commercially available yet. Nevertheless, the current trend to point-of-use applications may well create a market for such parts, which would thereby facilitate the future miniaturization of high-end analytics.

## 5.3 Digitalization: Machine Learning, Neuronal Networks, and Artificial Intelligence

The capacity for high-throughput analysis within microfluidic devices, in combination with advanced analytics, can quickly generate a veritable mass of data which can itself become very difficult to evaluate and visualize. This is particularly true when the raw data is tough to quantify as, for example, is the case for microscopic images of cells or complex sequence analysis. Machine learning, neuronal networks, and artificial intelligence have all been suggested as tools for efficiently combing through such data [101]. Possible microfluidic applications include cell classification [102], signal processing [103], DNA base calling for DNA sequencing [104], flow sculpting for microchannel design [105], and cell segmentation [106]. Moving forward, it will only become increasingly important to set up systems that facilitate the global sharing and evaluation of large data sets in real-time. For example, environmental pollution of the air might 1 day be tracked by smartphone compatible LOCs – which would then feed the data generated into cloud saving and deep learning tools that can be used to immediately identify possible causes, direct further measurements, and make useful predictions.

6 Integrated Point-of-Use Devices for Monitoring, Understanding, and Controlling Bioprocesses

Currently, the primary benefit of point-of-use devices is mostly seen in their portability, time efficiency, cost efficiency, and easy-to-use handling [107, 108]. But all of these abilities are really just basic requirements that will ultimately help to enable integrated point-of-use devices that facilitate unprecedented opportunities to constantly monitor important parameters and immediately react to alterations. Wherever there are processes which will benefit from creating such a real-time monitoring and feedback control loop, integrated point-of-use devices point the way towards an even more efficient and integrated future.

One prominent example of this phenomenon from the field of biotechnology is the bioreactor. Monitoring bioprocess parameters like pH, biomass, oxygen, glucose, and product concentration – and, in turn, controlling these parameters via a live feed – is the key to maximize product yields and purities [109]. While some basic
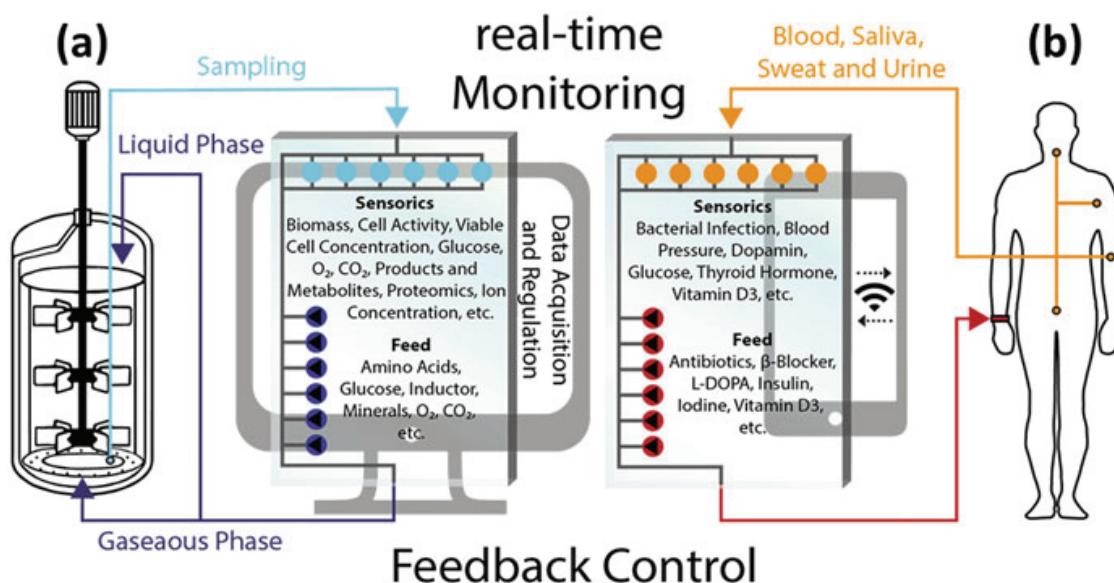
Fig. 10 The use of integrated point-of-use microfluidic devices for optimizing bioprocesses. The concept is illustrated using the example of a bioreactor (**a**) and a human being (**b**). These two bioprocesses can be monitored, analyzed, and controlled to improve either an industrial production or the state of health. Therefore, each LOC contains a sensor system, a connection to modern data analysis with computers or smartphones and an integrated feed. This results in a fully automatable control loop for permanent optimization, which in principle could be transferred to any bioprocess in all areas of life

parameters such as pH, temperature, and dissolved oxygen concentration are already being monitored on-line, various parameters still remain dependent on sampling for off-line detection. There is thus a clear need for novel on-line or at-line microfluidic, analytical, and data processing techniques that can be implemented within a single or multiple LOCs for multi-parameter monitoring. As illustrated in Fig. 10a, at-line LOCs could allow for the delivery and processing of samples and feedback-controlled feeding in a quasi on-line process with minimal dead volumes, dead time, and without unwanted influence on the process. Future advances in analytics will undoubtedly offer a wide variety of on-chip biosensors, spectrometers, microscopes, and other elements all aimed at measuring and calibrating an endless array of parameters with minimal time or sample requirements. In addition, LOCs could also exceed current feeding methods due to their ability to facilitate the precise mixing and distribution of a variety of independently controlled substances, enabling even the most complex feeding strategies for any kind of bioreactor. Finally, digitalization (including machine learning and neuronal networks) could foreseeably be used to interpret complex changes in bioprocess parameters and correlate them with a feedback control – effectively creating a full-automated bioreactor.

Similar to bioreactors, the objective of current POC devices is to understand, optimize, and control the human physiological (and in particular, pathological) processes. At present, most microfluidic POC devices obtain body fluids used for off-line analysis and subsequent therapy via drugs or other therapeutic strategies. But with miniaturized biosensors and micropumps, online monitoring and instantaneous

feedback-controlled drug therapy may foreseeably become available in the future. Exciting current examples of this young technology are implantable or on-skin glucose sensors in combination with insulin pumps [110, 111], dopamine monitoring [112], and online supplementation by infusion pumps [113]. Completely integrated point-of-use LOC devices for monitoring and feedback control could, in principle, be applied for nearly every biomarker in body fluids (Fig. 10b). This would create an invaluable tool in the fight against public health scourges like diabetes and hypertension – and it would also help physicians to recognize serious conditions (like lactate acidosis) as they are in the process of actively developing. To go even one step further, in the distant future, LOCs may 1 day become key tools in enhancing human physiology; for example, extracorporeal membrane oxygenation (ECMO) has already been intensively used to increase oxygenation in the blood of premature neonates [114] and COVID-19 patients [115]. And recently developed ECMO-on-a-chip systems [116, 117] may not only replace current ECMO devices – they could even be applied to increase athletic performance. Novel cancer treatment approaches are already exploring LOCs for on-chip immunotherapy [118]. Immunotherapy-on-a-chip could theoretically extract, sort, genetically modify, and return immune cells to the blood in a faster, less toxic, and more reproducible manner. Genetic modifications may also increase the effectiveness of immune cells against tumor cells [119] – and, in principle, other cells and other cell properties could also be modified, as well. In short, within our lifetimes LOCs may well become a valuable tool not only to develop a whole host of novel disease treatments, but also to optimize what even a healthy human being is capable of doing.

7 Concluding Remarks

Spearheaded by LOCs, microfluidics technology is an increasingly important tool across the field of biotechnology. Many successful proof-of-concept studies have already demonstrated the high potential for its application, and enterprising companies have already started to further realize this potential by introducing commercially available LOCs for routine applications (with a predominant focus, to date, on POC, screening, single-cell analytics, and novel organ-on-a-chip devices). Like with any emerging technology, significant challenges still block the path to full realization – including laborious and costly fabrication, inconvenient handling, and unsatisfactory standardization. Fast and easy fabrication by novel multimaterial 3D-printing, higher robustness via passively actuated chips as well as modularity, and the adoption of a unified and common biomicrofluidic language represent promising – but, as yet, not-fully-realized – solutions to these challenges. When these problems have been addressed and this technology is further buttressed via advanced microfluidic handling, advanced analytics, and digitalization, the practical applications promised by fully-mature microfluidic systems are nearly limitless: for example, the overwhelming number of analytical instruments currently used for monitoring and controlling processes could be simplified into a single, fully integrated point-of-use LOC. These

new opportunities will undoubtedly raise a whole host of thorny ethical considerations, up to and including the question of whether these new advances actually make our lives easier and better or instead threaten to fundamentally alter our very physical existence. In closing, such is the promise of this exciting field that it may not ultimately be a question of what we can do with microfluidics – but rather, what we *want* to do with it.

References

1. Scheler O, Postek W, Garstecki P (2019) Recent developments of microfluidics as a tool for biotechnology and microbiology. Curr Opin Biotechnol 55:60–67. https://doi.org/10.1016/j.copbio.2018.08.004
2. Bai Y, Gao M, Wen L et al (2018) Applications of microfluidics in quantitative biology. Biotechnol J 13:e1700170. https://doi.org/10.1002/biot.201700170
3. Arshavsky-Graham S, Segal E (2020) Lab-on-a-chip devices for point-of-care medical diagnostics. Adv Biochem Eng Biotechnol. https://doi.org/10.1007/10_2020_127
4. Maschmeyer I, Kakava S (2020) Organ-on-a-chip. Springer, Berlin, pp 1–32
5. Khan ZA, Siddiqui MF, Park S (2019) Progress in antibiotic susceptibility tests: a comparative review with special emphasis on microfluidic methods. Biotechnol Lett 41:221–230. https://doi.org/10.1007/s10529-018-02638-2
6. Frey LJ, Krull R (2020) Microbioreactors for process development and cell-based screening studies. Springer, Berlin
7. Dusny C, Grünberger A (2020) Microfluidic single-cell analysis in biotechnology: from monitoring towards understanding. Curr Opin Biotechnol 63:26–33. https://doi.org/10.1016/j.copbio.2019.11.001
8. Matuła K, Rivello F, Huck WTS (2020) Single-cell analysis using droplet microfluidics. Adv Biosyst 4:1900188. https://doi.org/10.1002/adbi.201900188
9. Payne EM, Holland-Moritz DA, Sun S et al (2020) High-throughput screening by droplet microfluidics: perspective into key challenges and future prospects. Lab Chip 20:2247–2262. https://doi.org/10.1039/D0LC00347F
10. Fluidicmems (2020) Microfluidic companies | fluidicmems. https://www.fluidicmems.org/microfluidic-companies. Accessed 5 Dec 2020
11. Google My Maps (2020) FluidicMEMS.com's list of microfluidics/lab-on-a-chip companies – Google My Maps. https://www.google.com/maps/d/u/0/viewer?ie=UTF8&hl=en&msa=0&z=2&mid=1e7udQl9Wyzaq4RVk48vWv8P59GM&ll=16.911338356870246%2C-6.3215279999999865. Accessed 5 Dec 2020
12. The MicroFluidic Circle (2020) Emerging microfluidic companies – the microfluidic circle. https://www.ufluidix.com/circle/microfluidic-companies/. Accessed 6 Dec 2020
13. Swerdlow H, Gesteland R (1990) Capillary gel electrophoresis for rapid, high resolution DNA sequencing. Nucleic Acids Res 18:1415–1419. https://doi.org/10.1093/nar/18.6.1415
14. Northrup MA, Gonzalez C, Hadley D et al (1995) A mems-based miniature DNA analysis system. In: Proceedings of the international solid-state sensors and actuators conference – TRANSDUCERS'95. IEEE, pp 764–767
15. Bahnemann J, Grünberger A (2021) Biotechnologie ganz klein. Zukunftsforum Biotechnologie (Hrsg.), DECHEMA e.V., Frankfurt. [ISBN] 978-3-89746-232-8

16. Quan P-L, Sauzade M, Brouzes E (2018) dPCR: a technology review. Sensors 18:1271. https://doi.org/10.3390/s18041271

17. Samiei E, Tabrizian M, Hoorfar M (2016) A review of digital microfluidics as portable platforms for lab-on a-chip applications. Lab Chip 16:2376–2396. https://doi.org/10.1039/c6lc00387g

18. Samandari M, Julia MG, Rice A et al (2018) Liquid biopsies for management of pancreatic cancer. Transl Res 201:98–127. https://doi.org/10.1016/j.trsl.2018.07.008

19. Cheng Z, Wu X, Cheng J et al (2017) Microfluidic fluorescence-activated cell sorting (μFACS) chip with integrated piezoelectric actuators for low-cost mammalian cell enrichment. Microfluid Nanofluid 21:9. https://doi.org/10.1007/s10404-017-1847-1

20. Manak MS, Varsanik JS, Hogan BJ et al (2018) Live-cell phenotypic-biomarker microfluidic assay for the risk stratification of cancer patients via machine learning. Nat Biomed Eng 2:761–772. https://doi.org/10.1038/s41551-018-0285-z

21. Nimir M, Ma Y, Jeffreys SA et al (2019) Detection of AR-V7 in liquid biopsies of castrate resistant prostate cancer patients: a comparison of AR-V7 analysis in circulating tumor cells, circulating tumor RNA and exosomes. Cell 8:688. https://doi.org/10.3390/cells8070688

22. Mahler L, Du G, Dajkovic A et al (2020) Rethinking culture-based microbiology – deep insights into any microbiota. Biomillenia, Romainville

23. Josephides D, Davoli S, Whitley W et al (2020) Cyto-mine: an integrated, picodroplet system for high-throughput single-cell analysis, sorting, dispensing, and monoclonality assurance. SLAS Technol 25:177–189. https://doi.org/10.1177/2472630319892571

24. Hengoju S, Tovar M, Man DKW et al (2020) Droplet microfluidics for microbial biotechnology. Adv Biochem Eng Biotechnol. https://doi.org/10.1007/10_2020_140

25. Mirasol F (2020) Shaping IR spectroscopy into a powerful tool for biopharma characterizations. BioPharm Int 33:42–47

26. Vaclavek T, Prikryl J, Foret F (2019) Resistive pulse sensing as particle counting and sizing method in microfluidic systems: designs and applications review. J Sep Sci 42:445–457. https://doi.org/10.1002/jssc.201800978

27. Globus T, Ferrance J, Moskaluk C et al (2018) Sub-terahertz spectroscopic signatures from micro-rna molecules in fluid samples for ovarian cancer analysis. Case Rep Liter Rev 2(2):1–3

28. Tsai A (2019) Ultra-sensitive chemical and nanoparticle sensing with optical microcavities. Periodic 7:16. http://www.chem.ox.ac.uk/periodic2019/

29. Zhang B, Radisic M (2017) Organ-on-a-chip devices advance to market. Lab Chip 17:2395–2420. https://doi.org/10.1039/c6lc01554a

30. Bahnemann J, Enders A, Winkler S (2021) Microfluidic systems and organ (human) on a chip. In: Basic concepts on 3D cell culture. Springer, Heidelberg. ISBN: 978-3-030-611 66749-8. https://doi.org/10.1007/978-3-030-66749-8

31. Chiu DT, deMello AJ, Di Carlo D et al (2017) Small but perfectly formed? Successes, challenges, and opportunities for microfluidics in the chemical and biological sciences. Chem 2:201–223. https://doi.org/10.1016/j.chempr.2017.01.009

32. Dekker S, Isgor PK, Feijten T et al (2018) From chip-in-a-lab to lab-on-a-chip: a portable Coulter counter using a modular platform. Microsyst Nanoeng 4:34. https://doi.org/10.1038/s41378-018-0034-1

33. Andersson H, van den Berg A (2006) Where are the biologists? Lab Chip 6:467–470. https://doi.org/10.1039/b602048h

34. Kandelousi MS (2018) Microfluidics and nanofluidics. InTech, London

35. Nguyen H-T, Thach H, Roy E et al (2018) Low-cost, accessible fabrication methods for microfluidics research in low-resource settings. Micromachines 9:461. https://doi.org/10.3390/mi9090461

36. Kotz F, Helmer D, Rapp BE (2020) Emerging technologies and materials for high-resolution 3D printing of microfluidic chips. Adv Biochem Eng Biotechnol. https://doi.org/10.1007/10_2020_141

37. Rupal BS, Garcia EA, Ayranci C et al (2019) 3D printed 3D-microfluidics: recent developments and design challenges. JID 22:5–20. https://doi.org/10.3233/jid-2018-0001

38. Preuss J-A, Nguyen GN, Berk V et al (2020) Miniaturized free-flow electrophoresis – production, optimization and application using 3D printing technology. Electrophoresis. https://doi.org/10.1002/elps.202000149

39. Enders A, Siller IG, Urmann K et al (2019) 3D printed microfluidic mixers-a comparative study on mixing unit performances. Small 15:e1804326. https://doi.org/10.1002/smll.201804326

40. Siller IG, Preuss J-A, Urmann K et al (2020) 3D-printed flow cells for aptamer-based impedimetric detection of *E. coli* crooks strain. Sensors 20:4421. https://doi.org/10.3390/s20164421

41. Lavrentieva A, Fleischhammer T, Enders A et al (2020) Fabrication of stiffness gradients of GelMA hydrogels using a 3D printed micromixer. Macromol Biosci 20:e2000107. https://doi.org/10.1002/mabi.202000107

42. Siller IG, Enders A, Gellermann P et al (2020) Characterization of a customized 3D-printed cell culture system using clear, translucent acrylate that enables optical online monitoring. Biomed Mater 15:55007. https://doi.org/10.1088/1748-605X/ab8e97

43. Siller IG, Epping N-M, Lavrentieva A et al (2020) Customizable 3D-printed (co-)cultivation systems for in vitro study of angiogenesis. Materials 13:4290. https://doi.org/10.3390/ma13194290

44. Siller IG, Enders A, Steinwedel T et al (2019) Real-time live-cell imaging technology enables high-throughput screening to verify in vitro biocompatibility of 3D printed materials. Materials 12:2125. https://doi.org/10.3390/ma12132125

45. Li F, Macdonald NP, Guijt RM et al (2018) Increasing the functionalities of 3D printed microchemical devices by single material, multimaterial, and print-pause-print 3D printing. Lab Chip 19:35–49. https://doi.org/10.1039/c8lc00826d

46. MacDonald E, Wicker R (2016) Multiprocess 3D printing for increasing component functionality. Science 353:aaf2093. https://doi.org/10.1126/science.aaf2093

47. Begolo S, Zhukov DV, Selck DA et al (2014) The pumping lid: investigating multi-material 3D printing for equipment-free, programmable generation of positive and negative pressures for microfluidic applications. Lab Chip 14:4616–4628. https://doi.org/10.1039/c4lc00910j

48. Li F, Smejkal P, Macdonald NP et al (2017) One-step fabrication of a microfluidic device with an integrated membrane and embedded reagents by multimaterial 3D printing. Anal Chem 89:4701–4707. https://doi.org/10.1021/acs.analchem.7b00409

49. O'Neil GD, Ahmed S, Halloran K et al (2019) Single-step fabrication of electrochemical flow cells utilizing multi-material 3D printing. Electrochem Commun 99:56–60. https://doi.org/10.1016/j.elecom.2018.12.006

50. Duarte LC, Chagas CLS, Ribeiro LEB et al (2017) 3D printing of microfluidic devices with embedded sensing electrodes for generating and measuring the size of microdroplets based on contactless conductivity detection. Sensors Actuators B Chem 251:427–432. https://doi.org/10.1016/j.snb.2017.05.011

51. Fornells E, Murray E, Waheed S et al (2020) Integrated 3D printed heaters for microfluidic applications: ammonium analysis within environmental water. Anal Chim Acta 1098:94–101. https://doi.org/10.1016/j.aca.2019.11.025

52. Scotti G, Nilsson SME, Haapala M et al (2017) A miniaturised 3D printed polypropylene reactor for online reaction analysis by mass spectrometry. React Chem Eng 2:299–303. https://doi.org/10.1039/C7RE00015D

53. Yuan R, Lee J, Su H-W et al (2018) Microfluidics in structured multimaterial fibers. Proc Natl Acad Sci U S A 115:E10830–E10838. https://doi.org/10.1073/pnas.1809459115

54. Sanchez D, Nordin G, Munro T (2020) Microfluidic temperature behavior in a multi-material 3D printed chip. American Society of Mechanical Engineers Digital Collection, New York

55. Kitson PJ, Rosnes MH, Sans V et al (2012) Configurable 3D-printed millifluidic and microfluidic 'lab on a chip' reactionware devices. Lab Chip 12:3267–3271. https://doi.org/10.1039/c2lc40761b

56. Kaminski TS, Scheler O, Garstecki P (2016) Droplet microfluidics for microbiology: techniques, applications and challenges. Lab Chip 16:2168–2187. https://doi.org/10.1039/c6lc00367b

57. Narayanamurthy V, Jeroish ZE, Bhuvaneshwari KS et al (2020) Advances in passively driven microfluidics and lab-on-chip devices: a comprehensive literature review and patent analysis. RSC Adv 10:11652–11680. https://doi.org/10.1039/D0RA00263A

58. Carrell C, Kava A, Nguyen M et al (2019) Beyond the lateral flow assay: a review of paper-based microfluidics. Microelectron Eng 206:45–54. https://doi.org/10.1016/j.mee.2018.12.002

59. Case DJ, Liu Y, Kiss IZ et al (2019) Braess's paradox and programmable behaviour in microfluidic networks. Nature 574:647–652. https://doi.org/10.1038/s41586-019-1701-6

60. Zaidon N, Nordin AN, Ismail AF (2015) Modelling of microfluidics network using electric circuits. In: 2015 IEEE regional symposium on micro and nanoelectronics (RSM). IEEE, pp 1–4

61. Duncan PN, Nguyen TV, Hui EE (2013) Pneumatic oscillator circuits for timing and control of integrated microfluidics. Proc Natl Acad Sci U S A 110:18104–18109. https://doi.org/10.1073/pnas.1310254110

62. Lee Y-S, Bhattacharjee N, Folch A (2018) 3D-printed quake-style microvalves and micropumps. Lab Chip 18:1207–1214. https://doi.org/10.1039/C8LC00001H

63. Ortseifen V, Viefhues M, Wobbe L et al (2020) Microfluidics for biotechnology: bridging gaps to foster microfluidic applications. Front Bioeng Biotechnol 8:1324. https://doi.org/10.3389/fbioe.2020.589074

64. Mohammed MI, Haswell S, Gibson I (2015) Lab-on-a-chip or chip-in-a-lab: challenges of commercialization lost in translation. Proc Technol 20:54–59. https://doi.org/10.1016/j.protcy.2015.07.010

65. Arnold FH (2018) Directed evolution: bringing new chemistry to life. Angew Chem Int Ed Engl 57:4143–4148. https://doi.org/10.1002/anie.201708408

66. Ma F, Chung MT, Yao Y et al (2018) Efficient molecular evolution to generate enantioselective enzymes using a dual-channel microfluidic droplet screening platform. Nat Commun 9:1030. https://doi.org/10.1038/s41467-018-03492-6

67. Waddington SN, Privolizzi R, Karda R et al (2016) A broad overview and review of CRISPR-cas technology and stem cells. Curr Stem Cell Rep 2:9–20. https://doi.org/10.1007/s40778-016-0037-5

68. McNutt M (2015) Breakthrough to genome editing. Science 350:1445. https://doi.org/10.1126/science.aae0479

69. Ahmadi F, Quach ABV, Shih SCC (2020) Is microfluidics the "assembly line" for CRISPR-Cas9 gene-editing? Biomicrofluidics 14:61301. https://doi.org/10.1063/5.0029846

70. Hajian R, Balderston S, Tran T et al (2019) Detection of unamplified target genes via CRISPR-Cas9 immobilized on a graphene field-effect transistor. Nat Biomed Eng 3:427–437. https://doi.org/10.1038/s41551-019-0371-x

71. Sinha H, Quach ABV, Vo PQN et al (2018) An automated microfluidic gene-editing platform for deciphering cancer genes. Lab Chip 18:2300–2312. https://doi.org/10.1039/c8lc00470f

72. Mondal S, Ben-Yakar A (2020) *Caenorhabditis elegans*-on-a-chip: microfluidic platforms for high-resolution imaging and phenotyping. In: Organ-on-a-chip. Elsevier, Amsterdam, pp 363–390

73. Kolluri N, Klapperich CM, Cabodi M (2017) Towards lab-on-a-chip diagnostics for malaria elimination. Lab Chip 18:75–94. https://doi.org/10.1039/c7lc00758b

74. Yang F, Gao C, Wang P et al (2016) Fish-on-a-chip: microfluidics for zebrafish research. Lab Chip 16:1106–1125. https://doi.org/10.1039/c6lc00044d

75. Jiang H, Xu Z, Aluru MR et al (2014) Plant chip for high-throughput phenotyping of Arabidopsis. Lab Chip 14:1281–1293. https://doi.org/10.1039/c3lc51326b
76. Grossmann G, Guo W-J, Ehrhardt DW et al (2011) The RootChip: an integrated microfluidic chip for plant science. Plant Cell 23:4234–4240. https://doi.org/10.1105/tpc.111.092577
77. Shapiro OH, Kramarsky-Winter E, Gavish AR et al (2016) A coral-on-a-chip microfluidic platform enabling live-imaging microscopy of reef-building corals. Nat Commun 7:10860. https://doi.org/10.1038/ncomms10860
78. Stanley CE, Grossmann G, i Solvas XC et al (2016) Soil-on-a-Chip: microfluidic platforms for environmental organismal studies. Lab Chip 16:228–241. https://doi.org/10.1039/c5lc01285f
79. Täuber S, Golze C, Ho P et al (2020) dMSCC: a microfluidic platform for microbial single-cell cultivation of Corynebacterium glutamicum under dynamic environmental medium conditions. Lab Chip 20:4442–4455. https://doi.org/10.1039/d0lc00711k
80. Wang H, Chen L, Sun L (2017) Digital microfluidics: a promising technique for biochemical applications. Front Mech Eng 12:510–525. https://doi.org/10.1007/s11465-017-0460-z
81. Edel JB, Ivanov A, Kim M (eds) (2017) Nanofluidics: nanoscience and nanotechnology. In: RSC nanoscience & nanotechnology, vol 41, 2nd edn. Royal Society of Chemistry, Cambridge
82. Bocquet L (2020) Nanofluidics coming of age. Nat Mater 19:254–256. https://doi.org/10.1038/s41563-020-0625-8
83. Barboiu M (2016) Artificial water channels--incipient innovative developments. Chem Commun 52:5657–5665. https://doi.org/10.1039/c6cc01724j
84. Ghasemi A, Amiri H, Zare H et al (2017) Carbon nanotubes in microfluidic lab-on-a-chip technology: current trends and future perspectives. Microfluid Nanofluidics 21:151. https://doi.org/10.1007/s10404-017-1989-1
85. Serra PA (2011) New perspectives in biosensors technology and applications. InTech, London
86. Prante M, Segal E, Scheper T et al (2020) Aptasensors for point-of-care detection of small molecules. Biosensors 10:108. https://doi.org/10.3390/bios10090108
87. Bhalla N, Jolly P, Formisano N et al (2016) Introduction to biosensors. Essays Biochem 60:1–8. https://doi.org/10.1042/EBC20150001
88. Preuß J-A, Reich P, Bahner N et al (2020) Impedimetric aptamer-based biosensors: applications. Adv Biochem Eng Biotechnol 174:43–91. https://doi.org/10.1007/10_2020_125
89. Aćimović SS, Šípová H, Emilsson G et al (2017) Superior LSPR substrates based on electromagnetic decoupling for on-a-chip high-throughput label-free biosensing. Light Sci Appl 6:e17042. https://doi.org/10.1038/lsa.2017.42
90. Liu B, Chen X, Cai H et al (2016) Surface acoustic wave devices for sensor applications. J Semicond 37:21001. https://doi.org/10.1088/1674-4926/37/2/021001
91. Zhao Y, Tong R-J, Xia F et al (2019) Current status of optical fiber biosensor based on surface plasmon resonance. Biosens Bioelectron 142:111505. https://doi.org/10.1016/j.bios.2019.111505
92. Inan H, Poyraz M, Inci F et al (2017) Photonic crystals: emerging biosensors and their promise for point-of-care applications. Chem Soc Rev 46:366–388. https://doi.org/10.1039/c6cs00206d
93. Montagut Y, Garcia J, Jimenez Y et al (2011) QCM technology in biosensors. In: Serra PA (ed) Biosensors – emerging materials and applications. InTech, London
94. Paiè P, Bragheri F, Bassi A et al (2016) Selective plane illumination microscopy on a chip. Lab Chip 16:1556–1560. https://doi.org/10.1039/c6lc00084c
95. Pirnstill CW, Coté GL (2015) Malaria diagnosis using a mobile phone polarized microscope. Sci Rep 5:13368. https://doi.org/10.1038/srep13368
96. Tang Q, Liang M, Lu Y et al (2016) Microfluidic devices for terahertz spectroscopy of live cells toward lab-on-a-chip applications. Sensors 16:476. https://doi.org/10.3390/s16040476
97. Costanzo MT, Boock JJ, Kemperman RHJ et al (2017) Portable FAIMS: applications and future perspectives. Int J Mass Spectrom 422:188–196. https://doi.org/10.1016/j.ijms.2016.12.007

98. Zhai Y, Feng Y, Wei Y et al (2015) Development of a miniature mass spectrometer with continuous atmospheric pressure interface. Analyst 140:3406–3414. https://doi.org/10.1039/c5an00462d

99. Zalesskiy SS, Danieli E, Blümich B et al (2014) Miniaturization of NMR systems: desktop spectrometers, microcoil spectroscopy, and "NMR on a chip" for chemistry, biochemistry, and industry. Chem Rev 114:5641–5694. https://doi.org/10.1021/cr400063g

100. Bomers M, Charlot B, Barho F et al (2020) Microfluidic surface-enhanced infrared spectroscopy with semiconductor plasmonics for the fingerprint region. React Chem Eng 5:124–135. https://doi.org/10.1039/C9RE00350A

101. Riordon J, Sovilj D, Sanner S et al (2019) Deep learning with microfluidics for biotechnology. Trends Biotechnol 37:310–324. https://doi.org/10.1016/j.tibtech.2018.08.005

102. Heo YJ, Lee D, Kang J et al (2017) Real-time image processing for microscopy-based label-free imaging flow cytometry in a microfluidic chip. Sci Rep 7:11651. https://doi.org/10.1038/s41598-017-11534-0

103. Han S, Kim T, Kim D et al (2018) Use of deep learning for characterization of microfluidic soft sensors. IEEE Robot Autom Lett 3:873–880. https://doi.org/10.1109/LRA.2018.2792684

104. Boža V, Brejová B, Vinař T (2017) DeepNano: deep recurrent neural networks for base calling in MinION nanopore reads. PLoS One 12:e0178751. https://doi.org/10.1371/journal.pone.0178751

105. Stoecklein D, Lore KG, Davies M et al (2017) Deep learning for flow sculpting: insights into efficient learning using scientific simulation data. Sci Rep 7:46368. https://doi.org/10.1038/srep46368

106. Zaimi A, Wabartha M, Herman V et al (2018) AxonDeepSeg: automatic axon and myelin segmentation from microscopy data using convolutional neural networks. Sci Rep 8:3816. https://doi.org/10.1038/s41598-018-22181-4

107. Vashist SK, Luong JHT (2019) An overview of point-of-care technologies enabling next-generation healthcare monitoring and management. In: Vashist SK, Luong JHT (eds) Point-of-care technologies enabling next-generation healthcare monitoring and management. Springer, Cham, pp 1–25

108. Vashist SK, Luong JHT (eds) (2019) Point-of-care technologies enabling next-generation healthcare monitoring and management. Springer, Cham

109. Stanke M, Hitzmann B (2013) Automatic control of bioprocesses. Adv Biochem Eng Biotechnol 132:35–63. https://doi.org/10.1007/10_2012_167

110. Vettoretti M, Facchinetti A (2019) Combining continuous glucose monitoring and insulin pumps to automatically tune the basal insulin infusion in diabetes therapy: a review. Biomed Eng Online 18:1–17. https://doi.org/10.1186/s12938-019-0658-x

111. Kim J, Campbell AS, Wang J (2018) Wearable non-invasive epidermal glucose sensors: a review. Talanta 177:163–170. https://doi.org/10.1016/j.talanta.2017.08.077

112. Godinho C, Domingos J, Cunha G et al (2016) A systematic review of the characteristics and validity of monitoring technologies to assess Parkinson's disease. J Neuroeng Rehabil 13:24. https://doi.org/10.1186/s12984-016-0136-7

113. Kim HJ, Jeon BS, Jenner P (2017) Hallmarks of treatment aspects: Parkinson's disease throughout centuries including l-dopa. Int Rev Neurobiol 132:295–343. https://doi.org/10.1016/bs.irn.2017.01.006

114. Fletcher K, Chapman R, Keene S (2018) An overview of medical ECMO for neonates. Semin Perinatol 42:68–79. https://doi.org/10.1053/j.semperi.2017.12.002

115. Bartlett RH, Ogino MT, Brodie D et al (2020) Initial ELSO guidance document: ECMO for COVID-19 patients with severe cardiopulmonary failure. ASAIO J 66:472–474. https://doi.org/10.1097/MAT.0000000000001173

116. Dabaghi M, Saraei N, Fusch G et al (2018) An ultra-thin highly flexible microfluidic device for blood oxygenation. Lab Chip 18:3780–3789. https://doi.org/10.1039/c8lc01083h
117. Gimbel AA, Flores E, Koo A et al (2016) Development of a biomimetic microfluidic oxygen transfer device. Lab Chip 16:3227–3234. https://doi.org/10.1039/c6lc00641h
118. Lagae L (2018) Boosting cell therapy production. Genet Eng Biotechnol News 38:20. https://doi.org/10.1089/gen.38.09.08
119. Li D, Li X, Zhou W-L et al (2019) Genetically engineered T cells for cancer immunotherapy. Signal Transduct Target Ther 4:35. https://doi.org/10.1038/s41392-019-0070-9

## 3.1.2 Additive Fertigung mikrofluidischer Systeme

Die additive Fertigung (3D-Druck) mikrofluidischer Systeme gewinnt zunehmend an Popularität und bietet insbesondere Biowissenschaftler:innen einen kostengünstigen Zugang zur Mikrofluidik. Zurecht wird sie auch als „die kommende 3D-Druck-Revolution der Mikrofluidik" bezeichnet [7]. Dabei sind insbesondere folgende Vorteile zu nennen:

- Stark **reduzierte Entwicklungszeiten** der Systeme durch iteratives Anpassen des Designs (*Rapid Prototyping*) [22, 23],

- **Verzicht auf spezielle Infrastruktur,** wie Reinräume und Spezialgeräte zur Fertigung von mikrostrukturierten Gussformen [23–25],

- **kostengünstiger** [7, 26],

- **erleichterter Zugang und Anwendung** für Wissenschaftler:innen ohne technischen Hintergrund [7, 26, 27],

- **zusätzliche Freiheitsgrade** im Design,

- leichtere **Integration externer Komponenten,** wie Konnektoren [28, 29], Sensoren [30], Membranen [31] etc.,

- **größere Materialvielfalt** mit transparenten [32–34], hitzebeständigen [32, 35], flexiblen [34, 36] und/oder biokompatiblen [37] Eigenschaften.

Durch das Auslaufen vieler Patente im letzten Jahrzehnt ist mittlerweile eine hohe Vielfalt an 3D-Druckern und Materialien kommerziell erhältlich [38, 39]. Die Drucker basieren auf ähnlichen Prinzipien, die sich zu übergreifenden 3D-Druckverfahren zusammenfassen lassen (s. **Abbildung 1**). Beim viel verwendeten *fused deposition modelling* (FDM, dt.: Schmelzschichtung) wird das Modell durch das schichtweise Aufschmelzen eines i.d.R. aus Polymer bestehenden Filaments erzeugt [40]. Dieses Druckprinzip ist besonders kostengünstig und benötigt kaum anschließende Bearbeitungsschritte. Oft weniger beachtet wird, dass sich die chemische Zusammensetzung des Baumaterials während des Druckprozesses kaum oder gar nicht verändert. Im Gegensatz dazu benötigen photopolymerisierende Druckprinzipien die nachträgliche Entfernung des nicht polymerisierten, potentiell toxischen Baumaterials, sodass die Chancen für eine Biokompatibilität des 3D-gedruckten Materials schlechter stehen. Allerdings ist der FDM-Druck eher ungeeignet für die Herstellung mikrofluidischer Systeme. Dies liegt einerseits an der weniger präzisen Fertigung kleiner Kanalstrukturen [41] und andererseits daran, dass eine vollständige Versiegelung zwischen den Schichten nicht immer gegeben ist und bei dünnen Strukturen Undichtigkeiten wahrscheinlich sind [42]. Ein vermehrt für die Herstellung mikrofluidischer Systeme angewendetes Druckverfahren ist der Stereolithographie-Druck (SLA). Hier wird Laserlicht über einen beweglichen Spiegel gezielt auf ein flüssiges Baumaterial proji-

ziert [43]. Sobald alle zu polymerisierenden Stellen einer Schicht einmal belichtet wurden wird dieser Prozess für die nächste Schicht wiederholt. Die Verwendung von Licht ermöglicht eine deutlich bessere Druckauflösung, allerdings führt dies dazu, dass nicht-polymerisiertes Material nachträglich aufwendig entfernt werden muss. Zudem bewirkt ein Durchscheinen des Lichts die Polymerisation in tieferliegenden Schichten, was zu verschlossenen oder unscharfen Kanälen bei der Herstellung von Mikrosystemen führen kann. Im Vergleich zu anderen Drucktechniken ist die Oberfläche des Modells besser versiegelt und deutlich weniger rau [44], sodass i.d.R. eine höhere Transparenz für mikroskopische Anwendungen und eine bessere Dichtfähigkeit für mikrofluidische Anwendungen gegeben ist. Eine Weiterentwicklung des SLA-Drucks ist das *digital light processing* (DLP), bei dem das Laserlicht nicht durch einen einzigen Spiegel, sondern ein Spiegelarray auf die gesamte Materialschicht gleichzeitig projiziert wird [45]. Demzufolge zeigt der DLP-Druck eine deutlich höhere Druckgeschwindigkeit. Eine spezielle Kombination aus DLP- und SLA-Verfahren ist die *projection micro stereolithography* (PμSL, dt.: Projektionsmikro-Stereolithographie). Hierbei wird das durch den Mikrospiegelarray erzeugte Bild des DLP-Verfahrens durch einen weiteren Spiegel nur auf einen kleinen Bereich projiziert. Somit werden hier besonders hohe Auflösungen von bis zu 0,6 μm erreicht [46].
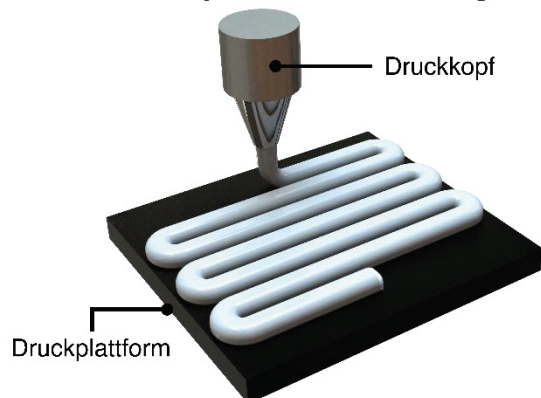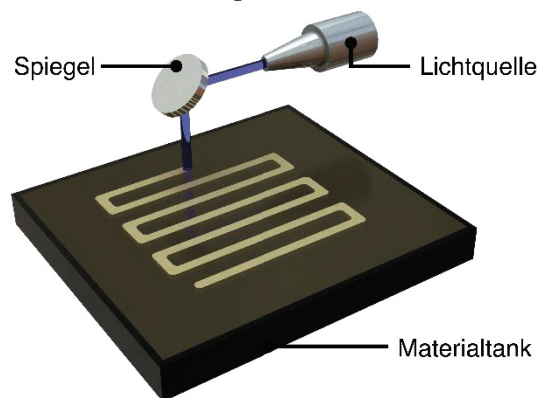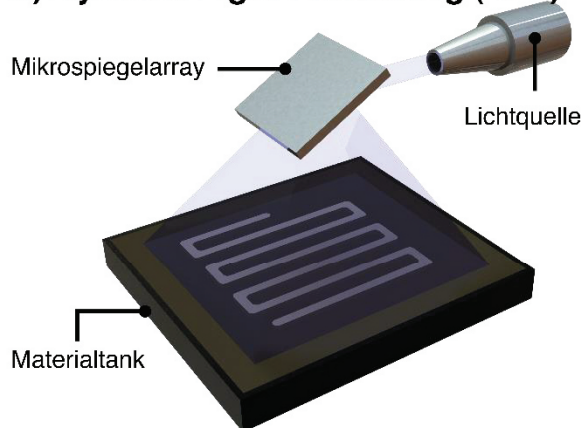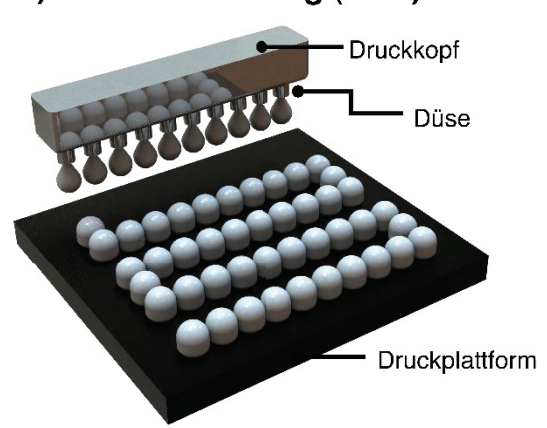
Abbildung 1: Schematische Darstellung verschiedener 3D-Druckverfahren. **A)** Beim *fused-deposition modelling* (FDM) Druck wird Druckfilament schichtweise auf der Druckplattform durch einen heizbaren Druckkopf aufgeschmolzen. **B)** Der Stereolithographie (SLA) Druck und das *digital light processing* (DLP) nutzen UV-Licht zur ge-

zielten Polymerisation eines flüssigen Baumaterials. **C)** Im Gegensatz zum SLA- wird beim DLP-Druck ein Mikrospiegelarray zur gleichzeitigen Belichtung der zu polymerisierenden Stellen einer Ebene genutzt. **D)** *Das multi-jet printing* (MJP) trägt gezielt feine Tröpfchen des Baumaterials auf der Druckplattform auf, welche anschließend durch UV-Licht verfestigt werden. (Eigene Darstellung erstellt mit SOLIDWORKS® 2022 und Adobe Illustrator 2019)

Das in dieser Arbeit verwendete Druckverfahren, das *multi-jet printing* (MJP, dt.: Mehrstrahldruck), ist ebenso wie das SLA/DLP Verfahren besonders geeignet für die additive Herstellung mikrofluidischer Bauteile. Hierbei wird das flüssige Material durch eine Vielzahl von Düsen schichtweise aufgesprüht und photopolymerisiert [47]. Besonders von Vorteil ist das zusätzliche Aufsprühen eines separaten Stützmaterials, welches die Designfreiheit erhöht und im Gegensatz zum SLA- oder DLP-Druck spezielle Strukturen, wie Überhänge oder auch komplett freie Strukturen, innerhalb eines Bauteils ermöglicht. Beispielsweise konnten so bereits miniaturisierte und integrierte Rückschlagventile gedruckt werden, welche eine frei bewegliche Kugel zur Dichtung nutzen [48]. Das Stützmaterial wird dabei durch nachgelagerte Aufreinigungsschritte entfernt. Je nach Stützmaterial und der Komplexität des Kanalsystems kann die vollständige Entfernung jedoch mit größeren Schwierigkeiten verbunden sein. Bei besonders komplexen Kanalsystemen können Hitze, Ultraschall oder auch separate, für das Spülen vorgesehene Kanaleingänge das Entfernen des Stützmaterials erleichtern. Ein weiterer großer Vorteil des MJP Drucks besteht in der Möglichkeit, verschiedene Modellmaterialien gleichzeitig drucken zu können, was durch manche Hersteller bereits realisiert wurde [49]. Dies ermöglicht prinzipiell die Integration von beispielsweise festen und flexiblen Materialien für die Integration von mechanischen Bauteilen oder Dichtungen während des Druckprozesses [25]. Ein Nachteil des MJP-Verfahrens besteht darin, dass die Verwendung von Düsen besondere Ansprüche an die Eigenschaften des Baumaterials, wie z.B. der Viskosität, stellt. Dies bedeutet, dass nicht jedes polymerisierbare Material verwendet werden kann, sondern zur Gewährleistung der Druckerfunktionalität die Auswahl i.d.R. auf das Angebot des Druckerherstellers begrenzt ist. Dies schafft wiederum eine größere Abhängigkeit.

Weitere jedoch weniger verwendete Drucktechniken sind das Selektive Lasersintern (SLS) und die Zweiphotonenpolymerisation (engl.: *two-photon polymerization*, 2PP). Das Selektive Lasersintern basiert auf einem ähnlichen Prinzip wie das SLA-Verfahren, wobei hier keine Polymerisation durch das Laserlicht hervorgerufen wird, sondern ein in Pulverform vorliegendes Material punktuell durch Schmelzen verfestigt wird [42]. Durch die Verwendung eines leistungsstarken Lasers können auch Metalle, Keramiken und Glas gesintert werden. Aufgrund der hohen chemischen Beständigkeit dieser Materialien werden mit dem SLS Verfahren hergestellte Systeme unter anderem in der Durchflusschemie eingesetzt [50]. Im Gegensatz zu photopolymerisierten Kunststoffen ist bei chemisch inerten Materialien wie Glas von einer deutlich höheren Biokompatibilität auszugehen. Somit zeigt auch das Lasersintern Potential für 3D-gedruckte Systeme in der Zellkultur. Mit Kanalabmessungen im Millimeter- bis oberen Mikrometerbereich ist die Auflösung des Lasersinterns zurzeit jedoch weniger für die Herstellung mikrofluidischer Systeme geeignet. Der 2PP-Druck nutzt ein Phänomen aus, bei dem ein Molekül zwei Photonen geringerer Wellenlänge fast gleichzeitig absorbiert und auf diese Weise die Elektronen des Photoinitiators angeregt werden. Diese Technologie

besitzt eine wesentlich bessere Auflösung, sodass Strukturen mit Abmessungen unterhalb der Abbeschen Beugungsgrenze – definiert als die halbe Wellenlänge des Anregungslichtes – gedruckt werden können [51, 52]. Aufgrund der nicht-linearen Abhängigkeit der Zweiphotonenanregung von der Intensität des eingestrahlten Lichts ist der Intensitätsgrenzwert, ab dem die Polymerisation ausgelöst wird, wesentlich schärfer [53]. Es werden folglich nur Bereiche ausgehärtet, die sich oberhalb der jeweiligen kritischen Anregungsintensität befinden. Zum Fokuspunkt direkt benachbarte Regionen nur leicht unterhalb der kritischen Intensität polymerisieren im Gegensatz zur Einphotonenabsorption nicht. Auch wenn der Zugang zu diesen Druckverfahren aufgrund der kostenintensiven Anschaffung schwierig ist, so sind hiermit Auflösungen im zweistelligen Nanometerbereich und 3D-gedruckte Nanostrukturen möglich [54]. Diese können beispielsweise zur Fertigung einer räumlichen Matrix für die Ausbildung von Mikrozellverbänden verwendet werden [55]. Außerdem werden wie beim MJP-Verfahren keine Stützstrukturen benötigt.

3.2 Anforderungen und Biokompatibilitätsbestimmung 3D-gedruckter Systeme zum Einsatz in der tierischen Zellkultur

Der 3D-Druck bietet insbesondere in der Forschung und Entwicklung einen hohen Grad an Designfreiheit und ermöglicht somit die unabhängige Fertigung von Zellkultursystemen und -werkzeugen auf Maß. Die Anwendung in der tierischen Zellkultur – adhärent als auch in Suspension – stellt jedoch besonders hohe Anforderungen an die spezifischen Materialeigenschaften. Dabei entscheiden verschiedene Faktoren über die potentiellen Anwendungen eines Materials. Möglichkeiten der Sterilisation durch beispielsweise Dampf oder Bestrahlung sind besonders bei Zelllinien, die ohne Antibiotikum kultiviert werden müssen, von hoher Wichtigkeit. Um die Systeme auch mikroskopieren zu können, sollten die Materialien eine gute Transparenz und geringe Autofluoreszenz aufweisen. Eine Kultivierung von Zellen direkt innerhalb der Systeme ist oft nur möglich, wenn eine Sauerstoff/Kohlenstoffdioxid Permeabilität sowie die Adhäsion von Zellen bzw. die Funktionalisierbarkeit für die Beschichtung (engl.: *coatings*) durch Proteine gegeben ist. Die Biokompatibilität des Materials gegenüber eines verwendeten Organismus als Grundvoraussetzung für die Verwendung in der Zellkultur ist jedoch das wichtigste Kriterium.

Biokompatibilität ist gegeben, wenn ein Material keinen, als signifikant betrachteten negativen Einfluss an einem gegebenen Organismus verursacht [56]. Fälschlicherweise wird die Biokompatibilität oftmals einzig und allein als intrinsische Eigenschaft eines Materials verstanden. Bei nicht-inerten Materialien – was für die meisten verwendeten Kunststoffen bei 3D-Druckverfahren der Fall ist – ist eine potentielle Toxizität des Materials jedoch von weiteren Bearbeitungsschritten des Materials, vom Organismus und den Testbedingungen des Biokompatibilitätstests abhängig (s. **Abbildung 2**).

3D-Druckmaterial

Baumaterial

- Materialtyp
- Materialzusätze
- Rückstände durch Produktion

Drucker

- Druckprinzip
- Verunreinigungen
- Druckbedingungen (Temperatur, Belichtung, etc.)

Nachbearbeitung

- Nachhärtung
- Extraktion
- Sterilisation

Organismus

- Spezies (z.B. Mensch, Maus)
- Form (z.B. ganze Tiere oder Zellen in Kultur)
- Kultivierungsbedingung (z.B. adhärent/Suspension, Art des Mediums)

Testbedingungen

- Sachgerechte Anwendung von Standards (ISO 10993, USP)
- Form der Exposition
- Expositionsdauer
- Art der Analyse

Biokompatibilität

Abbildung 2: Einflussfaktoren auf die Biokompatibilitätsbestimmung 3D-gedruckter Materialien. Die Eigenschaften des 3D-gedruckten Materials hängen nicht nur von der Art des Baumaterials, sondern auch vom Drucker und der Nachbearbeitung ab. Zudem nimmt die Wahl des Organismus als auch der Testbedingungen Einfluss auf das Biokompatibilitätsergebnis. (Eigene Darstellung erstellt mit Adobe Illustrator 2019)

Ursache für eine potentielle Toxizität sind oft sogenannte *leachables* (dt.: herlauslösbare Bestandteile), die sich aus dem Material herauslösen. Die Zusammensetzung der *leachables* ist abhängig vom Baumaterial, der Druckbedingungen wie Druckprinzip und Druckereinstellungen sowie von weiteren Nachbearbeitungsschritten wie beispielsweise der nachträglichen Entfernung nicht polymerisierten 3D-Druckmaterials. Die Art des Baumaterials hat dabei einen großen Einfluss. Insbesondere photopolymerisierende Materialien enthalten durchaus toxische Radikalstarter und Monomere, die nicht immer vollständig abreagieren und somit im 3D-gedruckten Bauteil verbleiben [57]. Die Einstellungen des Druckers wie beispielsweise Belichtungsintensität und –Zeit können wiederum das Druckergebnis und somit auch die Art oder Menge der *leachables* beeinflussen. Selbst bei nicht-photopolymerisierenden Druckprinzipien wie dem FDM Druck können zu hohe Temperaturen des Druckkopfes zu einer teilweisen Zersetzung des Materials führen und somit auch die Biokompatibilität unbedenklicherer Materialien wie Polylactid negativ beeinflussen [58]. Bei Druckverfahren mit Polymerisation wie SLA, DLP oder MJP spielt auch die Nachbearbeitung (engl.: *post-processing*) des Materials eine entscheidende Rolle, da sie maßgeblich die Menge an potentiell toxischen Stoffen wie Radikalstarter und Mono– bzw. Oligomere beeinflussen kann. So werden insbesondere Nachhärteverfahren durch Erhitzen und Bestrahlung mit UV-Licht [59, 60] und Extraktionen mit Lösungsmitteln (wie z.B. Ethanol oder Isopropanol [61, 62]) zur Verbesserung der Biokompatibilität verwendet. Allerdings können sich auch hier wiederum Rückstände von Lösungsmitteln und Detergenzien negativ auf

die Biokompatibilität auswirken. Auch die Sterilisation 3D-gedruckter Zellkultursysteme als eine Form der Nachbearbeitung kann die Biokompatibilität negativ oder positiv beeinflussen [63].

Auch wenn das 3D-gedruckte Material unter standardisierten Druckbedingungen und Aufarbeitungsschritten hergestellt wird, hängt die Biokompatibilität immer noch von dem verwendeten Organismus ab. Dabei spielt einerseits die Spezies (z.B. Mensch oder Maus) als auch die Form (*in vivo* oder *in vitro*) eine große Rolle. Bei unterschiedlichen Spezies, ergeben sich beispielsweise Unterschiede in der Zellmembran, der Signaltransduktion oder des Zellmetabolismus. Diese wirken sich auf die Aufnahme, den Wirkmechanismus und den Abbau und somit auch auf die potentielle Toxizität der *leachables* aus. Beispielsweise reagieren Bakterien und Hefen weniger empfindlich auf Toxine als tierische Zellen, da sie eine deutlich robustere Zellmembran bzw. Zellwand besitzen. Die Wirkstoffforschung der pharmazeutischen Industrie steht zudem vor dem Problem, dass sich auch Unterschiede zwischen Mensch und Tier bezüglich Toxizität und Wirkung eines Wirkstoffs ergeben. Somit können vielversprechende Wirkstoffkandidaten beim Übergang von präklinischen zu klinischen Phasen scheitern [64]. Diese Unterschiede sind folglich auch für *leachables* anzunehmen. Selbst bei gleicher Spezies eines Organismus ist die Biokompatibilität immer noch anhängig von der Form des Organismus. Werden Zellen in Kultur (*in vitro*) statt ganzer Tiere (*in vivo*) verwendet, so vereinfacht sich die komplexe Pharmakokinetik eines Toxins deutlich, und Aufnahme-, Distributions-, Metabolismus- oder Eliminationsprozesse (ADME) fehlen oder laufen nur in stark veränderter Form ab. Somit ist auch eine Biokompatibilität eines Materials, das *in vitro* getestet wurde, nicht direkt auf *in vivo* Modelle übertragbar und umgekehrt.

Um die Biokompatibilität von Werkstoffen näher zu definieren und somit eine Nutzung für den kommerziellen Vertrieb 3D-gedruckter Materialien in Medizin, Forschung und Industrie zu ermöglichen, werden verschiedene, standardisierte Biokompatibilitätstests verwendet. Hierbei ist insbesondere die Normreihe 10993 der Internationalen Organisation für Normung (engl.: International Standard Organization, ISO) zur Biokompatibilitätstestung von Medizinprodukten zu nennen. Die Abschnitte ISO 10993-5 zur Testung auf *in vitro* Zytotoxizität und ISO 10993-12 zur Probenvorbereitung spielen bei der Anwendung 3D-gedruckter Materialien in der Zellkultur eine wichtige Rolle [65, 66]. Hierbei werden zunächst Extraktionsmedien hergestellt, um potentielle Schadstoffe aus dem Material herauszulösen, und anschließend zur Kultivierung genutzt. Dabei werden beispielweise die in der ISO angegebenen adhärenten Zelltypen, wie die von Mausembryonen isolierten BALB/c 3T3 Zellen, V79 Zellen des Chinesischen Hamsters und L929 Mausfibroblasten, auf Veränderungen der Proliferation, Viabilität, Zellaktivität oder auch Morphologie untersucht. Die Analysemethoden zur qualitativen und quantitativen Bestimmung eines toxischen Effekts sind dabei nicht eindeutig geregelt. Einfach zugängliche und damit oft angewendete Verfahren sind i.d.R. biochemische Assays, wie der sogenannte *Cell-Titer-Blue* (CTB) Assay oder der 3-(4,5-Dimethylthiazol-2-yl)-2,5-diphenyltetrazoliumbromid (MTT) Assay [67, 68]. In beiden Assays erfolgt eine vorwiegend mitochondrielle Reduktion und die anschließende photometrische Detektion von Farbstoffen, sodass die Zellviabilität und das Zellwachstum indirekt über die mitochondrielle Aktivität quantifiziert werden können. Allerdings konnten

selbst bei diesen sehr ähnlichen Assays Unterschiede in der Zytotoxität von identischen Proben in Biokompatibilitätstests ausgemacht werden, sodass auch hier eine Feststellung einer Toxizität bzw. Biokompatibilität vom Testverfahren abhängt [69]. Weitere Verfahren sind die Mikroskopie, die insbesondere zur morphologischen Untersuchung eingesetzt werden kann. Auf diese Weise können Zellabrundungen oder DNA-Fragmentierungen als Phänotypen des Zelltods erkannt werden [70, 71]. Zusätzlich ermöglicht die Lebendzellmikroskopie (engl.: *live-cell-imaging*) die Quantifizierung der Zellviabilität und des Zellwachstums durch eine Algorithmen-gestützte Analyse der Konfluenz und Identifikation der durch Farbstoffe markierten toten und lebenden Zellen [72]. Der Nutzen der Lebendzellmikroskopie für die effektive Biokompatibilitätstestung 3D-gedruckter Materialien wurde bereits durch Siller *et al.* umfangreich dargestellt und bietet den entscheidenden Vorteil einer von der mitochondriellen Aktivität unabhängigen Analyse [73]. Ein weiteres wichtiges Verfahren ist die Fluoreszenz-aktivierte Zellsortierung (engl.: *Fluorescence-activated cell sorting*, FACS). Dieses wird angewendet, um insbesondere die Art des Zelltodes – Apoptose oder Nekrose – festzustellen [74, 75].

Neben der Testung nach ISO 10993 gibt es noch weitere wichtige Biokompatibilitätsstandards und Prüfrichtlinien, die zur Biokompatibilitätsbestimmung verwendet werden. Die Artikel 87 und 88 der von den USA herausgegebenen United States Pharmacopeia (USP) legen die Vorgaben für die *in vitro* und *in vivo* Biokompatibilitätsbestimmung fest [76, 77]. Dabei werden sechs USP-Biokompatibilitätsklassen für Kunststoffe beschrieben, bei denen Materialien mit der höchsten Biokompatibilität in die Stufe VI eingeordnet werden. Wie bei der ISO 10993 kann auch die USP Klassifizierung von Herstellern zur Lizensierung ihrer Materialien und Produkte verwendet werden. Auch die durch die Organisation für wirtschaftliche Zusammenarbeit und Entwicklung (OWZE) ausgegebene Prüfrichtlinie zur Testung akuter Toxizität in Zebrafisch-Embryonen wird zur Biokompatibilitätstestung von 3D-Druckmaterialien verwendet [78, 79]. Dabei können zusätzlich zur Zytotoxizität auch negative Auswirkungen auf empfindliche Prozesse wie der Embryogenese festgestellt werden.

3.3 Mikrofluidische Zellkultursysteme

Medizin, Medizintechnik und Pharmaforschung verfolgen ambitionierte Ziele, wie z.B. die Abschaffung von Versuchstieren in der Wirkstoffforschung [80, 81], die schnelle, personalisierte Medizin am Krankenbett [1, 82], die Heilung von Krankheiten wie Alzheimer durch Zelltherapien [83], bis hin zur Entwicklung künstlicher Organe [84]. Alle diese Ziele setzen ein tieferes Verständnis zellphysiologischer, zellpathogener und pharmakologischer Prozesse voraus, welche durch physiologisch relevantere und damit komplexere Zellkultursysteme umfangreicher erforscht werden können. Dabei spielt neben dem klassischen *Tissue Engineering* (dt.: Gewebetechnik) mit Spheroiden, Organoiden und Hydrogelen zunehmend die Mikrofluidik eine größere Rolle, indem sie die räumliche und chemische Mikrostrukturierung auf zellulärer bis subzellulärer Ebene ermöglicht. Vielversprechende Anwendungsbeispiele sind das Nachahmen von Stammzellnischen

durch Mikrokavitäten für die Erforschung von Leukämie [85], die Integration von Mikrokanälen zur Gestaltung Neuronaler Netze [86, 87] oder auch die Erzeugung von Sauerstoffgradienten zur Untersuchung von Hypoxie in Tumorzellen [88, 89].

Diese Verwendung mikrofluidischer Systeme als *in vitro* Zellkulturplattformen wird in dem nachfolgenden Übersichtsartikel „*Microfluidic Systems and Organ (Human) on a Chip*", veröffentlicht in dem Textbuch „*Basic Concepts on 3D Cell Culture*" der Buchserie „*Learning Materials in Biosciences*", behandelt. Hierbei liegt neben der allgemeinen Anwendung mikrofluidischer Systeme in der Zellkultur ein spezieller Fokus auf sogenannte *organ-on-a-chip* (OOC, dt.: Organ auf einem Chip) Systemen. OOCs stellen eine Kombination aus mikrofluidischen Systemen und Zellen in verschiedensten Formen dar (als Monolayer, Co-Kultur, als Spheroid/Organoid, als Zellverband im Hydrogel, etc.), welche die grundlegendsten Funktionen eines Organs nachzuahmen versuchen. Neben der Funktionsweise, Konstruktion sowie verschiedenen Beispielen von OOC-Systemen aus der Literatur werden auch die pharmakologische Bedeutung von OOCs sowie die *human-on-a-chip* und *disease-on-a-chip* Systeme diskutiert.

Microfluidic Systems and Organ (Human) on a Chip

8

Janina Bahnemann, Anton Enders, and Steffen Winkler

Contents

J. Bahnemann (✉) · A. Enders · S. Winkler
Institute of Technical Chemistry, Leibniz University Hannover, Hannover, Germany
e-mail: jbahnemann@iftc.uni-hannover.de

175

41

What You Will Learn in This Chapter

In the previous chapters we learned how cells are cultivated in 3D and how the surrounding gel matrix is optimized. However, to achieve even higher physiologically relevant cell culture conditions, the surrounding environment must be controlled by emerging microfluidic systems. Thus, in the first part of this chapter we will learn about the tremendous benefits of microfluidic devices, their fabrication, and finally their implementation in novel and highly controlled biological and cell culture applications.

On this basis, the second part of this chapter will focus on the complete control of biochemical and biomechanical cell culture parameters, which results in sophisticated organ-on-a-chip systems. You will learn how the blood–tissue barrier and the minimal functional unit of an organ are reconstructed to mimic specific organ functions. Finally, the combination of several different organ-on-a-chip systems results in the so-called human-on-a-chip systems. Although these systems are still in its infancy, we will elaborate on first design concepts and point out their future role in drug development processes in industry.

8.1　　Introduction to Microfluidics

Microfluidics is an emerging interdisciplinary field that holds great promise for applications in such diverse realms as chemistry, biochemistry, and biological applications. Generally speaking, microfluidic systems involve the precise control of minute amounts of fluids (measured in the microliter scale) within complex channel systems at low flow rates. Because most microfluidic applications currently lie in chemical or biological analysis, these systems are also frequently referred to as Micro Total Analysis System (µTAS). The primary advantages of microfluidic systems over more traditional methods are comparatively small sample and reagent volumes, shorter analysis time, and lower cost.

But these are not the only advantages—other emerging applications in this field are leveraging the possibility of including several different analytic steps (i.e., mixing, diluting, and separating) in parallel within a single microfluidic system. Such systems are colloquially known as "Lab-on-a-Chip," and they hold great promise across a wide range of applications in the fields of biology and biochemistry—for example, by facilitating protein crystallization, cell growth analysis, or cultivation optimization [1]. And microfluidic devices are also increasingly being deployed within the biomedical field—for example, in the form of ready-to-use diagnostic systems for the so-called point-of-care diagnosis [2].

8.2   Characteristics of the "Microfluidic Environment"

Most microfluidic systems exploit specific characteristics of the unique environment that is created within these miniaturized conditions. As discussed below, such micro-environments are characterized by three important elements: (1) a small physical size, (2) an increased surface-to-volume ratio, and (3) a comparatively stable laminar flow.

The main advantage created by the small physical size of these systems is their decreased inner volume. This decrease in systemic volume allows for significantly lessened reagent and sample consumption as compared to more traditional methods. In addition, when using cells or particles, this small physical size also allows the user to influence every single cell more directly, via the introduction of nutrients, hormones, or other signaling molecules.

Surface-to-volume ratio also naturally increases as a direct function of decreasing channel size within these systems. This, in turn, has three corollary effects: First, a correlative increase in heat transfer across all parts of the system, which results in higher control and less dispersion. Second, a correlative increase in gas exchange. And third, a decrease in diversity within and across fluids within the system.[1]

Finally, due to the small physical dimensions and high surface-to-volume ratios typically found in microfluidic systems, fluid flow is typically dominated by viscous forces. As a result, the characteristic "Reynolds number" (defined as $Re = \rho v d / \eta$, where ρ is the density of the fluid, v is the velocity, d is the hydraulic diameter, and η is the dynamic viscosity of the fluid) in these systems is typically well below the threshold value of 2300—which means that the flow rate in microfluidic systems can be considered to be highly laminar. Unlike turbulent flow, where fluidic streamlines often cross (envision pouring milk into coffee or the turbulent water channels created by the movement of a ship's propeller), fluidic streamlines move "side-by-side" within a laminar flow (Fig. 8.1). As a result of this even and parallel motion, fluidic mixing is only caused by diffusion *at the interface of these streams*. This feature allows the architect of a microfluidic system to
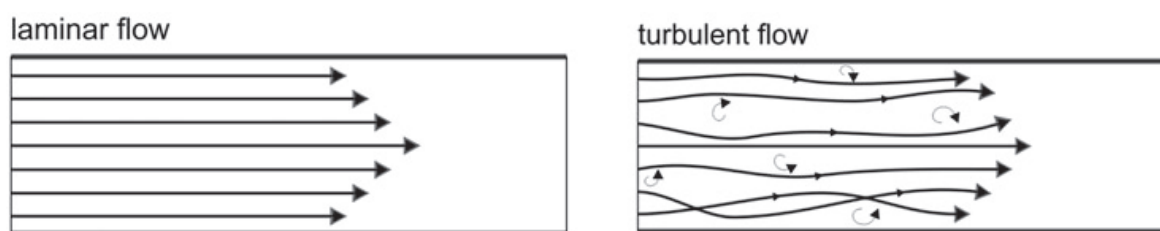
Fig. 8.1 Schematic visualization of fluidic streamlines within laminar vs. turbulent flows

---

[1]Conversely, it should be noted that adsorption effects on channel walls also tend to increase. This is worth mentioning because adsorption can potentially lead to *unwanted* binding effects (e.g., with nonspecific proteins).

readily design channels that foster a stable concentration of different gradients [3] within several different units. If mixing is thereafter desired, then micromixer channels can also be introduced (see Chap. 4.3).

There are multiple ways to propel fluids in microfluidic systems. In some applications, like paper microfluidics, the effects of water interacting with the chip material are sufficient to propel the fluid forward. However, in more complex microfluidic systems, active pumps are needed to achieve suitable flow rates.

Some applications, like the Organ-on-a-Chip or Human-on-a-Chip designs discussed later in this chapter, rely on pulse-free slow fluid motion, which can be created best using pressure driven pumps. Pressure driven pumps use pressurized gas to force fluids into microfluidic channels. Other devices do not rely on pulse-free motion and can be used with more common peristaltic pumps, where a rotor is squeezing a pump tube in a revolving motion, thereby forcing the fluid inside the tube to move. Another common type of pump is the syringe pump, which provides accurate flow control and nearly pulse-free flow by pushing or pulling on a syringe filled with fluid but is also limited by the volume of the syringe used. Some designs even include a way to move fluids inside of the microfluidic system itself. In these devices, elastic properties of the chip material are used as a kind of membrane, which can be actuated using pressurized gas or force applied from the outside of the device. Therefore, the fluid motion can be controlled on the microfluidic device directly.

8.3   Microfluidic Fabrication Techniques

Perhaps not surprisingly, the roots of the field of microfluidics lie in the microelectronics industry. The very first microfluidic systems were etched into silicon wafers, using traditional electronics manufacturing principles. But silicon is expensive and opaque (which is a critical limitation with respect to designing biological experiments). As a result, biologists eager to take advantage of this emerging technology quickly began exploring glass and plastics as fabrication materials. The soft elastomer polydimethylsiloxane (PDMS) is widely used today in biological applications, where it is prized for its optical transparency, elastic features, biocompatibility, and permeability to gases [3]. The production process of PDMS systems usually involves several steps (see Fig. 8.2). First, a mold is created. The layout of the channels within this mold is printed directly onto a mask via a high-resolution printer. This mold is then used to outline the channel positions on photoresistant material on a silicon wafer, using a photolithographic process. The cured material is left protruding off the silicon. This is called the "master." The PDMS system is thereafter cast using the master and cured for 2 h at 60 °C. After the curing process is complete, the PDMS stamp is removed. The PDMS system now has the channel structures etched at the bottom and can be adhered to another flat sheet of PDMS, glass, or other materials, in order to seal the channels. For more complex three-dimensional channel systems, multiple PDMS stamps can also be adhered to one another [4].
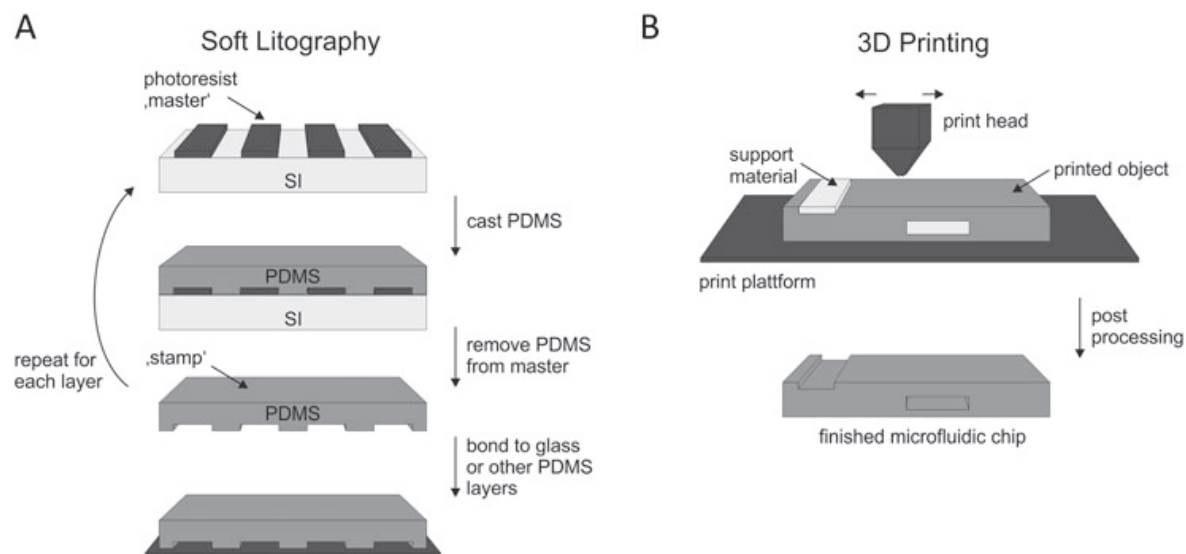
Fig. 8.2 Common fabrication techniques for creating microfluidic systems: (**a**) soft lithography (PDMS molding) and (**b**) 3D printing

In recent years, 3D printing has become more widely available, with the advent and popularization of new printing techniques, greater material selection, cheaper printers, and more refined printing resolution. As a result, 3D printing—which can frequently be done even more quickly, efficiently, and cost-effective than PDMS molding (Fig. 8.2)—has emerged as a highly promising alternative method for manufacturing microfluidic systems. Having said that, a note of caution is warranted: the materials used in "traditional" 3D printing applications (such as mechanical engineering and design) frequently are not biocompatible or chemically stable when exposed to solvents. This imposes a substantial limitation in the current use of 3D printing to create microfluidic systems within the biochemical and medical fields. Furthermore, even with recent advances in 3D printing techniques, current printing resolution still cannot compete with the smallest channel sizes achieved by using PDMS molding and photolithography. Nevertheless, the authors anticipate that the march of technological progress on this front will result in 3D printing becoming the "preferred" production mechanism for microfluidic systems in the near- to medium-term future, as biocompatible and chemically stable materials are being released [5, 6] and print resolutions continue to improve.

8.4 Overview of Biological and Cell Culture Applications

Numerous microfluidic devices have already been manufactured for use in various biological and cell culture applications [7]. Below, we highlight just a few of these devices and also briefly discuss the advantages they offer over more traditional methods.

45

8.4.1 DNA Sequencing

Blazej et al. have integrated all three steps of the Sanger sequencing protocol (e.g., thermal cycling reaction, sample purification, and electrophoresis) onto a single microfluidic chip—thereby effectively automating this multi-step procedure while simultaneously decreasing the amount of DNA that is needed to accomplish DNA sequencing [8]. This device is fabricated from two glass wafers—with features etched into both glass surfaces as well as a PDMS membrane—and another glass wafer at the bottom of the device (Fig. 8.3). The two top glass wafers form enclosed reaction chambers and capillary electrophoresis chambers, and the second wafer also includes resistive thermal probes. The elastic PDMS membrane underneath is used to actuate integrated microvalves for fluid control, by applying pressure through the integrated manifold lines etched into the bottom glass layer.

For the Sanger sequencing procedure, a sample mixed with both a sequencing reagent and primers is first loaded onto the chip and then moved into the thermal cycling chamber via the integrated valves. This mixture is then thermal cycled 35 times between 95 °C and 60 °C, at which point complementary DNA strands are synthesized. Each of these synthesized DNA strands is called Sanger extension fragments. Afterwards, the sample is pumped into the purification chamber, where a small polyacrylamide gel with single strand of DNA (complementary to the 3′ end) captures these Sanger extension fragments. Salts,
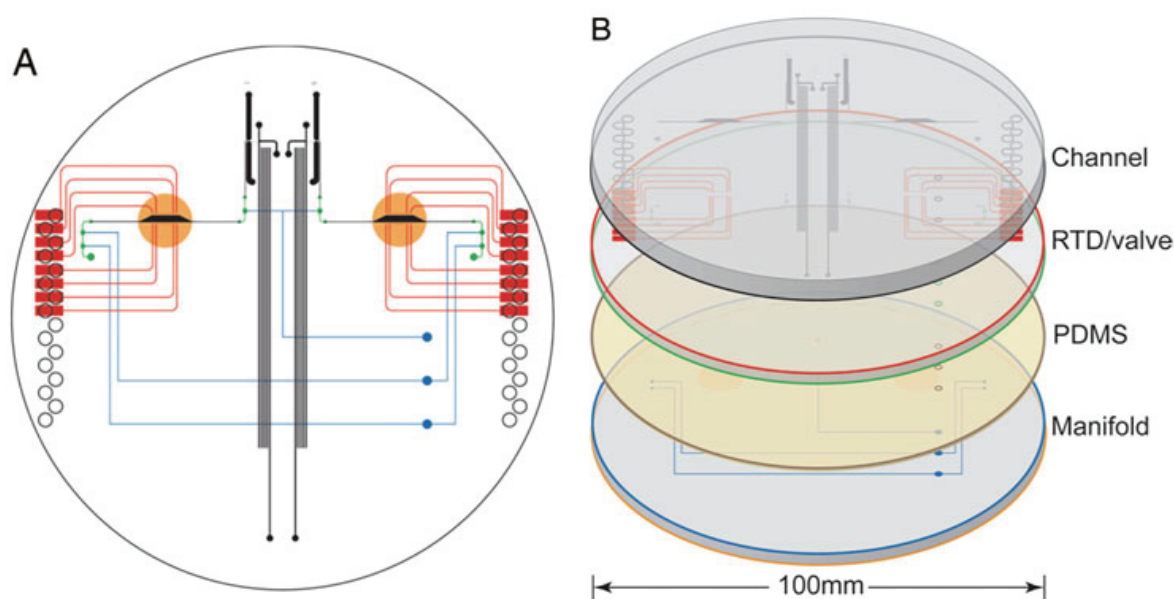
Fig. 8.3 An integrated nanoliter-scale DNA bioprocessor for Sanger sequencing. (**a**) schematic visualization of the top glass plates—illustrating the channel system for sample loading (red), the reaction chamber (orange), and the purification chamber and capillary electrophoresis (black); (**b**) overview of the entire system—showing the top glass plate which contains the channel system; the second glass plate which contains the thermistors and valve system; the elastic PDMS membrane which is used for valve actuation; and the bottom glass plate which contains the manifold channel system used to actuate the PDMS membrane via pressurized air. Blazej et al. [8] Copyright (2006) National Academy of Sciences, U.S.A.

primer, and excess sample DNA are then passed through the gel and removed. After capture, the Sanger extension fragments are released by heating the purification chamber and thereafter moved into the separation capillary where capillary electrophoresis is performed. At the end of the capillary, the four-color sequence data is collected on a radial scanner. Through this mechanism, Blazej et al. were able to achieve a sequence accuracy of 99% using only 1 fmol of DNA template while demonstrating long read lengths suitable for the de novo sequencing of complex genomes. The integration of all three steps onto one system also reduces both the manual labor required to operate the system and the volumes of reagents and DNA needed to conduct the analysis.

Aborn et al. have also developed a system for high-throughput DNA sequencing by parallelizing the electrophoresis step of the Sanger method. In this approach, polyacrylamide gel is pumped into 384 enclosed separation lanes [9]. Afterwards, the prepared Sanger fragments are loaded onto the lanes, and electrophoresis is performed. At the end of these lanes, a multi-line laser is used to excite the DNA and a scanning detector is used to capture the fluorescence data. Using two of these 384-lane plates in parallel, they were able to parallelize the cleaning and loading steps for a 768-lane complete system—which can sequence more than four million bases per day. This system highlights the great potential that microfluidic systems hold for parallelizing operations on a micro-scale.

8.4.2   Point-of-Care Diagnostics

The possibility of miniaturization inherent to microfluidics not only allows for new and improved methods of analytical procedures, but also facilitates new applications in medical diagnostics. The field of point-of-care (POC) diagnostics uses microfluidic systems to develop small, low cost, and self-contained devices that provide analysis directly at the patient instead of relying on analytical laboratories. Major advantages include not just the reduced timeframe to complete a diagnosis, but also the greater independence from infrastructure—which is particularly beneficial in developing countries and/or in disaster situations.

The iSTAT device by Abbott is one of the oldest and most successful commercially available POC devices. This handheld, battery-powered microfluidic device is used for detection of blood chemistries (like potassium, sodium, and glucose), coagulation, and cardiac markers. The analyzer handles drops of whole blood (approximately 100 μL) without sample preparation and uses internal calibration. The calibration reagents are integrated on disposable plastic test cartridges containing an air bladder for fluid movement, a small channel system, and a silicon microchip. Micro-fabricated thin-film electrodes on this microchip coated with ionophores or enzymes are used for detection of various analytes. For fluid movement of the sample and calibration fluids, an electric motor in the handheld device presses on the air bladder on the test cartridge. The handheld nature and power-independence of the device makes it an excellent example of a practical POC device [10].

Another commercially available POC device is the PIMA CD4 counter, manufactured by Abbott. This device is used to count CD4 cells in AIDS/HIV patients—a disease especially prevalent in developing countries. The device employs static image analysis for cell counting. The sample (25 μL of capillary blood) is pumped into a disposable cartridge with dry sealed reagents. In the first compartment, fluorescent anti-CD3 and anti-CD4 antibodies bind to their respective target cells. Then the sample is transferred to a detection area, where the stained cells are imaged and analyzed using image analysis algorithms. The whole process takes just 20 min and can be performed with minimal training in a small desktop system [10]. Although there are a few established systems already on the market, the development of miniaturized, personalized, low-cost, and easy-to-use POC diagnostic systems continues to be a focus of research. In particular, the integration of suitable (bio)sensors into microfluidic systems has already increased sensor selectivity and sensitivity for the detection of specific biomarkers (such as proteins) [11]. In addition, integrated microfluidic POC devices offer the possibility of parallelizing and automating sample processing and analysis.

8.4.3 Handling of Suspension Cells

The ability to handle liquids with high precision in small volumes also makes microfluidics attractive for handling suspended cells. Often, these systems seek to combine several laborious steps into a single system to allow for parallelization, automation, and easier handling.

One example for these systems is an integrated system for fast dynamic quantitative analysis of the metabolism of mammalian suspension cells from a bioreactor [12]. This system combines the sample treatment, mixing, incubation, and sequential separation as well as media exchange in one system with two temperature zones to ensure physiological conditions (37 °C) as well as improved cell quenching at 4 °C. Therefore, the system does not only massively reduce the time and manual labor needed for sample processing, but also offers advantages by providing greater temperature control [13].

Another example of a microfluidic device for cell culture applications is a continuous system for transient transfection of Chinese hamster ovary (CHO) cells. The system aims to combine the necessary lab steps for DNA vector integration in CHO-K1 cells into one system: (1) mixing of DNA vector, chemical transfection reagent, and cell suspension, (2) incubation, and (3) separation of the cells (Fig. 8.4).

The first functional unit of the illustrated transfection system consists of an integrated micromixer. Enders et al. have demonstrated the efficiency of four different passive micromixers in a comparative analysis [14]. While the environment in microfluidic systems is typically laminar—which limits the mixing phenomena to slow diffusion—passive micromixers can be used to overcome the poor mixing in microfluidics by rearranging the flow and disturbing the parallel flow lines. One example for disturbing the flow lines is the popular Tesla-like mixing structure. This mixer splits the flow vertically and leads one
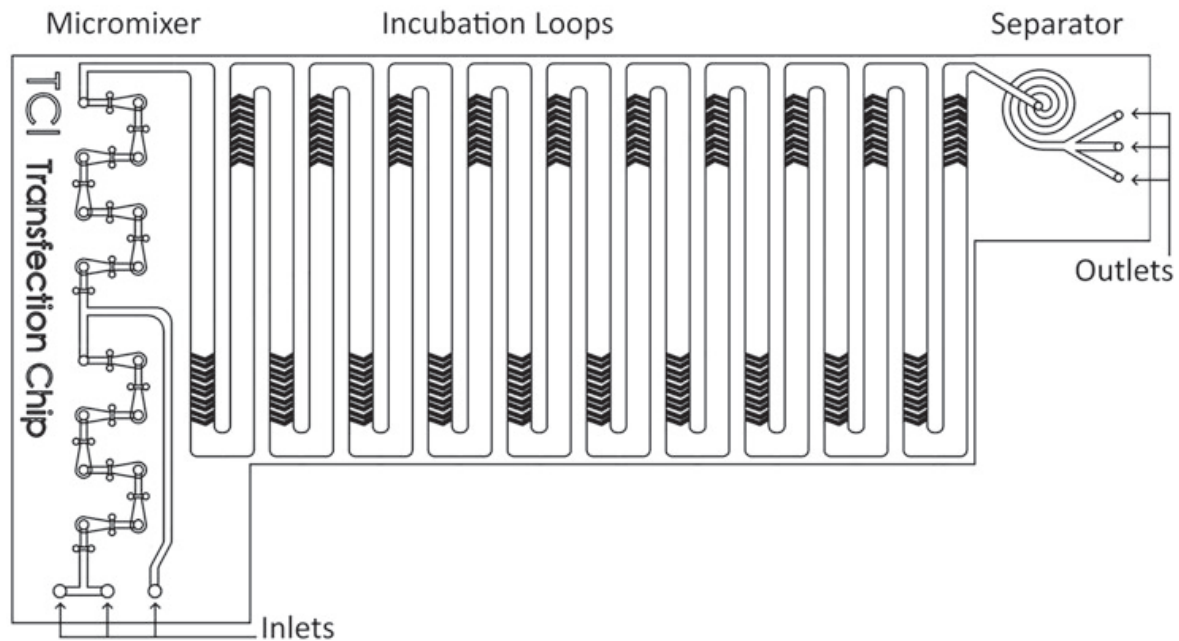
Fig. 8.4 Microfluidic system for transient cell transfection. This system combines cell and fluid mixing, incubation, and separation steps in one microfluidic device

half of the flow in a 180° turn to recombine with the other half head on. Conversely, the F-type mixers split the flow vertically and recombine it horizontally, which create an alternating pattern and decrease the distance for diffusion. Additional information on both passive and active micromixers can be found from Capretto et al. [15] or Nguyen et al. [16].

Enders et al. also used 3D printing to quickly fabricate the complex channel structures of the different micromixers. Figure 8.5 illustrates the printing workflow. Additionally, the 3D printing workflow is shown in our video, which can be viewed via the following link (https://youtu.be/Wc4gjoxfhOw) and the QR code in Fig. 8.5. The complete printing process is dependent on the model dimensions, but generally takes about 2–4 h in total.

Another functional unit of the microfluidic transfection system is the separation of cells following the transfection. The aim is to preserve cell viability by separating the cells from the toxic transfection reagent. Microfluidic separation systems can focus particles of various sizes at specific points inside a microfluidic channel. An example of a simple separation system is a spiral separator. While particles converge to stable positions inside a channel in a laminar flow environment naturally, a channel with a rectangular cross-section only has two stable positions in a horizontal plane. When winding a rectangular channel into a spiral, a pressure difference is created between the flow at the outer wall and the inner wall of the spiraling channel. This leads to a new flow pattern orthogonal to the main flow direction (called "dean flow"), which leads the outer stable position in the channel to become unstable [17]. Thereafter, only one stable position—towards the inner wall of the channel—remains. The spiral separator is an ideal tool for focusing cells from suspension at this position.
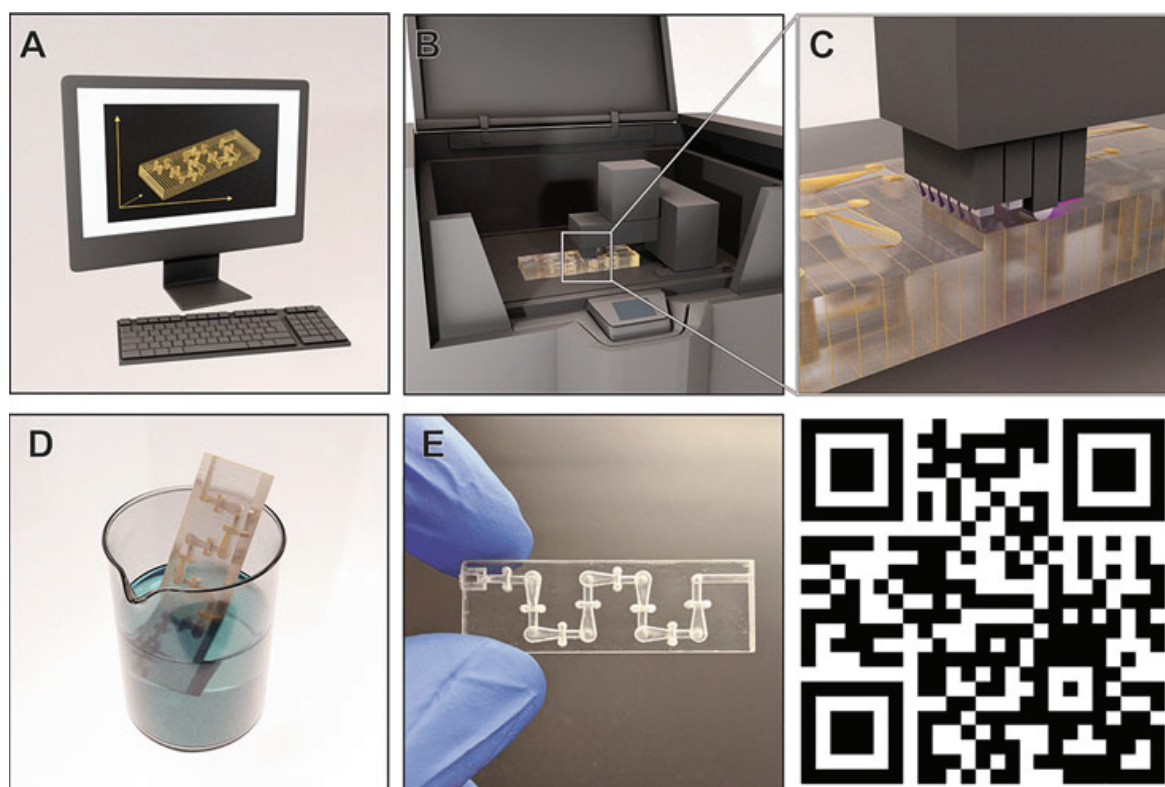
Fig. 8.5 3D printing workflow used by Enders et al. (**A**) computer aided design (CAD); (**B**) the CAD file is sent directly to the 3D printer; (**C**) detailed view of the print head, which places the print model material and support material; (**D**) the channels are filled with support material during the printing process, which is removed during post-processing; (**E**) the finished 3D-printed micromixer

8.4.4 Analysis of Single Cells

Conventional analytical methods used for analyzing suspended cells (e.g., in cell culture or blood) frequently use the averaged results of a sample size of hundreds or thousands of cells. However, these methods do not consider cells as single individuals, so the information reflects only the average state of a population of cells. The use of microfluidic platforms opens the possibility of analyzing single cells.

Grünberger et al. have developed several systems consisting of very small bioreactors on microfluidic chips to perform various analysis on individual cells [18, 19]. The smallest system is a cell trap for a singular bacterial cell, which holds the cell in place while fresh medium flows around the cell. The group was able to trap *E. coli* cells and monitor the cell growth over several hours, showing constant division times and typical morphology (which indicates that the system exerted no inhibiting effects tarpon the cell) (Fig. 8.6). This system allows for live-cell imaging and analysis over extended periods of time in a perfectly controlled environment, which facilitates more granular analysis and observation of the response of a single bacteria to short term environmental fluctuations (e.g., in pH, temperature, etc.).
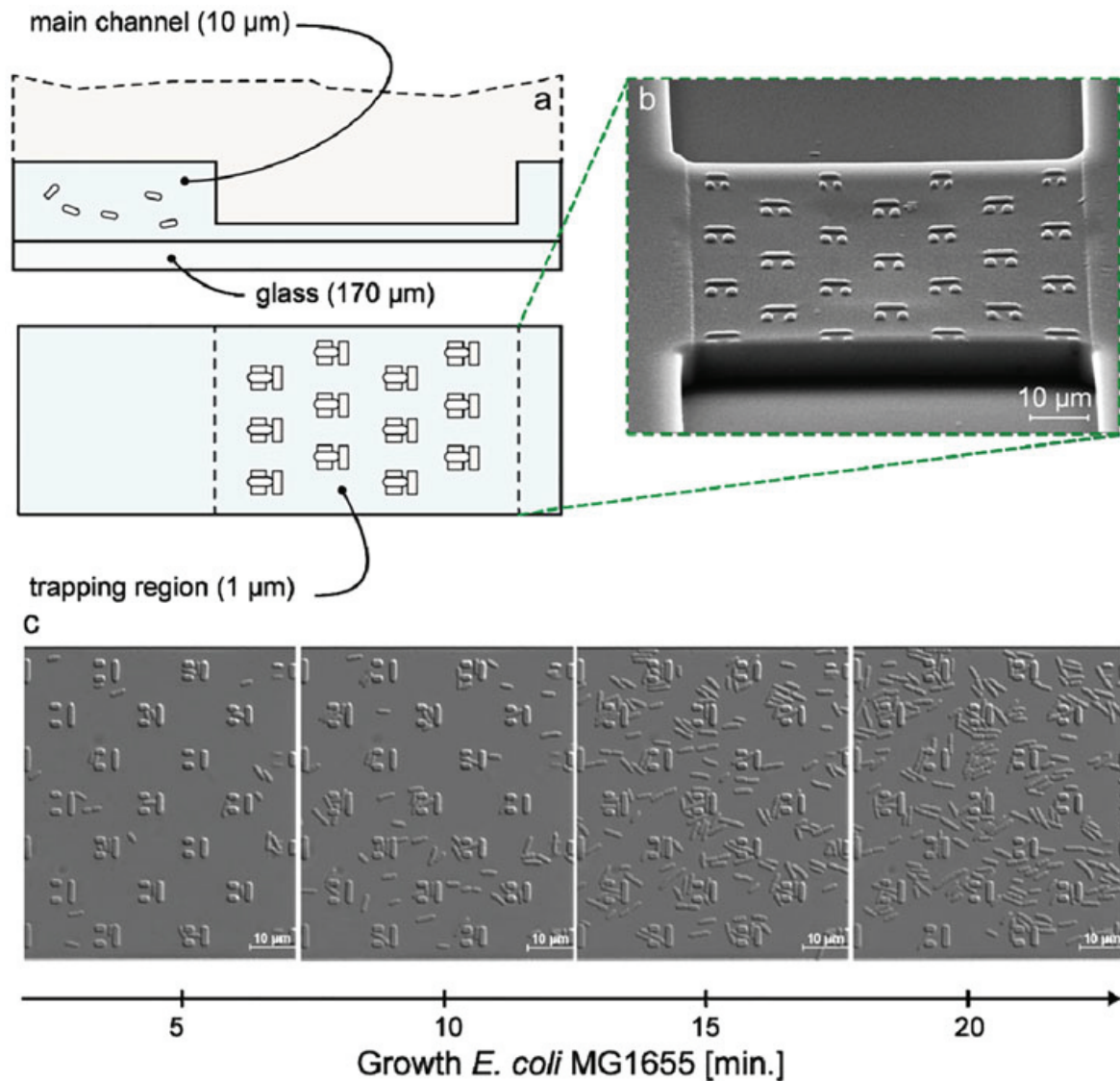
Fig. 8.6 Cell traps for single cell cultivation and studies by Grünberger et al. (**a**) schematic illustration of the complete chip and the trapping region, (**b**) microscopic view of the trapping region, (**c**) microscopic images demonstrating the growth of *E. coli* over time

Gao et al. have developed another microfluidic system for use in biological cell studies [20]. Unlike other cell analysis protocols, this system focuses on the analysis of a single cell. The team used human blood cells to conduct an analysis of intracellular constituents via a simple microfluidic device which consists of only four channels (sample input, buffer input, sample waste, and a capillary electrophoresis channel) leading to a single crossing point. First, the human blood cells (in suspension) were pipetted onto the chip and flowed into the channel system via hydrodynamic force. Then, a single cell was captured using electrophoretic means at the crossing point by applying a set of potentials at the end of the four channels. This cell was docked at the channel walls and then lysed by applying even higher voltages. This docked-lysing approach led to reduced dispersion of the released cell

constituents. Next, capillary electrophoresis was performed in the capillary electrophoresis channel, and the cell constituents were analyzed using a fluorescence detector located at the end of the channel. Although the operation in this research was fully manually, it is worth noting that this process could also be easily automated—since only pipetting and voltage-switching are involved. It is also worth noting that multiple analyses of a single individual cell can provide researchers and/or doctors with far more nuanced and granular insights into the health of a patient's blood cells than using averaged results gained via more traditional homogenized samples taken from thousands of cells.

8.4.5   Parallel Cell Culture

Hung et al. have developed a microfluidic system for performing a parallel perfusion culture of mammalian cells (HeLa) [21]. The team manufactured a 10×10 grid of circular cultivation chambers in PDMS with an integrated gradient micromixer system. Each chamber featured a larger inlet and outlet channel at opposing sides, as well as several small perfusion channels surrounding the chamber. In experiments using this system, HeLa cells were first loaded in suspension and then left for 2 h to settle. Afterwards, these cells were fed using perfusion medium pumped at low flow rates through the perfusion feed, until the cells adapted to the new environment and cell growth stabilized at a normal rate (a time interval of 8 days). At that point, perfusion was stopped, and sample reagents were fed through the inlet channels. Using an integrated gradient micromixer system located in front of the inlet channels, ten different concentrations of reagents could be created, and ten wells could be utilized for each concentration. A Calcein AM cell assay with an observation time of 10 days (using fluorescence microscopy) was then deployed. This parallel perfusion culture system holds significant promise for future deployment in cell culture optimization and studies in tissue behavior. Again, comparatively small reagent and media volumes, as well as parallelization, enable more cost-effective assay methods within this microfluidic system when compared to more traditional methods.

Gómez-Sjöberg et al. have gone even farther and enhanced the idea of parallel cultivation of adherent mammalian cells by developing a fully automated cultivation system with 96 individually addressable cultivation chambers on a single chip (Fig. 8.7) [22]. Once again, every cultivation chamber was quite small—with a volume of just 40 nL—and the whole microfluidic chip was mounted on an automated microscope equipped with a motorized X-Y stage. During the cultivation process, each hour a phase contrast image was taken and then automatically analyzed. Even at the cell loading step, automatic cell counting was used to ensure that the exact same number of cells were placed into every cultivation chamber. Up to 16 reagents and culture media were connected to the system at the same time and mixed at different quantities.

Through this study, Gómez-Sjöberg et al. have amply demonstrated that a microfluidic system can simultaneously sustain proliferation while also stimulating the differentiation of human mesenchymal stem cells. By automating both the pumping of reagents/media and
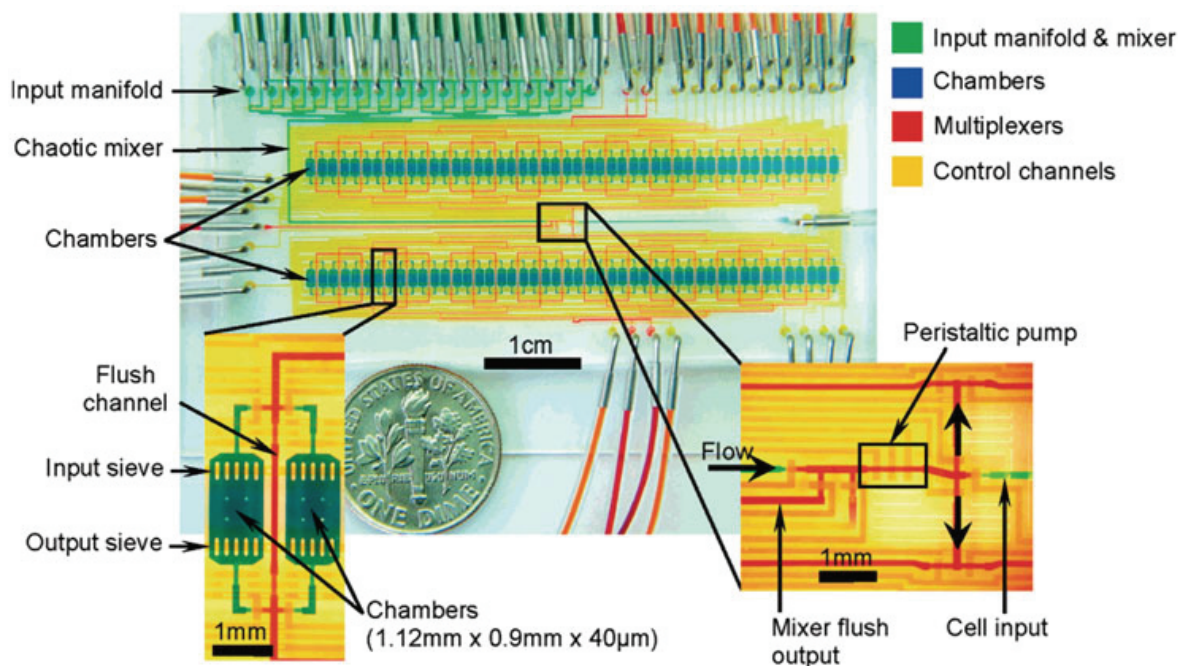
Fig. 8.7 A microfluidic cell culture array for perfusion culture, reprinted with permission from Gómez-Sjöberg et al. Copyright (2007) American Chemical Society

the microscopic imaging phases of their process, the group was able to implement complex and time-varying feeding and stimulation schedules while also taking time-lapse microscopic images of each cultivation chamber. As a result, they were able to study the effects of osteogenic differentiation factors on cell motility in a highly granular fashion.

A slightly different cultivation device was published by Siller et al. [23]: The 3D-printed cultivation vessel was used to co-cultivate endothelial and mesenchymal stem cells indirectly. A physical barrier was separating the cell types from one another, while medium was able to flow over that barrier. The 3D-printed material enabled phase contrast and fluorescence microscopy, which allowed for the observation of cell growth over time. These observations and further analysis revealed that endothelial cells form tubular-like structures when cultivated alongside mesenchymal stem cells, a feature that can be considered angiogenic. In addition, this study demonstrated that the 3D-printed material is biocompatible and thus suitable for the development of individual cell culture vessels.

The foregoing examples—which represent only a small sampling of some recent applications of microfluidic systems that have been deployed in recent years—illustrate the varied and numerous advantages that these systems can offer to researchers in the fields of biotechnology and bioengineering: parallelization, automation, small sample and reagent volumes, and more direct sample control chief among them.
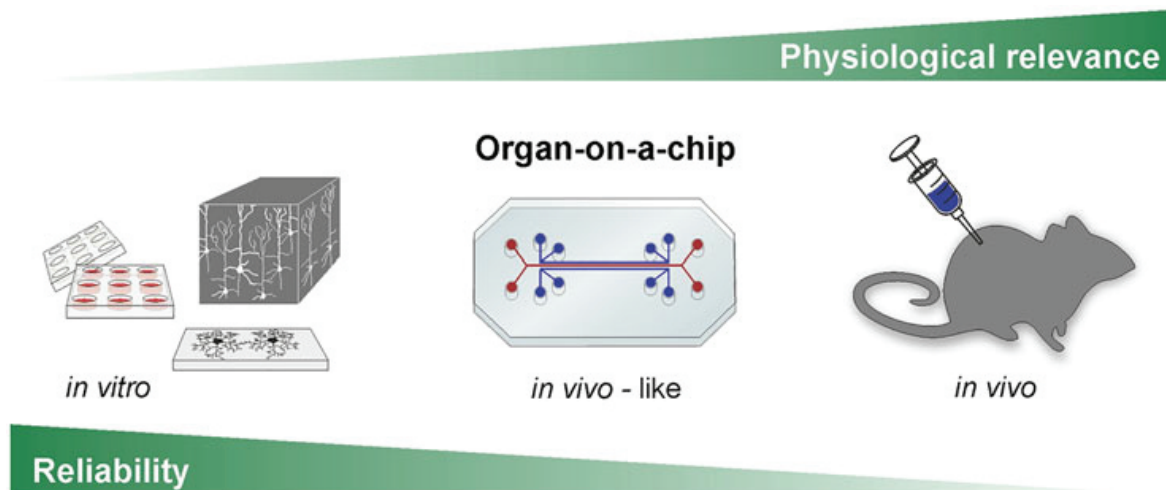
8.5 "Organ-on-a-Chip"

8.5.1 Introduction to the Concept of the "Organ-on-a-Chip" (OoC)

"Organ-on-a-chip" (OoC) systems represent one of the most promising biotechnologies that have been invented to date in the field of microfluidics. Just as the lab-on-a-chip is intended to facilitate the miniaturization and automatization of lab procedures, OoCs seek to mimic organ functions by deploying 3D cell culture techniques on a microfluidic chip. Importantly, the focus in these systems is *not* the reconstruction of complete organs—rather, it is merely the development of "minimal functional units" (MFUs) that accurately represent the core essence of these organs as it relates to experimental purposes. This innovative approach encompasses a wide range of concepts—including tissue engineering, hydrogel integration, cell integration, cell cultivation, and cell differentiation—and also makes use of a wide array of emerging technologies in the field, including pumps, valves, and the design of the microenvironment for targeted 3D culture formation and cultivation. Currently, advanced OoC systems are using established cell lines or primary cells. However, by its very nature, the microfluidic environment allows for the precise control of cell culture conditions and spatial- and time-dependent differentiation of stem cells within OoCs. As a result, adult or induced pluripotent stem cells are assuming an increasingly prominent role in this research field [24].

The highest potential for OoC technology lies in the pharmaceutical industry—particularly within the context of drug development. At present, the long pipeline of new drug development includes (without limitation) the synthesis of chemical compounds; high-throughput screenings for biological activity and toxicity by using in vitro enzymatic or cell-based assays; pre-clinical investigation of pharmacokinetics and dynamics by in vivo animal experiments; and, finally, three separate clinical phases culminating in studies featuring thousands of patients. Unfortunately, the second and third clinical testing phases (which occur relatively late in this chain) are the single most expensive steps for drug development—and they are also characterized by the highest failure rates. As a result, *ex ante* predictions of compound activity, toxicity, and other key benchmarks for drug candidates derived from data realized using current in vitro and in vivo techniques are notoriously unreliable.

OoC holds tremendous promise as a tool to help bridge the expensive and time-consuming gap that currently separates the pre-clinical and clinical phases [25]. It balances the advantages of high reliability of in vitro techniques with the higher physiological relevance of in vivo parameters by including novel in vivo-like parameters into the system (Fig. 8.8). These in vivo-like parameters are additional biomechanical parameters that more closely mimic actual in vivo conditions. For instance, mechanical stimulations have been demonstrated to influence cell behavior—in particular, the process of cell differentiation. This is because most, if not all, organs are exposed to (at least small) mechanical forces. For instance, a lung-on-a-chip system may help to stimulate the formation of the lung epithelial cell barrier by using a vacuum-induced cell strain. And even static organs are exposed to

Fig. 8.8 Organ-on-a-chip systems balance the advantages of high reliability of in vitro techniques with the higher physiological relevance of in vivo parameters by including novel in vivo-like parameters

the basic mechanical forces caused by the liquid flow of the blood within the organ tissue. OoCs have revealed a fluid flow shear stress that alters gene expression—to cite one example, this stress has been found to influence vasculature diseases [26]. Similar to the vascular system, the flow additionally allows the permanent supply and removal of anabolites and metabolites, thereby creating a constant pH value and a constant distribution of oxygen, medium, and drugs in a physiological liquid-to-cell ratio. These in vivo-like parameters make OoCs superior to the standard in vitro 3D cell culture. Furthermore, animal experiments can also be complemented, or even entirely supplanted, by OoCs. The applicability of animal models to human patients is notoriously limited. Indeed, this disjunction currently represents a major bottleneck for drug development. But OoCs have substantially better predictive capabilities, because they combine in vivo-like advantages with *human* cells. As a result, tests for compound properties (such as liver toxicity or skin irritations) can be more reliably conducted using human liver-on-a-chip or skin-on-a-chip systems. And in contrast to using animals as black boxes, the processes in OoC devices can also be electrochemically or optically monitored by integrated sensors or microscopic/spectroscopic techniques, resulting in a high data output that finally can be multiplied by automation and high-throughput screenings.

8.5.2 Engineering the Organ-on-a-Chip Microenvironment

Engineering in vivo-like complexity within the organ-on-a-chip microenvironment is highly dependent on an interdisciplinary combination of tissue engineering technology and microfluidic knowledge. This is accomplished in an iterative process, where the requirements for survival and function of cells and cell cultures—investigated and defined

by cell culture and tissue engineering research—are fulfilled by the microstructures and control of the chip, which is in turn based on technical knowledge gained within the microfluidic field. The first challenge for designing any OoC is therefore to ascertain these requirements, in order to reconstruct and maintain the basic organ-like functions of a cell culture. Depending on the organ, this can include hydrogels, membranes, electrical fields, gas or nutrient gradients, and dynamic mechanical stimulation, among many other aspects [27]. Defining these parameters is governed by a critical manta: "as much as necessary and as little as possible." In other words, an OoC must be usable and reliable in its application, but it should *not* (unnecessarily) mimic every function of a real organ.

An OoC can be built from either ex vivo tissues or 2D and 3D cell cultures. To begin, we will focus on general steps and techniques for OoC engineering using the type of 2D and 3D cell cultures that have been used in OoC research so far—saving further discussion of OoCs of important organs for later on.

Engineering a successful OoC is strongly dependent on the selection of a suitable cell source. Primary cells, "immortalized" cell lines, and various kinds of stem cells are all popular choices. Primary cells are unmodified mature cells, and, perhaps not surprisingly, their major advantage is their similarity to in vivo tissue. However, they also suffer from several distinct disadvantages—including ethical and practical difficulties associated with isolating them from other animal or human tissue; limited resources and lifetime; a comparatively difficult cultivation; and an unfortunate tendency to alternate gene expression and the loss of function after a few weeks of cultivation. As a consequence, many OoC platforms instead make use of the so-called immortalized cell lines that are derived from primary cells via a process of chemical or viral modification. Immortalized cells are easier to cultivate and also exhibit superior growth when compared with primary cells. Nonetheless, like the primary cells from which they are derived, immortalized cells also tend to display genotypic and/or phenotypic alternations as the culture matures. Stem cells are perhaps the most promising of all, because they offer the possibility of differentiation into complex in vivo-like tissues. Thus, OoC platforms could manage a targeted manipulation of cell differentiation to create a specific assembly of different cell types creating a more physiological, tissue-like cell culture. Depending on their origin, stem cells can be classified into embryonic stem cells (ESCs), adult stem cells, or induced pluripotent stem cells (iPSCs). iPSCs are of particular interest to researchers, because at least in principle they can be achieved by reprogramming skin cells isolated from any person—thereby enabling truly personalized OoC models.

After the appropriate cell type(s) have been selected and their requirements are ascertained and defined, the microenvironment can then be engineered. One of the primary engineering challenges faced by every OoC model is the reconstruction of the blood–tissue barrier, where the microfluidic nutrient flow represents the blood and the 3D cell culture organization represents the tissue [28]. This barrier is a central biological principle found in every organ, which allows the perfusion and nutrient supply of the 3D culture. Depending on the organ, additional barriers must be reconstructed to manage separation of, e.g., urine in kidneys; bile in liver; food in the gut; air in the lungs; etc. Several basic techniques for
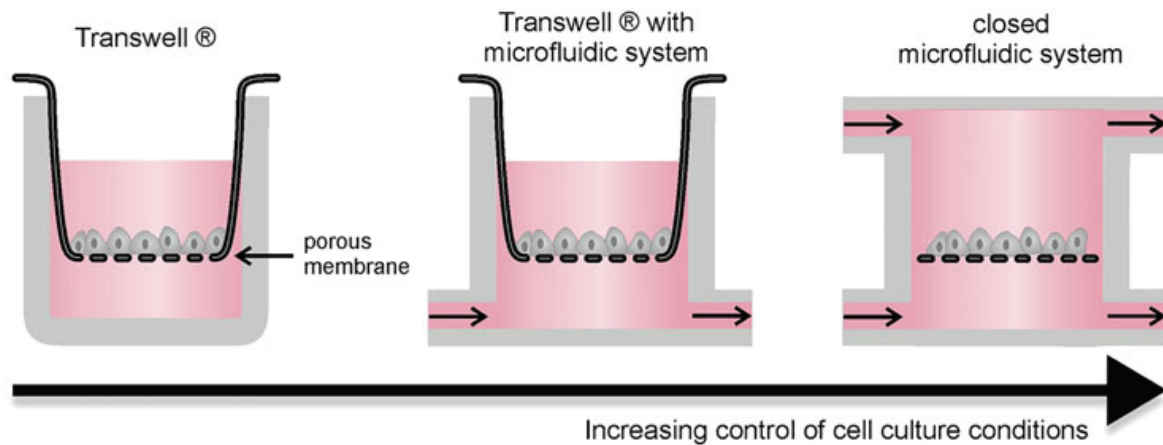
Fig. 8.9 The advances of membrane-based organ-on-a-chip systems. Early Transwell® systems included a permeable membrane, but no flow control (left). In contrast, many current membrane-based OoCs make use of microfluidic platforms for Transwell® integration (middle) or complete displacement (right), to allow liquid flow that results in an increased control of cell culture conditions

creating these interfaces inside the microfluidic chip have been developed. The use of porous membranes is very common.

The membrane allows the cultivation of 2D or 3D cell cultures on both sides: By manipulating the pore size, thickness, surface properties, elasticity, and other parameters, the membrane can be adapted to fulfill all of the complex functions that are required in a barrier (including selective permeability, cell attachment, cell migration, and cell alignment). Porous membranes also offer comparatively good transparency to facilitate microscopic observation. The so-called Transwell® is one of the simplest and best-known examples of a membrane-based OoC design (Fig. 8.9). Initially it was plugged in standard well-plates, but, with advances in microfluidics, it has been combined with microfluidic devices to enable a continuous flow. Today, many membrane-based OoCs replace the barrier by integrated membranes—allowing a closed design accompanied with markedly higher control of cell culture conditions. Unfortunately, the use of membranes in 3D cultures is limited by the fact that they cannot (presently) be freely modeled in all three dimensions.

As discussed in Chap. 5, 3D cultivation can be accomplished by using hydrogels to form a physiological extracellular matrix (ECM) for cell encapsulation. One approach to hydrogel integration—derived from microfluidic chips fabrication technology—is soft lithography. In this process, a non-polymerized gel is squeezed into a reusable template, which is then removed after gel polymerization occurs. Another approach is selective photopolymerization using photomasks with subsequent removal of non-polymerized gel. However, as 3D microstructures become more complicated, the challenges associated with using either of these methods quickly escalates. At a micro-scale, adhesion and capillary forces can be used to exclusively trap the gel in specific channels without blocking neighboring channels for fluid flow. Porous or degradable chip materials enable the construction of permeable or disappearing barriers between hydrogel and fluid channels

that will not be overgrown and blocked by cells due to the constant perfusion [29]. In combination with advancing 3D printing techniques, these channels can be fabricated in all dimensions of space—allowing a well-defined perfusion of the hydrogel. Likewise, 3D printing can directly be used for microstructuring hydrogel using bioprinting technologies (see Chap. 9).

Many current OoCs are membrane-based and thus do not require a sophisticated 3D tissue microstructure for fulfilling the requirements of their specific application. But OoC research is still in its infancy—and with the increasing success of OoCs spurring on ever-more-complex designs, the demands on OoC design will only continue to increase moving forward.

8.5.3 Reconstructing the "Minimal Functional Unit"

As discussed above, every organ contains its own "minimal functional unit" (MFU), which fulfills the basic functions of the organ. The overall aim of any OoC is to reconstruct this unit—and *only* this unit. In contrast to 2D, 3D, or even organoid cultures, the MFU encompasses biomechanical functions such as (by way of example) contraction, dilation, resorption, filtration, and excretion. However, mimicking *all* functions of the MFU is extremely challenging, and, as a result, current OoCs typically focus on only a few of them. Nevertheless, researchers all over the world are currently reconstructing organ functions for nearly every human organ—even the brain. Below, we briefly discuss how MFUs of the liver and kidney are mimicked by existing OoC systems.

Liver Because of the central role that it plays in metabolizing drugs within the human body, the liver is a common focus for OoC systems. The MFU of the liver is the liver sinusoid. The sinusoid is a capillary that combines oxygen-rich blood from the artery with nutrient-rich blood from the portal vein. Liver sinusoidal endothelial cells (LSECs), Kupffer cells, hepatic stellate cells, and hepatocytes [30] all act together to form a porous barrier between the capillary and the bile duct, where hepatocytes clean the blood by scavenging and metabolizing toxic substances. This blood–tissue barrier has most commonly been mimicked by using integration of permeable membranes to allow cultivation of LSECs and hepatocytes on opposing sides [30, 31]. Other approaches involve nanostructures which allow diffusion of nutrients and removal of waste products [32]. However, many liver-on-a-chip devices omit this barrier and instead merely contain 2D cell monolayers or 3D spheroids. This is because for studying the toxicity and metabolism of drugs, sinusoid-like structures are generally not absolutely mandatory. Nevertheless, the liver sinusoid *is* essential for observing urea secretion function—and as a result its inclusion in a liver-on-a-chip OoC is critical for studying pharmacokinetic and/or pharmacodynamic drug behavior [33].

Kidney The kidney is also of special interest for drug testing, since it eliminates xenobiotics and is highly involved in regulating blood pressure. The MFU of the kidney is the nephron, which consists of the glomerulus, proximal tubule, and the loop of Henle. Current microfluidic devices serve a specific purpose—such as characterizing drug transport and nephron toxicity [34]—and as a result they tend to focus on replicating glomeruli or tubule structures. The main function of the glomerulus is the filtration of blood. Similar to a liver-on-chip OoC, endothelia cells and glomeruli-specific cell types (such as podocytes) have been cultured on each side of a permeable membrane in kidney-on-a-chip OoCs. Furthermore, mechanical influences like pulsation of the renal blood flow have also been reconstructed via vacuum-driven deformation of the membrane [35]. The main function of the proximal tubule is the reabsorption of solute and fluid [36], which has similarly been reconstructed in several tubule-on-a-chip systems by a membrane-based design [34, 37, 38]. However, the tubule has also been designed by 3D cell culture techniques as well, using hollow fibers or bioprinting [39, 40]. The 3D gel matrix is formed in a tubular structure allowing cells to be cultured inside or on the surface of the matrix.

8.6 "Human-on-a-Chip" and "Disease-on-a-Chip"

8.6.1 The Principles of Multi-Organ-on-a-Chip

The concept of combining several different OoCs in a single chip is called human-on-a-chip (HoC), body-on-a-chip, multi-organ-on-a-chip, or micro-cell culture analogs (μCCAs) (Fig. 8.10). Although several multi-organ-on-a-chip devices have been created to date [41–44], no complete HoC has been successfully developed yet, because the reconstruction of all organs and their interactions remains a subject of active and ongoing research. Nevertheless, the concepts for multi-organ-on-a-chips and HoCs are essentially the same: A HoC must be a stable system where OoCs can interact and communicate with each other, while unwanted fluctuations that potentially lead to non-physiological functions are prevented or minimized.

To engineer such a stable system, OoCs must firstly be scaled down by using either allometric scaling or residence-time based scaling approach [45]. Allometric scaling miniaturizes organs relative to each other according to their scaling factors. But miniaturization of a human body from kilograms to grams, or even milligrams, does not follow a trivial linear (isometric) down-scaling of all organs. This is because different characteristics of an organ—such as mass, metabolization, blood volume, or oxygen consumption—all follow different scaling factors [46]. To illustrate this concept, consider cells that are already relatively rare within a normal, full-sized human body: An isometrically scaled HoC would include only a few leukocytes, and they would be inhomogeneously distributed within the system. In consequence, they could not fulfill their functions in all compartments of the chip. Moreover, scaling always changes ratios of physical quantities. Thus, diffusion has a significantly higher impact in small HoC devices than in a real full-sized body. One of
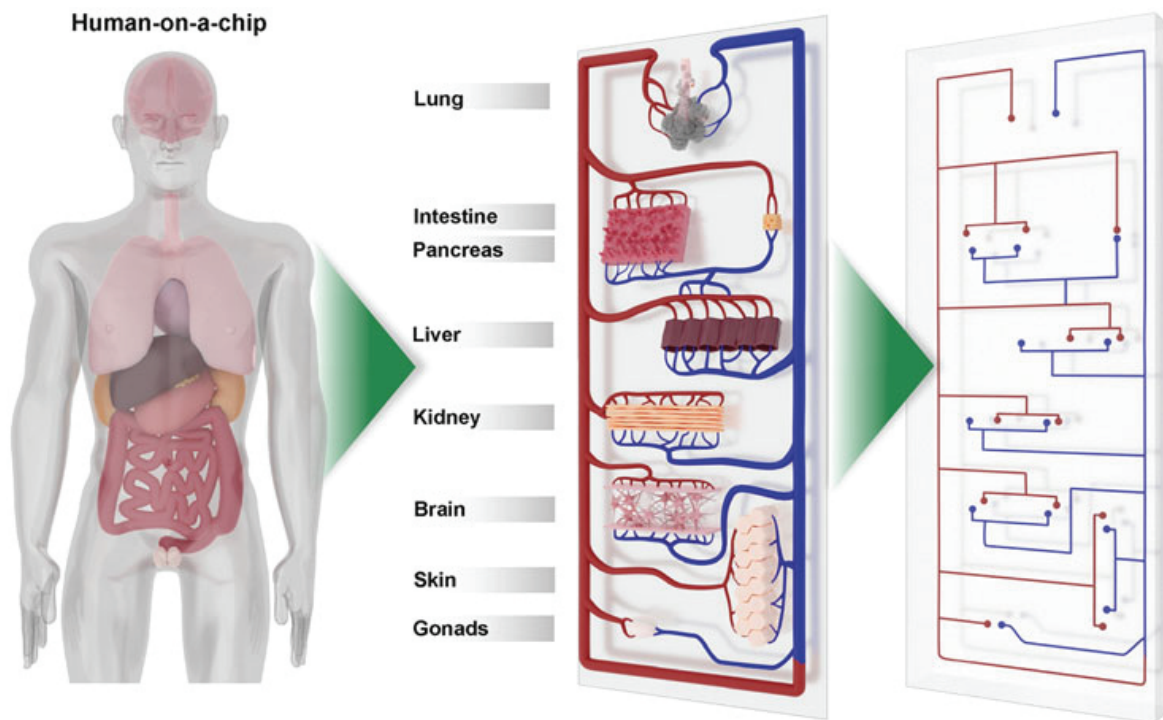
Fig. 8.10 Schematic presentation of a "human-on-a-chip" (HoC). In a HoC several different organ-on-a-chip systems are combined to simulate the physiology of the human body

the main issues with engineering HoCs for pharmacokinetic drug testing is that scaling does not change enzyme/protein affinities. As a result, a liver-on-a-chip may not produce a physiological relevant concentration of drug metabolites—which further cannot activate or block their targets or off-targets in a lung-on-a-chip. Residence-time-based scaling seeks to tackle this issue by determining the concentrations drugs and metabolites inside the OoCs and then replicating physiologically relevant drug concentrations.

OoCs must also be connected in the correct way within a HoC. For instance, nutrient uptake starts with absorption in the gut, which is first delivered to the liver via the portal vein, then modified and released into the bloodstream, and then partially excreted by the kidney. As a result, the chip must include interconnecting channels that mimic all of these different main connection pathways (e.g., the bloodstream, the urine stream, etc.). Depending on the device, organs can be created inside the chip simultaneously in a universal medium, separately with a subsequent combination, or even partially combined by connecting and counterbalancing two OoCs first [47]. The last two approaches offer the possibility of OoC exchange. In other words, a single impaired OoC can be readily replaced and does not necessarily lead to dysfunction within the larger system. Furthermore, culturing cells of different OoCs with a single medium is challenging, because a single common medium cannot satisfy the specific needs of every cell type, and the device may not maintain its supposed function. In consequence, a flexible approach had been proposed, where organs can be cultured separately and connected as soon as they are needed for an experiment [47].
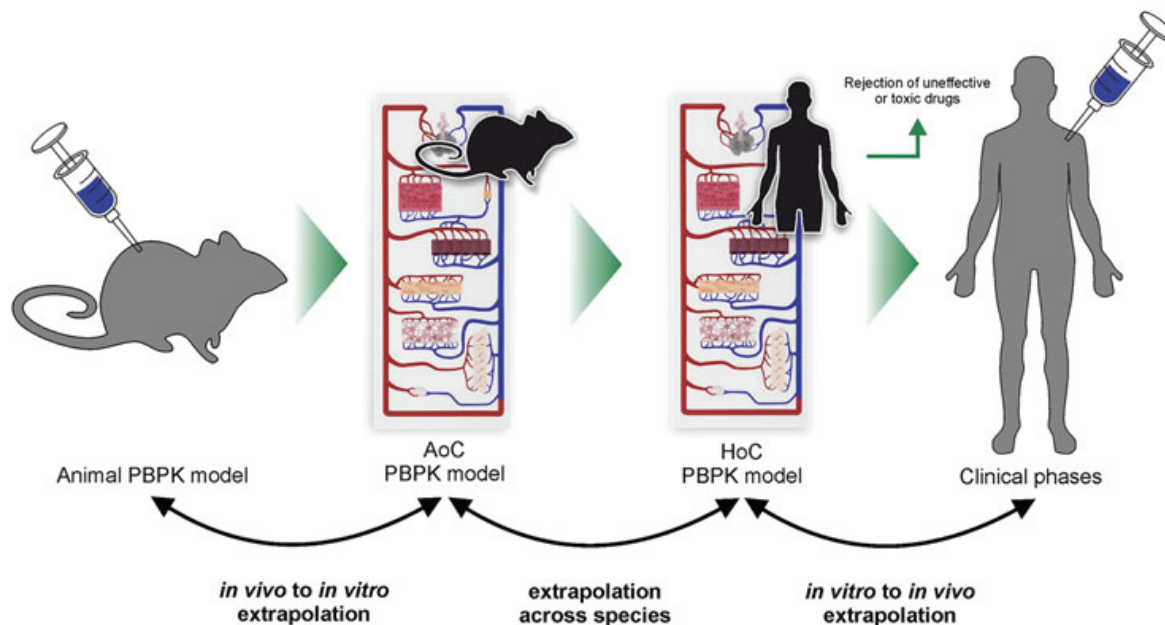
8.6.2 "Human-on-a-Chip"

To date, multi-organ-on-a-chip devices predominantly integrate OoCs which are of particular interest for pharmaceutical industry—such as the liver, kidney, gut, skin, and lungs. These organs are crucial for pharmacokinetic investigations of adsorption, distribution, metabolism, excretion, and toxicity (ADME-Tox) of pharmaceutical compounds within the human body.

The ADME-Tox behavior of a compound is currently described via animal experiments, and, as a result, the highest potential for HoCs using human cells can be seen in ADME-Tox characteristics that are highly species-dependent—such as metabolism and toxicity. The metabolism of a compound, particularly within the liver, often differs widely between animals and human—leading to very different by-products with different levels of toxicity. While in vitro cell cultures of human liver cells are already being used to investigate and assess these by-products for basic liver toxicity, detecting and understanding possible toxic effects within other organs remains a project for future studies. HoC technology promises to open that door to researchers. But many other parameters of the ADME-Tox process can also be monitored within HoCs: In contrast to animals, a HoC can be comprehensively modified and adapted to allow the integration of sensor spots or live cell imaging to monitor changes in the concentrations of pH, oxygen, or metabolites of interest, as well as cell morphologies and cell culture properties.

One important caveat: HoCs are still in development, and at this point, it remains highly challenging to attempt to mimic all important organ functions for reliable ADME-Tox predictions (and thereby truly replace animal testing). As a result, from a practical perspective, in the context of drug testing HoCs are perhaps best viewed as a gradual complement to animal testing rather than a complete replacement looming on the horizon. This complementation can be obtained by comparing physiologically based pharmacokinetic (PBPK) models gained from animal experiments, animal-on-a-chip (AoC) systems, and HoC systems (Fig. 8.11) [48]. The AoC acts as a linker for in vivo to in vitro extrapolation, where its PBPK is optimized to match the PBPK from animal experiments. Following this, the AoC PBPK can be extrapolated across species by comparing it to the PBPK of the corresponding HoC. Thus, in principle at least, a HoC with the same design should fit the AoC PBPK model, when a drug has the same behavior in animal and in human. In turn, differences in these models could help to identify deviant pharmacokinetic characteristics of a drug and thereby help to prevent drug failure in later (and more costly) clinical stages.

8.6.3 "Disease-on-a-Chip"

Engineering a disease-on-a-chip (DoC) is another promising application for tissue engineers. In principle, a DoC is nothing more than a slightly modified OoC. Nevertheless, in practice, the DoC is even more complex—because it needs to reconstruct disease processes as well as organ functions. This can include the use of genetically modified cells; the targeted integration or reconstruction of dysfunctional tissues; or the integration

Fig. 8.11 The future role of human-on-a-chip systems in drug development. Pharmacokinetic and pharmacodynamic data of animal experiments are summarized to a physiologically based pharmacokinetic model (PBPK). This model will be used for in vivo to in vitro extrapolation to develop a reliable animal-on-a-chip model (AoC). In turn, the PBPK of the AoC will be used for the extrapolation to human and for the development of a HoC. Finally, the HoC PBPK model will help to reject ineffective or toxic drugs before entering costly and time-consuming clinical phases

of tissue-unrelated cell types or even organisms. A simple example of reconstructing a disease is the thrombosis-on-a-chip [49]. A thrombosis includes the agglomeration of thrombocytes at the vascular wall that form a thrombus, which then blocks the blood flow in the vein. First, a vessel-on-a-chip system is constructed by forming hydrogel into a chip including channels for liquid flow, where endothelial cells have been seeded and cultured. Then, the disease element is integrated into the system by inducing thrombosis in a blood flow inside the channels using calcium chloride ($CaCl_2$).

Like OoCs, DoCs can serve as in vivo-like platforms to reduce animal experiments and offer higher reliabilities by using human cells. But DoCs can also be used to investigate the activity of drug candidates and observe how they counteract specific diseases. In contrast to using animal models, the comparative accessibility of a chip creates new opportunities for researchers to observe and understand disease processes—particularly on the microcellular or intercellular level. A cancer-on-a-chip platform is a prominent example of reconstructing and investigating tumor processes. The altered metabolism and the resulting tumor environment have been observed by culturing tumor cells in a 3D gel matrix with constant perfusion [50]. The artificial tumor created pH and oxygen gradients that led to different gene expression profiles dependent on the location in the tumor.

Cancer-on-a-chip platforms are also of particular interest for personalized DoCs, because tumor cells develop due to several random mutations in the cell genome, and

every tumor can therefore evidence a slightly different behavior—even when the main tumor growth-inducing mutations are nearly identical. As a result, personalized platforms are favored by integrating tumor cells of a single patient into DoCs for subsequent drug screenings to rapidly establish patient-specific therapies.

Although research into OoCs, HoCs, and DoCs remains at a very early stage at this time of this publication, these microfluidic 3D cell culture platforms are developing rapidly. Companies are investing extensively into promising new biotechnologies, and OoC start-ups are popping up all over the world—highlighting the tremendous promise that these systems offer to revolutionize the fields of cell cultivation, tissue engineering, and medical research in general.

> **Take-Home Message**
> - Microfluidics involve the precise control of minute amounts of fluids within complex channel systems at low flow rates.
> - "Lab-on-a-chip" systems are microfluidic chips that allow the miniaturization and automation of lab procedures such as DNA sequencing, point-of-care diagnostics, cell transfection, single cell analysis, and parallel cell culture.
> - Microfluidic chips are commonly fabricated via soft lithography or emerging 3D printing techniques.
> - An "organ-on-a-chip" (OoC) is a cell culture system typically inside a microfluidic chip that mimics the minimal functional unit of a specific organ.
> - A "human-on-a-chip" (HoC) combines several OoC systems to mimic human physiology.
> - A "disease-on-a-chip" (DoC) is an OoC or HoC system which additionally mimics a pathophysiologic process.
> - OoCs, HoCs, and DoCs all hold immense promise for revolutionizing drug testing in the pharmaceutical industry.

References

1. Whitesides GM. The origins and the future of microfluidics. Nature. 2006;442:368–73. https://doi.org/10.1038/nature05058.
2. Pandey CM, Augustine S, Kumar S, et al. Microfluidics based point-of-care diagnostics. Biotechnol J. 2018;13:1700047. https://doi.org/10.1002/biot.201700047.
3. Weibel DB, Whitesides GM. Applications of microfluidics in chemical biology. Curr Opin Chem Biol. 2006;10:584–91. https://doi.org/10.1016/j.cbpa.2006.10.016.
4. Whitesides GM, Ostuni E, Takayama S, Jiang X, Ingber DE. Soft lithography in biology and biochemistry. Annu Rev Biomed Eng. 2001;3(1):335–73.
5. Siller IG, Enders A, Steinwedel T, et al. Real-time live-cell imaging technology enables high-throughput screening to verify in vitro biocompatibility of 3D printed materials. Materials (Basel). 2019;12:2125. https://doi.org/10.3390/ma12132125.

6. Siller IG, Enders A, Gellermann P, et al. Characterization of a customized 3D-printed cell culture system using clear, translucent acrylate that enables optical online monitoring. Biomed Mater. 2020;15:055007. https://doi.org/10.1088/1748-605X/ab8e97.

7. Yeo LY, Chang H-C, Chan PPY, et al. Microfluidic devices for bioapplications. Small. 2011;7:12–48. https://doi.org/10.1002/smll.201000946.

8. Blazej RG, Kumaresan P, Mathies RA. Microfabricated bioprocessor for integrated nanoliter-scale sanger DNA sequencing. Proc Natl Acad Sci U S A. 2006;103:7240–5. https://doi.org/10.1073/pnas.0602476103.

9. Aborn JH, El-Difrawy SA, Novotny M, et al. A 768-lane microfabricated system for high-throughput DNA sequencing. Lab Chip. 2005;5:669–74. https://doi.org/10.1039/b501104c.

10. Chin CD, Linder V, Sia SK. Commercialization of microfluidic point-of-care diagnostic devices. Lab Chip. 2012;12:2118–34. https://doi.org/10.1039/c2lc21204h.

11. Arshavsky-Graham S, Enders A, Ackerman S, et al. 3D-printed microfluidics integrated with optical nanostructured porous aptasensors for protein detection. Microchim Acta. 2021;188:67. https://doi.org/10.1007/s00604-021-04725-0

12. Bahnemann J, Rajabi N, Fuge G, et al. A new integrated lab-on-a-chip system for fast dynamic study of mammalian cells under physiological conditions in bioreactor. Cell. 2013;2:349–60. https://doi.org/10.3390/cells2020349.

13. Rajabi N, Bahnemann J, Tzeng T-N, et al. Lab-on-a-chip for cell perturbation, lysis, and efficient separation of sub-cellular components in a continuous flow mode. Sensors Actuators A Phys. 2014;215:136–43. https://doi.org/10.1016/j.sna.2013.12.019.

14. Enders A, Siller IG, Urmann K, et al. 3D printed microfluidic mixers-a comparative study on mixing unit performances. Small. 2019;15:e1804326. https://doi.org/10.1002/smll.201804326.

15. Capretto L, Cheng W, Hill M, et al. Micromixing within microfluidic devices. Top Curr Chem. 2011;304:27–68. https://doi.org/10.1007/128_2011_150.

16. Nguyen N-T, Wu Z. Micromixers—a review. J Micromech Microeng. 2005;15:R1–R16. https://doi.org/10.1088/0960-1317/15/2/R01.

17. Di Carlo D. Inertial microfluidics. Lab Chip. 2009;9:3038–46. https://doi.org/10.1039/b912547g.

18. Probst C, Grünberger A, Wiechert W, et al. Polydimethylsiloxane (PDMS) sub-Micron traps for single-cell analysis of bacteria. Micromachines (Basel). 2013;4:357–69. https://doi.org/10.3390/mi4040357.

19. Grünberger A, Wiechert W, Kohlheyer D. Single-cell microfluidics: opportunity for bioprocess development. Curr Opin Biotechnol. 2014;29:15–23. https://doi.org/10.1016/j.copbio.2014.02.008.

20. Gao J, Yin X-F, Fang Z-L. Integration of single cell injection, cell lysis, separation and detection of intracellular constituents on a microfluidic chip. Lab Chip. 2004;4:47–52. https://doi.org/10.1039/b310552k.

21. Hung PJ, Lee PJ, Sabounchi P, et al. Continuous perfusion microfluidic cell culture array for high-throughput cell-based assays. Biotechnol Bioeng. 2005;89:1–8. https://doi.org/10.1002/bit.20289.

22. Gómez-Sjöberg R, Leyrat AA, Pirone DM, et al. Versatile, fully automated, microfluidic cell culture system. Anal Chem. 2007;79:8557–63. https://doi.org/10.1021/ac071311w.

23. Siller IG, Epping N-M, Lavrentieva A, et al. Customizable 3D-printed (co-)cultivation systems for in vitro study of angiogenesis. Materials (Basel). 2020;13:4920. https://doi.org/10.3390/ma13194290.

24. Zhang J, Wei X, Zeng R, et al. Stem cell culture and differentiation in microfluidic devices toward organ-on-a-chip. Future Sci OA. 2017;3:FSO187. https://doi.org/10.4155/fsoa-2016-0091.

25. Marx U, Andersson TB, Bahinski A, et al. Biology-inspired microphysiological system approaches to solve the prediction dilemma of substance testing. ALTEX. 2016;33:272–321. https://doi.org/10.14573/altex.1603161.

26. Cecchi E, Giglioli C, Valente S, et al. Role of hemodynamic shear stress in cardiovascular disease. Atherosclerosis. 2011;214:249–56. https://doi.org/10.1016/j.atherosclerosis.2010.09.008.

27. Zhang B, Radisic M. Organ-on-a-chip devices advance to market. Lab Chip. 2017;17:2395–420. https://doi.org/10.1039/c6lc01554a.

28. Zhang B, Korolj A, Lai BFL, et al. Advances in organ-on-a-chip engineering. Nat Rev Mater. 2018;3:257–78. https://doi.org/10.1038/s41578-018-0034-7.

29. Zhang B, Montgomery M, Chamberlain MD, et al. Biodegradable scaffold with built-in vasculature for organ-on-a-chip engineering and direct surgical anastomosis. Nat Mater. 2016;15:669. https://doi.org/10.1038/nmat4570.

30. Du Y, Li N, Yang H, et al. Mimicking liver sinusoidal structures and functions using a 3D-configured microfluidic chip. Lab Chip. 2017;17:782–94. https://doi.org/10.1039/c6lc01374k.

31. Domansky K, Inman W, Serdy J, et al. Perfused multiwell plate for 3D liver tissue engineering. Lab Chip. 2010;10:51–8. https://doi.org/10.1039/b913221j.

32. Lee PJ, Hung PJ, Lee LP. An artificial liver sinusoid with a microfluidic endothelial-like barrier for primary hepatocyte culture. Biotechnol Bioeng. 2007;97:1340–6. https://doi.org/10.1002/bit.21360.

33. Hedaya MA. Basic pharmacokinetics, Pharmacy education series. 2nd ed. Hoboken: CRC Press; 2012.

34. Jang K-J, Mehr AP, Hamilton GA, et al. Human kidney proximal tubule-on-a-chip for drug transport and nephrotoxicity assessment. Integr Biol (Camb). 2013;5:1119–29. https://doi.org/10.1039/c3ib40049b.

35. Musah S, Mammoto A, Ferrante TC, et al. Mature induced-pluripotent-stem-cell-derived human podocytes reconstitute kidney glomerular-capillary-wall function on a chip. Nat Biomed Eng. 2017;1:0069. https://doi.org/10.1038/s41551-017-0069.

36. Weinberg E, Kaazempur-Mofrad M, Borenstein J. Concept and computational design for a bioartificial nephron-on-a-chip. Int J Artif Organs. 2008;31:508–14. https://doi.org/10.1177/039139880803100606.

37. Sciancalepore AG, Sallustio F, Girardo S, et al. A bioartificial renal tubule device embedding human renal stem/progenitor cells. PLoS One. 2014;9:e87496. https://doi.org/10.1371/journal.pone.0087496.

38. Kim S, LesherPerez SC, Kim BCC, et al. Pharmacokinetic profile that reduces nephrotoxicity of gentamicin in a perfused kidney-on-a-chip. Biofabrication. 2016;8:15021. https://doi.org/10.1088/1758-5090/8/1/015021.

39. Ng CP, Zhuang Y, Lin AWH, et al. A fibrin-based tissue-engineered renal proximal tubule for bioartificial kidney devices: development, characterization and in vitro transport study. Int J Tissue Eng. 2013;2013:1–10. https://doi.org/10.1155/2013/319476.

40. Homan KA, Kolesky DB, Skylar-Scott MA, et al. Bioprinting of 3D convoluted renal proximal tubules on perfusable chips. Sci Rep. 2016;6:34845. https://doi.org/10.1038/srep34845.

41. Maschmeyer I, Lorenz AK, Schimek K, et al. A four-organ-chip for interconnected long-term co-culture of human intestine, liver, skin and kidney equivalents. Lab Chip. 2015;15:2688–99. https://doi.org/10.1039/c5lc00392j.

42. Skardal A, Murphy SV, Devarasetty M, et al. Multi-tissue interactions in an integrated three-tissue organ-on-a-chip platform. Sci Rep. 2017;7:8837. https://doi.org/10.1038/s41598-017-08879-x.

43. Miller PG, Shuler ML. Design and demonstration of a pumpless 14 compartment microphysiological system. Biotechnol Bioeng. 2016;113:2213–27. https://doi.org/10.1002/bit.25989.
44. Tsamandouras N, Chen WLK, Edington CD, et al. Integrated gut and liver microphysiological systems for quantitative in vitro pharmacokinetic studies. AAPS J. 2017;19:1499–512. https://doi.org/10.1208/s12248-017-0122-4.
45. Abaci HE, Shuler ML. Human-on-a-chip design strategies and principles for physiologically based pharmacokinetics/pharmacodynamics modeling. Integr Biol (Camb). 2015;7:383–91. https://doi.org/10.1039/c4ib00292j.
46. Wikswo JP, Block FE, Cliffel DE, et al. Engineering challenges for instrumenting and controlling integrated organ-on-chip systems. IEEE Trans Biomed Eng. 2013;60:682–90. https://doi.org/10.1109/TBME.2013.2244891.
47. Rogal J, Probst C, Loskill P. Integration concepts for multi-organ chips: how to maintain flexibility?! Future Sci OA. 2017;3:FSO180. https://doi.org/10.4155/fsoa-2016-0092.
48. Esch MB, King TL, Shuler ML. The role of body-on-a-chip devices in drug and toxicity studies. Annu Rev Biomed Eng. 2011;13:55–72. https://doi.org/10.1146/annurev-bioeng-071910-124629.
49. Zhang YS, Davoudi F, Walch P, et al. Bioprinted thrombosis-on-a-chip. Lab Chip. 2016;16:4097–105. https://doi.org/10.1039/c6lc00380j.
50. Ayuso JM, Virumbrales-Munoz M, McMinn PH, et al. Tumor-on-a-chip: a microfluidic model to study cell response to environmental gradients. Lab Chip. 2019;19:3461–71. https://doi.org/10.1039/c9lc00270g.
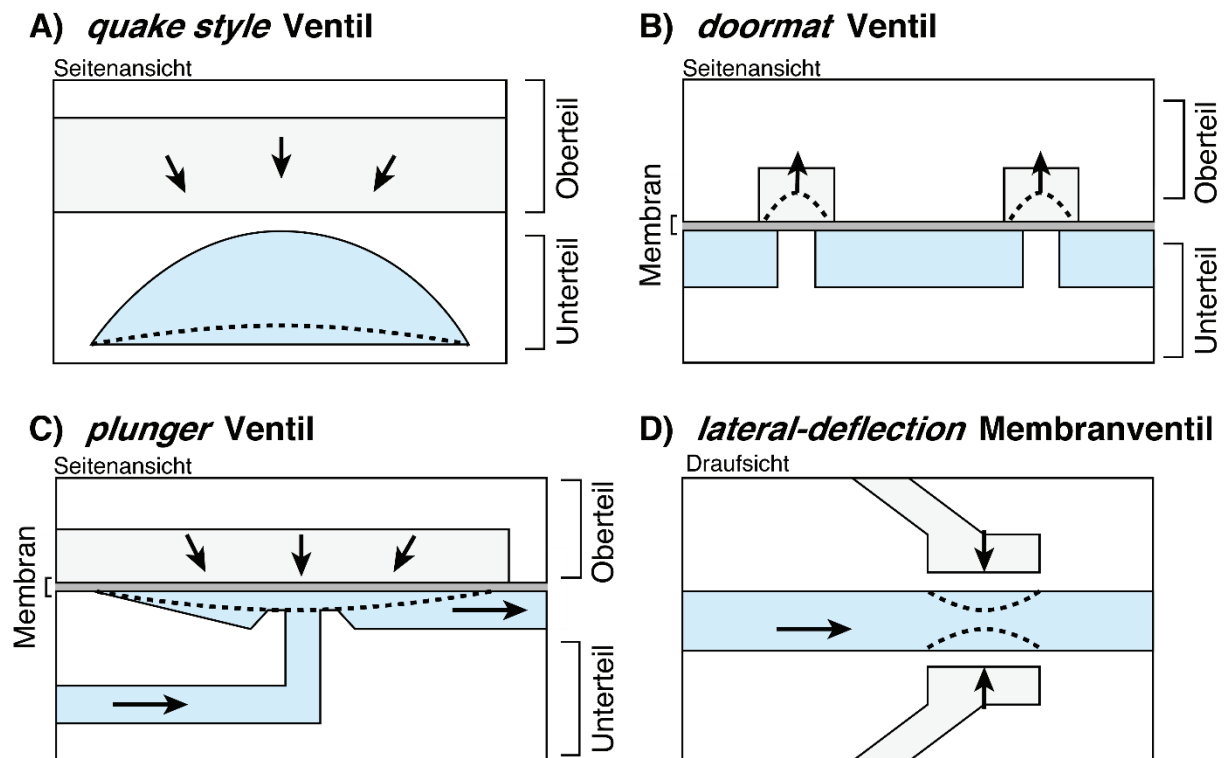
3.4 Automatisierung mikrofluidischer Zellkultursysteme

Zur Automatisierung sowie Parallelisierung mikrofluidischer Zellkultursysteme werden zunehmend soge-nannte Mikroventile genutzt. Mikroventile werden direkt während des Fertigungsprozesses in das mikro-fluidische System integriert und besitzen Abmessungen im Mikrometerbereich mit äußerst geringen inter-nen Volumina von wenigen Nanolitern [90]. Sie finden schon länger Anwendung für verschiedenste LOC-Systeme und können zur Steuerung der Mediumversorgung von integrierten Zellkulturkammern verwendet werden. Durch Verwendung multipler Mikroventile in einem System können diese Kammern parallelisiert werden. Dies ermöglicht unter anderem die Entwicklung und Automatisierung mikrofluidischer Zellkultur-assays, wie es in einer Machbarkeitsstudie auch Ziel dieser Arbeit ist.

Die Automatisierung von Zellkulturassays ist durch Pipettierroboter allerdings schon länger gegeben. Der Mehrwert automatisierter mikrofluidischer Ventilsysteme besteht vielmehr in der Möglichkeit, auch *organ-on-a-chip* Systeme automatisieren zu können. Viele dieser mikrofluidischen Zellkultursysteme müssen für eine ausreichende Versorgung mit Nährstoffen und Sauerstoff aktiv mit Medium durchströmt werden. Pi-pettierroboter können einen solchen Mediumstrom i.d.R. nicht erzeugen, mikrofluidische Ventilsysteme hingegen schon. Außerdem sind viele mikrofluidische Zellkultursysteme hoch individualisiert und entspre-chen selten den Formaten standardisierter Gewebekulturplatten, auf die Pipettierroboter spezialisiert sind. Insbesondere 3D-gedruckte mikrofluidische Ventilsysteme, wie das in Kapitel 4.2 (s. Seite 86) vorgestellte Mikroventilsystem, können leicht angepasst werden, um den unterschiedlichsten Formaten zu entsprechen.

Mikroventile setzen sich aus Ventiltyp und Aktuationsprinzip zusammen, welche in **Abbildung 3** bzw. **Abbildung 4** zusammengefasst sind [91]. Die am häufigsten verwendeten Ventiltypen (s. **Abbildung 3**) sind binäre Ventile, die das Schließen bzw. das Öffnen eines einzelnen Kanals ermöglichen. Diese liegen dabei entweder in einem normalerweise geschlossenen (engl.: *normally closed,* n.c.) oder normalerweise geöffneten (engl.: *normally open,* n.o.) Zustand vor. Die allerersten n.o. Mikroventile, die *quake style* Mikro-ventile benannt nach dem Entwickler Prof. Dr. Stephen R. Quake, bestehen aus zwei mikrostrukturierten PDMS-Schichten [92]. Durch Anlegen einer äußeren Kraft (i.d.R. pneumatisch) presst sich das Oberteil des Chips in einen halbzirkularen, mikrofluidischen Kanal des Unterteils und blockiert ihn. Ein Ventiltyp in normalerweise geschlossener Stellung ist das *doormat* (dt.: Fußmatte) Ventil, welches eine Membran als flexibles Element besitzt und i.d.R. durch Anlegen von Unterdruck geöffnet wird [93]. Das in dieser Arbeit (s. Kapitel 4.2) verwendete Design des *plunger* Mikroventils (dt.: Kolbenventil), welches sich von dem klas-sischen Kolbenventil ableitet, besitzt ebenfalls eine Membran, welche jedoch nicht parallel sondern ortho-gonal zum zu verschließenden Kanal orientiert ist [94]. Die Membran wird ausgelenkt und verschließt durch Anpressen an einen Ventilsessel die runde Kanalöffnung. Das *lateral-deflection membrane valve* (dt.: seit-lich auslenkendes Membranventil) besitzt eine Membran, welche den Kanal wiederum seitlich verschließt [95]. Dies bringt Vorteile in der Fertigung, da die Membran als Teil einer Schicht eines PDMS-Chips gefertigt

werden kann und nicht nachträglich integriert werden muss. Allerdings können dadurch nur Kanäle mit rechteckigem Querschnitt gebildet werden, was in einer unvollständiger Ventilschließung resultiert [91].

A) *quake style* **Ventil**

Seitenansicht

B) *doormat* **Ventil**

Seitenansicht

C) *plunger* **Ventil**

Seitenansicht

D) *lateral-deflection* **Membranventil**

Draufsicht

Abbildung 3: Schematische Darstellung des Funktionsprinzips zur Automatisierung mikrofluidischer Systeme verwendeter Mikroventile in ihrer Standardkonfiguration (weiß: mikrofluidischer Chip; blau: mikrofluidischer Kanal; grau: Kontrollkanal, an den zur Schließung/Öffnung des Ventils Druck bzw. Vakuum angelegt wird). **A)** Beim *quake style* Mikroventil wird der mikrofluidische Kanal durch Luftdruck von einem darüber liegenden Kontrollkanal verschlossen. **B)** Das *doormat* Ventil ist ein normalerweise geschlossenes Mikroventil, bei dem über das Anlegen von Unterdruck die verschließende Membran verformt und der Kanal geöffnet wird. **C)** Beim *plunger* Ventil wird eine Membran auf einen darunter liegenden Ventilsessel gedrückt und eine Kanalöffnung des mikrofluidischen Kanals verschlossen. **D)** Beim *lateral-deflection* Membranventil liegen Kontrollkanäle und der mikrofluidische Kanal in einer Ebene. Durch Verformung einer dünnen Membran wird der Kanal seitlich geschlossen. (Eigene Darstellung erstellt mit Adobe Illustrator 2019)

Das Aktuationsprinzip von Mikroventilen (s. **Abbildung 4**), also der Mechanismus zur Öffnung und Schließung eines Ventils, ist entscheidend für die Automatisierbarkeit, Herstellung und den Fußabdruck (die auf dem Chip eingenommene Fläche) der Ventile. Eines der wichtigsten Prinzipien ist die pneumatische Aktuation, bei der eine dünne Silikonwand bzw. eine integrierte flexible Membran durch das Anlegen von Über- bzw. Unterdruck an einen über dem zu steuernden Kanal befindlichen Kontrollkanal ausgelenkt wird [96, 97]. Dabei wird das eigentliche Schaltsignal für das Ventil an ein externes, an den Kontrollkanal angeschlossenes Magnetventil verlagert. Dadurch ist der Fußabdruck eines Ventils besonders klein. Zudem können etablierte Magnetventile als externe Ventile eingesetzt werden, wodurch die Verlässlichkeit des Systems erhöht wird. Zentrale Nachteile dieses Prinzips sind die Notwendigkeit zusätzlicher Kontrollkanäle und die dafür notwendigen zusätzlichen Anschlüsse am Chip sowie der Einsatz von Zuleitungen, externen Ventilen und einer Pneumatikquelle. Dies vergrößert Aufbauten, erhöht die Kosten, verkompliziert die Steuerung und erhöht die generelle Fehleranfälligkeit des Systems. Wichtige Alternativen zur pneumatischen

Aktuation sind die piezoelektrische [98], (elektro)magnetische [99], thermische [100] oder mechanische [101] Aktuation. Diese sind im Vergleich zur pneumatischen Steuerung oftmals mit einem größeren Fußabdruck und aufwendigerer Fertigung verbunden, ergeben jedoch meist einen kompakteren Gesamtaufbau. Zudem werden auch sehr spezielle Aktuationsmechanismen entwickelt, wie die Steuerung der Ventile über Licht, akustische Wellen oder sogar biologische Sensoren [96].

A) pneumatisch   B) piezoelektisch   C) magnetisch

D) thermisch   E) mechanisch
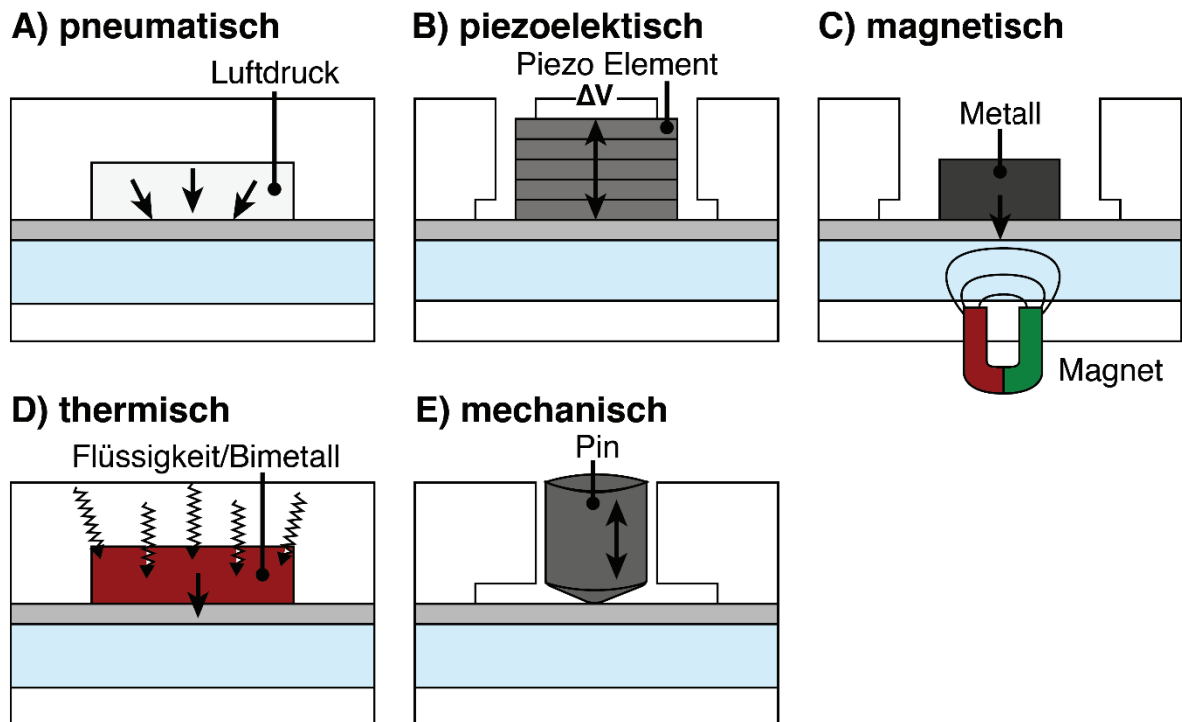
Abbildung 4: Schematische Darstellung verschiedener Aktuationsprinzipien mikrofluidischer Ventile. **A)** Bei der pneumatischen Aktuation wird die Membran zur Ventilschließung durch Luftdruck (nicht gezeigt) verformt. **B)** Piezoelektrisch geschaltete Ventile nutzen den Piezoelektrischen Effekt, bei dem die Verformung eines Piezoelements durch Anlegen einer Spannung das Ventil schließt bzw. öffnet. **C)** Bei (elektro)magnetischen Mikroventilen wird die Anziehung zwischen Metall und Magnet zur Schließung des Ventils ausgenutzt. **D)** Eine thermische Ventilschließung wird über die Ausdehnung von Flüssigkeiten oder Bimetallen, die sich unter Erhitzung Ausdehnen bzw. verformen, erreicht. **E)** Die mechanische Schließung kann durch das vertikale Anpressen eines Pins oder einer Schraube erreicht werden. (Eigene Darstellung erstellt mit Adobe Illustrator 2019)

Neben binär schaltbaren Ventilen werden auch miniaturisierte Proportionalventile entwickelt, welche durch eine partielle Schließung den Durchfluss gezielt regulieren können [102, 103]. Auf diese Weise können mikrofluidische Zellkultursysteme konstant mit Medium perfundiert werden und gleichzeitig der Anteil von Mediumzusätzen variiert werden. Somit ist einerseits ein permanenter Medium- und Sauerstoffaustausch gegeben und andererseits können komplexe, zeit- und konzentrationsaufgelöste Assays durchgeführt werden. Allerdings sind die Fertigung und präzise Steuerung dieses Mikroventiltyps schwieriger. Außerdem benötigt es für exakt dosierte Volumenströme bei Systemen mit mehreren Eingangs- und Ausgangskanälen i.d.R. eine Durchflusskontrolle und Regelung, da sich gebildete Differenzdrücke an verschiedenen Ventilen gegenseitig beeinflussen können. Des Weiteren können auch passive Mikroventile einge-

setzt werden wie z.B. das *check valve* (dt.: Rückschlagventil) [104, 105] oder das *burst valve* (dt.: Bruch-ventil) [106], welche einen Rückfluss verhindern bzw. ab einem vordefinierten Druck brechen. Diese werden jedoch weniger für die Automatisierung mikrofluidischer Zellkultursysteme eingesetzt.

Neben integrierten Mikroventilen für die Automatisierung mikrofluidischer Systeme können auch klassi-sche Magnetventile genutzt werden. Beispielsweise konnte durch die Verwendung miniaturisierter Mag-netventile, welche an den mikrofluidischen Chip angeschraubt werden, bereits komplexe Schaltungen re-alisiert werden [48]. Solche Ventile sind jedoch für die Regelung von Medienströmen für die Zellkultur aufgrund der auszuschließenden Sterilisation integrierter elektronischer Bauteile durch Heißdampf oder Bestrahlung weniger geeignet.

Zur Automatisierung mikrofluidischer Zellkultursysteme werden derzeit oft pneumatische Systeme ver-wendet. Beispielsweise wurden mesenchymale Stammzellen in 96 unabhängige mikrofluidische Kammern als Monolayer integriert und anschließend die Auswirkungen vorprogrammierter Protokolle auf die Prolife-ration, osteogene Differenzierung und Bewegung untersucht [107]. Eine Automatisierung der Versorgung erster 3D-Zellkulturen, wie Tumor-Organoiden, konnte durch eine Kombination aus einer mikrofluidischen Zellkulturplattform und einem mikrofluidischen Ventilsystem realisiert werden [108]. Interessant ist dabei die Trennung des mikrofluidischen Ventilsystems von der mikrofluidischen Zellkulturplattform. Diese Mo-dularität ermöglicht den nachträglichen Austausch der Zellkulturplattform. Somit kann das Design der Zellkulturplattform weitesgehend unabhängig vom mikrofluidischen System gestaltet werden. Dieser Vor-teil kann mitunter auch in einer getrennten Fertigung der beiden Module genutzt werden [28].

4 Experimenteller Teil

Die vorliegende Dissertation besteht aus vier verschiedenen Teilen, die sich mit dem Einsatz der Mikrofluidik für die Biotechnologie mit speziellem Fokus auf mikrofluidische Zellkultursysteme sowie den 3D-Druck zur Herstellung automatisierter mikrofluidischer Zellkultursysteme befassen. Jeder Teil wurde separat in peer-reviewten Fachzeitschriften veröffentlicht.

Dabei wurde in dem bereits beschriebenen ersten Teil dieser Arbeit (s. Kapitel 3.1.1, Seite 5) die Rolle der Mikrofluidik in der Biotechnologie diskutiert und Zukunftstechnologien dieses interdisziplinären Forschungsfeldes identifiziert. Durch die Charakterisierung einiger hundert Biotechnologieunternehmen, die mikrofluidische Systeme in ihren Produkten verwenden, konnten Hauptanwendungsfelder der Mikrofluidik in der Biotechnologie identifiziert und deren Zukunftspotential eingeschätzt werden. Außerdem wurden besonders vielversprechende Technologien der Mikrofluidik und ihre Verwendung als sogenannte *point-of-use* (dt.: an dem Ort der Anwendung verwendbar) Systeme in der Biotechnologie diskutiert. In einem weiteren vorrausgehenden Teil dieser Arbeit (s. Kapitel 3.3, Seite 39) wurde der Einsatz mikrofluidischer Systeme in der Zellkultur behandelt und der Nutzen, die Funktionsweise und die Anwendungen von *organ-on-a-chip* (OOC) Systemen erörtert.

Der experimentelle Teil setzt sich aus dem dritten und vierten Teil dieser Arbeit zusammen. Im dritten Teil wurde die Biokompatibilität des 3D-Druckmaterials VisiJet M2S-HT90 (3D Systems Inc.) gegenüber verschiedenen Zelltypen untersucht. Dieses mit dem hochauflösendem MJP 3D-Druckverfahren hergestellte, hitzestabile Polyacrylat erlaubt prinzipiell die Fertigung autoklavierbarer, mikrofluidischer Systeme. Um es auch für die Fertigung neuartiger Zellkultursysteme wie OOC Systeme einsetzen zu können, wurde es auf Biokompatibilität getestet. Dabei wurden gezielt Zelltypen verwendet, die vielfach in Forschung und Industrie eingesetzt werden. Des Weiteren wurde der Einfluss der Heißdampfsterilisation als gängigste Sterilisationsmethode auf die Biokompatibilität untersucht. Die Biokompatibilität gegenüber Mausfibroblasten und Hefen blieb nach Heißdampfsterilisation unbeeinflusst. Die Ergebnisse erlauben somit die Verwendung eines neuartigen, hitzebeständigen 3D-Druckmaterials zur Fertigung 3D-gedruckter, autoklavierbarer mikrofluidischer Zellkultursysteme.

In dem letzten Teil dieser Arbeit konnte das charakterisierte 3D-Druckmaterial zur Fertigung eines 3D-gedruckten, mikrofluidischen Ventilsystems zur Automatisierung von Zellkulturassays verwendet werden. Dieses System zeigt eindrucksvoll den Prozess vom ersten Design bis zur automatisierten Anwendung in drei Schritten: 1) Dem Design und der Entwicklung des 3D-gedruckten Ventilsystems, 2) dessen Automatisierung durch Motoren, Pumpen und Computer und 3) letztendlich der Charakterisierung und Anwendung in einem automatisierten Zellkulturassay. Besonders hervorzuheben ist, dass das 3D-gedruckte, mikrofluidische Ventilsystem eine hohe Mischungsgenauigkeit aufweist. Somit konnten in einem automatisierten mikrofluidischen Zytotoxizitätsassay als Machbarkeitsstudie ebenso gute Ergebnisse erzielt werden wie in einem pipettierten Assay.

Im Gegensatz zu Pipettiertechniken kann das entwickelte mikrofluidische Ventilsystem nicht nur zur Automatisierung von 2D Zellkulturassays sondern prinzipiell auch zur Automatisierung mikrofluidischer Zellkultursysteme genutzt werden. Außerdem wurden mit dieser Arbeit alle verwendeten Originaldateien der 3D-Modelle und der für die Automatisierung benötigten Python Skripte veröffentlicht. Somit können auch andere Wissenschaftler:innen das System individualisieren und auf diese Weise von den Vorteilen der 3D-Druck Technologie profitieren.

Diese Arbeit demonstriert den vollständigen Prozess von der Biokompatibilitätstestung eines neuen 3D-Druckmaterials bis hin zur Anwendung 3D-gedruckter mikrofluidischer Systeme in der Zellkultur. Von nun an können Wissenschaftler:innen das untersuchte Material zur Fertigung eigener autoklavierbarerer Zellkultursysteme nutzen. Für die Automatisierung ihrer Systeme können sie dabei unmittelbar auf ein bereits charakterisiertes, automatisiertes mikrofluidisches Ventilsystem zurückgreifen. Auf diese Weise wird dazu beigetragen, dass mikrofluidische Systeme in Zukunft vermehrt auch in der Zellkultur genutzt werden können.

4.1 *In vitro* Biokompatibilitätsbestimmungen eines hitzebeständigen 3D-Druckmaterials zur Anwendung in der Zellkultur
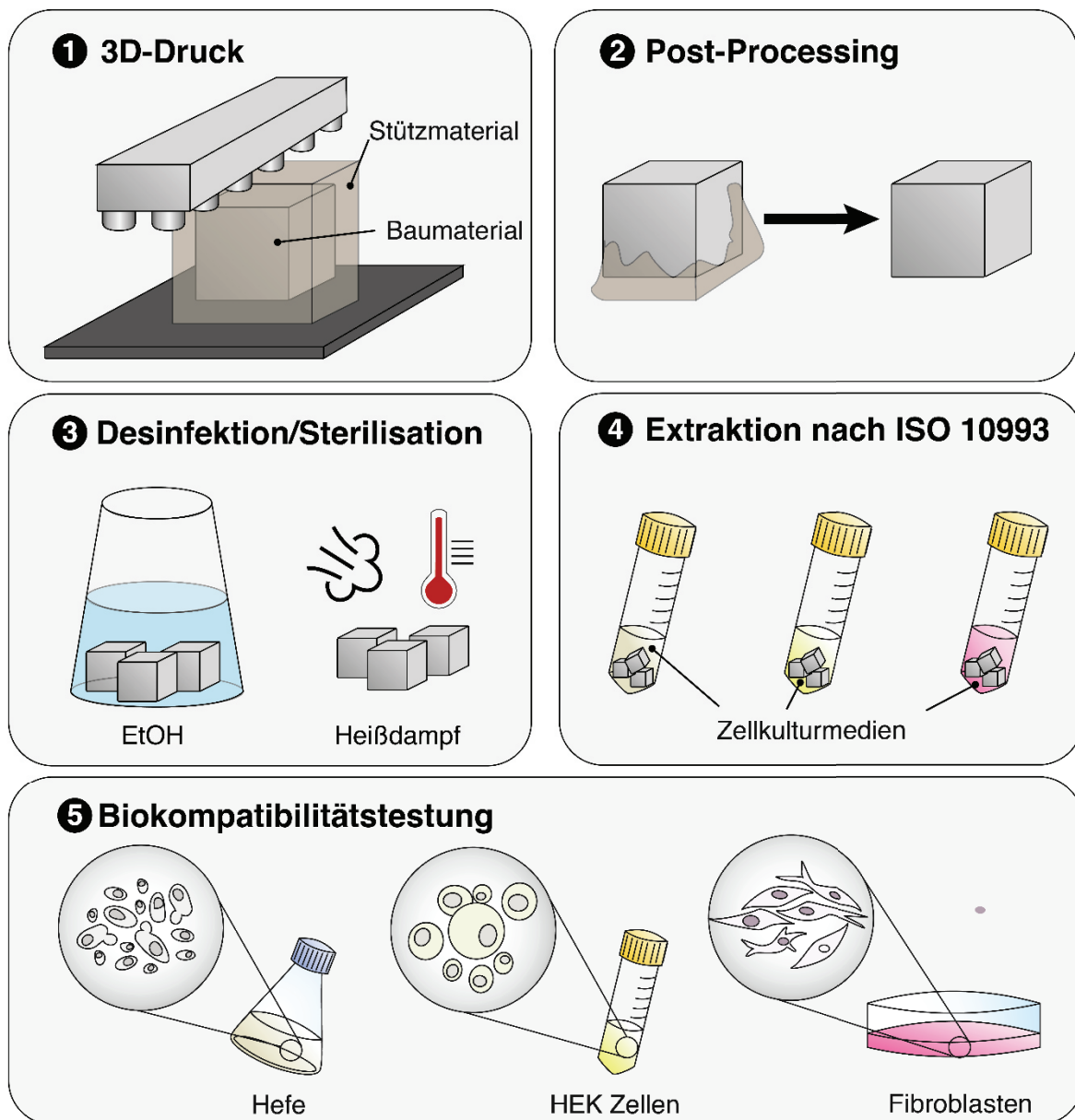
Abbildung 5: *Graphical Abstract* von „*In vitro biocompatibility evaluation of a heat-resistant 3D printing material for use in customized cell culture devices"*. (Eigene Darstellung erstellt mit Adobe Illustrator 2019)

Während auf der einen Seite die 3D-Druckindustrie exponentiell wächst und gleichzeitig der Nutzen und die Verwendung dieser Technologie für Medizin und Forschung steigt, entsteht auf der anderen Seite zunehmend ein Mangel an verlässlichen Biokompatibilitätsstudien [79]. Im Gegensatz zu gut etablierten Zellkulturmaterialien wie Polystyrol, ist die Biokompatibilität insbesondere neuerer 3D-Druckmaterialien noch unerforscht und muss zunächst umfangreich getestet werden. Dies erschwert den Einsatz des 3D-Drucks für biologische Anwendungen und seine Vorteile – wie beispielsweise die schnelle Fertigung mikrostrukturierter Zellkultursysteme – bleiben ungenutzt.

Aus diesem Gründen wurde in der dargelegten Arbeit ein neu erschienenes, hitzebeständiges 3D-Druck-material (VisiJet M2S-HT90, 3D Systems Inc.) auf seine *in vitro* Biokompatibilität gegenüber verschiedenen Zelltypen untersucht.

Bei dem verwendeten 3D-Druckmaterial handelt es sich um ein festes Polyacrylat, welches unter anderem zur Fertigung mikrofluidischer Systeme eingesetzt werden kann. Das Material wird vom Hersteller nach ISO 10993 Testung an L929 Mausfibroblasten sowie nach USP Klasse IV Testung an Ratten als biokompa-tibel beworben. Allerdings reagieren unterschiedliche Zelltypen oder Organismen auf dasselbe Material durchaus unterschiedlich. Daher muss die Biokompatibilität immer für den jeweiligen individuellen Einsatz neu bestimmt werden. Dies wird auch von dem Hersteller des 3D-Druckmaterials empfohlen. Zudem han-delt es sich bei dem Material um ein neu auf dem Markt erschienenes Produkt, welches sich besonders durch eine hohe Hitzebeständigkeit auszeichnet. Durch diese Eigenschaft kann es prinzipiell für die Hit-zesterilisation 3D-gedruckter Zellkultursysteme genutzt werden, welche für aus Kunststoff bestehende 3D-Druckmaterialien i.d.R. nicht gegeben ist. Hitze kann jedoch das Austreten zellschädlicher Stoffe her-vorrufen und damit Einfluss auf die Biokompatibilität des Materials nehmen. Daher wurde das Material zunächst zur Entfernung des Stützmaterials schrittweise aufgereinigt und anschließend durch Heißdampf sterilisiert bzw. als Kontrolle durch Ethanol (70 %, v/v) desinfiziert. Die weitere Probenvorbereitung für die *in vitro* Biokompatibilitätstestung erfolgte entsprechend der ISO 10993-12, bei der das Material in einem bestimmten Oberflächen-zu-Volumen-Verhältnis mit jeweiligen Zellkulturmedien zur Extraktionsmedien-herstellung in Kontakt gebracht wird. Um einen möglichst breiten Einsatz des Materials in Forschung und Industrie zu ermöglichen, wurde die Biokompatibilität an vielfach genutzten adhärenten Mausfibroblasten (L929), menschlichen embryonalen Nierenzellen in Suspension (engl.: *human embryonal kidney cells* (HEK 293E)) sowie der Hefe *Saccharomyces cerevisiae* (*S. cerevisiae*) untersucht.

Dabei konnte kein negativer Einfluss der Extraktionsmedien auf Viabilität und Wachstum der L929-Zellen und Hefezellen gegenüber Kontrollen mit unbehandeltem Medium festgestellt werden. Ferner konnte ge-zeigt werden, dass die Sterilisation durch Heißdampf im Vergleich zur Desinfektion durch Ethanol die Bio-kompatibilität nicht signifikant beeinflusst. Im Gegensatz dazu wiesen die HEK 293E-Suspensionszellen nach wenigen Tagen ein stark vermindertes Wachstum und nach zwei Tagen eine niedrige Viabilität von nur etwa 50 % auf.

Die Ergebnisse zeigen, dass durch die Wahl des Organismus das Ergebnis der Biokompatibilität maßgeblich beeinflusst werden kann. Wissenschaftler:innen sollten daher gezielt Biokompatibilitätstestung für ihre Anwendungen durchführen und die Testbedingungen zu einer von Herstellern möglicherweise angegebe-nen Biokompatibilität genau prüfen. Durch die Hitzesterilisierbarkeit und Biokompatibilität des in dieser Arbeit betrachteten Materials gegenüber Mausfibroblasten und Hefen, kann das Material dennoch für An-

wendungen in der Zellkultur zum Einsatz kommen. Damit zeigt das Material ein hohes Potential zur Fertigung hochkomplexer, individualisierbarer und sterilisierbarer Systeme mittels hochauflösendem 3D-Druck, was für die Prototyp-Entwicklung in Wissenschaft und Industrie von großem Interesse ist.

Im nachfolgenden Artikel „*In vitro biocompatibility evaluation of a heat-resistant 3D printing material for use in customized cell culture devices*", welcher in der Fachzeitschrift „*Engineering in Life Sciences*" veröffentlicht wurde, werden die Methoden und Ergebnisse ausführlich beschrieben und diskutiert.

Engineering
in Life Sciences

RESEARCH ARTICLE

In vitro biocompatibility evaluation of a heat-resistant 3D printing material for use in customized cell culture devices

Steffen Winkler[1] | **Katharina V. Meyer[1]** | **Christopher Heuer[1]** |
Carlotta Kortmann[1] | **Michaela Dehne[1]** | **Janina Bahnemann[1,2]**

[1]Institute of Technical Chemistry, Leibniz University Hannover, Hannover, Germany

[2]Cell Culture Technology, Faculty of Technology, Bielefeld University, Bielefeld, Germany

Correspondence
Janina Bahnemann, Institute of Technical Chemistry, Leibniz University Hannover, Callinstraße 5, 30167 Hannover, Germany.
Email: jbahnemann@iftc.uni-hannover.de

Steffen Winkler and Katharina V. Meyer are co-first author, these authors contributed equally to this work.

Abstract

Additive manufacturing (3D printing) enables the fabrication of highly customized and complex devices and is therefore increasingly used in the field of life sciences and biotechnology. However, the application of 3D-printed parts in these fields requires not only their biocompatibility but also their sterility. The most common method for sterilizing 3D-printed parts is heat steam sterilization—but most commercially available 3D printing materials cannot withstand high temperatures. In this study, a novel heat-resistant polyacrylate material for high-resolution 3D Multijet printing was evaluated for the first time for its resistance to heat steam sterilization and in vitro biocompatibility with mouse fibroblasts (L929), human embryonic kidney cells (HEK 293E), and yeast (*Saccharomyces cerevisiae* (*S. cerevisiae*)). Analysis of the growth and viability of L929 cells and the growth of *S. cerevisiae* confirmed that the extraction media obtained from 3D-printed parts had no negative effect on the aforementioned cell types, while, in contrast, viability and growth of HEK 293E cells were affected. No different effects of the material on the cells were found when comparing heat steam sterilization and disinfection with ethanol (70%, v/v). In principle, the investigated material shows great potential for high-resolution 3D printing of novel cell culture systems that are highly complex in design, customized and easily sterilizable—however, the biocompatibility of the material for other cell types needs to be re-evaluated.

KEYWORDS
3D printing, biocompatibility, cell culture, heat steam sterilization, rapid prototyping

1 | INTRODUCTION

Additive manufacturing or 3D printing is considered a revolutionizing technology already changing the way of fabri-

Abbreviations: EM, extraction medium; S. cerevisiae, Saccharomyces cerevisiae

cation in diverse industrial fields. It enables the bottom-up single-step production of most complex building parts, creating structure elements, such as inaccessible cavities, where standard top-down fabrication technologies would fail. In addition, product development processes benefit from rapid prototyping due to the high degree of customizability of the design. There are multiple different additive

manufacturing technologies, such as Fused Deposition Modeling (FDM), Stereolithography (SLA), MultiJet Printing (MJP), Two-Photon Polymerization, and many more [1], some of them with printing resolutions down to the micro- to nanometer scale [2–4]. Furthermore, diverse materials (e.g., polymers [5], silicones [6], ceramics [7], or even metals [8]) can be printed, enabling products that are translucent, flexible, highly stable, or conductive. In addition, multi-material printing enables printing different materials at the same time, which allows gaskets or conductive paths to be integrated directly into a device [9].

3D printing is increasingly used for medical applications, such as dental prosthetics [10] or transplants for surgery [11, 12]. It is also used in life sciences and biotechnology, for example, to develop 3D-printed bioreactors [13] and "lab-on-a-chip" or "organ-on-a-chip" systems for cell cultivation [14–16] and tissue engineering [17]. To enable microscopic or spectroscopic analysis, transparent materials are preferred for use in cell culture applications. Therefore, 3D- printed cell culture devices are predominantly printed from transparent photopolymers [13, 18, 19].

Especially for applications in cell culture and medical technology, the sterility of a product must be guaranteed. Typically, heat steam sterilization (autoclaving) is used to sterilize bioreactors and equipment because it is easily accessible and applicable. However, this method has significant disadvantages, such as deformation or degradation of many polymers under heat or humidity [20, 21] Therefore, sterilization or disinfection of 3D-printed objects is often achieved by UV irradiation or chemicals (e.g., ethanol or ethylene dioxide) [22]. Despite the challenges in developing a heat-resistant 3D printable polymer material, several heat-resistant materials for additive manufacturing have already been reported, such as polyetheretherketones(PEEK), fluorinated polymers, polyurethanes, and polyacrylates [23–29]. Another important requirement for the use of a material for cell culture or medical device applications is its biocompatibility.

A generally approved definition of the concept of biocompatibility was adopted in 1986 at a consensus conference on "Definitions in Biomaterials" organized by D. F. Williams: "Biocompatibility is the ability of a material to perform with an appropriate host response in a specific application" [30, 31]. This definition already implies that biocompatibility is a characteristic of a system and not of a material per se. Additionally, the response of an organism to a 3D printing material is particularly dependent on the duration and nature of the interaction and therefore needs to be uniquely defined for each application and product [31–33]. To develop suitable assays and to gather information on biocompatibility test methods, the extensive information provided by international standards—such as ISO 10993—can be consulted [34].

PRACTICAL APPLICATION

3D printing enables rapid manufacturing of highly individual and complex designs and is therefore revolutionizing the production and prototyping of customized parts for various applications in different disciplines. In the medical and biotechnology sectors, where 3D printing can be used to fabricate cell culture devices or bioreactors, the availability of sterile products is of particular importance. Heat steam sterilization is the easiest way to sterilize 3D-printed parts. However, among the wide variety of 3D printing materials, few are commercially available that can withstand heat steam sterilization and have shown biocompatibility. In this study, a polyacrylate material (VisiJet M2S-HT90) shows great potential to fulfill both criteria for cell culture applications with adherent fibroblast cells and yeast cells, and is therefore a promising material for the development of customized cell culture devices.

In most cases, initial cytotoxicity screening is based on cell culture methods because these methods are sensitive, reliable and reproducible [35]. Continuous (immortalized) cell lines such as HeLa, L929, 3T3, WI-38 or Chinese hamster ovary (CHO) cells are usually selected for these screening steps [35]. For further investigations, cells are selected depending on the anticipated use of the material under study. For example, fibroblasts such as mouse L929 cells are an appropriate choice for skin contact materials because they play a physiological role in the wound healing process around implanted devices [35]. One reason for a cytotoxic effect of a material may be the formation of substances that are leachable or extractable from the material. Common leachables and extractables that may originate from polymers include additives, processing aids, and to a lesser extent monomers and oligomers [35].

A variety of in vitro methods are available for testing cytotoxic effects, ranging from counting viable/dead cells under the microscope to biochemical assays, flow cytometric analysis, and real-time live-cell imaging technology [33, 35–37]. While microscopic observations – including counting of viable/dead cells using vital dyes such as trypan blue – and observations of changes in cell morphology provide an initial assessment of cytotoxic effects, biochemical assays provide more reliable and specific information [33, 35, 36]. Flow cytometric analysis and real-time live-cell imaging technologies offer even more specific data, but typically require costly instrumentation and more manual labor compared to traditional screening assays.
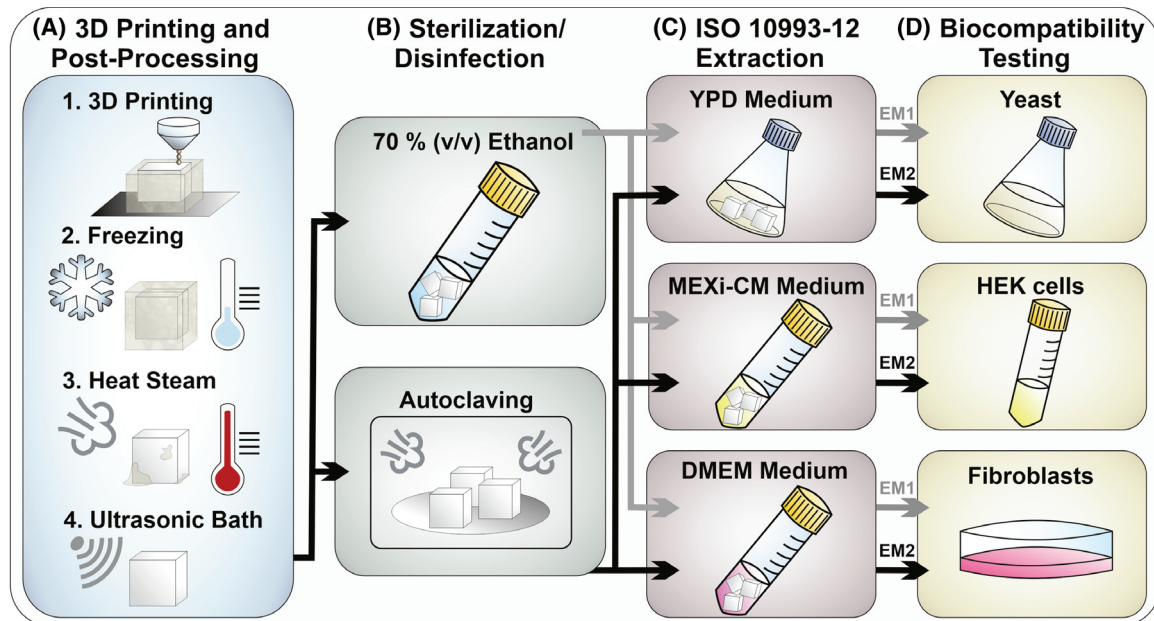
FIGURE 1 Schematic representation of the experimental procedure. The whole procedure includes 3D printing, post-processing and sterilization/disinfection of the cubes (Section 2.2), preparation of extraction media in accordance to ISO 10993-12 (Section 2.3) and biocompatibility testing using three different cell types (Section 2.5 - 2.7). (EM 1: Extraction medium obtained by incubation of ethanol (70 %, v/v) disinfected 3D-printed cubes; EM 2: Extraction medium obtained by incubation of autoclaved 3D-printed cubes)

Despite the immense number of 3D printing materials already available, materials that are biocompatible and can also be used in heat steam sterilization procedures are hard to find. The aim of this study is to investigate the potential of a novel, heat-resistant polyacrylate material (VisiJet M2S-HT90) for cell culture applications. For this purpose, the material was printed using a high-resolution Multi-Jet 3D printer and then post-processed to remove the support material (VisiJet M2 Sup). After this post-processing procedure, the 3D-printed parts were sterilized by heat steam sterilization or disinfected with ethanol (70% v/v) to reveal any effect of the disinfection/sterilization process on the 3D printing material. Subsequently, all of the post-processed objects were analyzed, and extraction media were obtained according to the ISO 10993:12 standards. The suitability of the material for cell culture applications with *Saccharomyces cerevisiae*(*S. cerevisiae*), suspension human embryonic kidney (HEK) cells and mouse L929 cells was then investigated.

2 | MATERIALS AND METHODS

2.1 | Experimental procedure

The experimental procedure is illustrated in Figure 1. The experiments started with 3D printing of 5 x 5 x 5 mm cubes (representing a total surface area of 1.5 cm² per cube) with translucent polyacrylate material and support material.

Subsequently, the printed cubes were cleaned in a post-processing process and sterilized or disinfected either by autoclaving (30 min, 121°C) or incubation in ethanol (70% v/v; Merck KGaA, Darmstadt, Germany). To study the in vitro biocompatibility of the 3D printing material, extraction media were prepared according to ISO 10993:12. These were used to evaluate the effect of the 3D printing material on adherent mouse fibroblast cells (L929), suspension human embryonic kidney cells (HEK 293E), and suspension yeast cells (*S. cerevisiae* NCYC 1024).

2.2 | 3D printing, post-processing and sterilization/disinfection of 3D-printed objects

Cubes with 5 x 5 x 5 mm were designed using SolidWorks 2020 (Dassault Systemes Deutschland GmbH, Stuttgart, Germany) and 3D-printed using the high-resolution MultiJet 3D printer ProJet® MJP 2500 Plus (3D Systems, Rock Hill, SC, USA). The resolution of the printer in xyz is 800 x 900 x 790 DPI creating layers of 32 μm [38]. The 3D printing material tested within this study is referred to by the manufacturer as VisiJet® M2S-HT90. According to the safety data sheet, the non-polymerized model material contains several hazardous chemicals [39]. However, in the printed form, the model material is declared as biocompatible in accordance with USP-class IV by the manufacturer [40]. In addition, the material is declared as heat-stable with a heat

distortion stability of 0.45 MPa at 90-100 °C [41]. As support material, VisiJet® M2 Sup was used, which according to the safety data sheet is a hydroxylated resin that has no evidenced toxic effects [42].

After the printing process was completed, the printing plate was incubated for 10 min at -18 °C. This allows to remove the cubes from the plate and transfer them in a heat steam bath of an EasyClean unit (3D systems, Rock Hill, SC, USA) for 45 min.

Subsequently, the objects were incubated in an ultrasonic bath (Bandelin electronic, Berlin, Germany) with detergent (1% (v/v); Fairy Ultra Plus, Procter and Gamble, CT, USA) for 30 min at 65 °C. Afterwards, water (Arium Sartorius Stedim Biotech GmbH, Göttingen, Germany) and detergent were renewed, and the incubation step was repeated. Following incubation with detergent, the 3D-printed objects were incubated in water for 30 min at 65 °C and then dried for 30 min at 70 °C.

In this study, chemical disinfection by incubation in ethanol (70 %, v/v) for 1 h at room temperature and sterilization by autoclaving the objects for 30 min at 121 °C (Systec VX-150, Systec GmbH, Linden, Germany) were compared. The material showed no distortion after heat steam sterilization. Finally, all cubes were washed thoroughly with sterile phosphate-buffered saline (PBS; Life Technologies Limited, Paisley, United Kingdom).

2.3 | Preparation of extraction media (EM) for biocompatibility studies

To study potential leaching properties of the 3D printing material, extraction medium (EM) was prepared according to ISO 10993-12:2021(E) (Biological evaluation of medical devices — Part 12: Sample preparation and reference materials) [34]. Following the post-processing and sterilization/disinfection steps, extraction media were obtained by incubating the 3D-printed cubes for 72 ± 2 h at 37 °C (with a surface area/volume ratio of 3 cm^2 ml^{-1}) in the respective culture media. EM obtained by incubation of ethanol disinfected 3D-printed cubes is referred to as EM 1. EM obtained by incubation of autoclaved 3D-printed cubes is referred to as EM 2. In all biocompatibility experiments, the respective cell culture medium incubated for 72 h at 37 °C without 3D-printed cubes served as a control.

2.4 | Flow cytometric analysis of extraction media

To detect particles that may have detached from the 3D printing material during incubation in the media, the EM

(for culturing L929 and HEK 293E) and the corresponding control media were analyzed using a BD Accuri™ C6 (Becton Dickinson, NY, USA) flow cytometer. All samples were filtered through a 70 μm cell strainer (Corning Incorporated, Corning, USA) prior to the experiment, and 20 μL of each medium was analyzed. Each particle within the sample was detected by the instrument as an event. BD Accuri C6 software (Becton Dickinson, USA) was used for data analysis, and all media samples were compared to a size calibration sample containing polystyrene microspheres of known diameter (1.0, 2.0, 4.0, 6,0, 10, and 15 μm (Thermo Fisher Scientific Inc., Waltham, USA)).

2.5 | L929 culture conditions and viability assessment

2.5.1 | Cell line and cell culture conditions

L929 cells (DSMZ-German Collection of Microorganisms and Cell Cultures GmbH, Braunschweig, Germany, No. ACC2) were routinely cultivated in 75 cm^2 cell culture flasks (Corning, CellBind Surface, Corning, NY, USA) in Dulbecco's Modified Eagle's Medium (DMEM; Sigma-AldrichChemie GmbH, Steinheim, Germany), supplemented with 10% fetal calf serum (Sigma-AldrichChemie GmbH, Steinheim, Germany) and 1% Penicillin/Streptomycin (Sigma-AldrichChemie GmbH, Steinheim, Germany) in a 5% CO$_2$, humidified atmosphere at 37 °C (Heracell 240 incubator, Thermo Fisher Scientific Inc., Waltham, USA) and harvested at 70-85 % confluency by Trypsin/EDTA solution (Biochrom GmbH, Berlin, Germany) treatment. Experiments were performed with cells of passage numbers below 13. 24 h prior to the start of an experiment, cells were seeded in 96-well plates (Sarstedt AG and Co. KG, Nümbrecht, Germany) at a density of 15,000 cells per well and 7,500 cells per well in 200 μL cell culture medium.

2.5.2 | CellTiter blue (CTB) viability assay

Cell viability of the L929 cells was determined by CellTiter-Blue® cell viability assay (Promega GmbH, Mannheim, Germany) using the background and standard controls given in the accompanying manual. In metabolically active cells, blue resazurin is reduced to purple fluorescent resorufin [33, 43, 44]. The resulting fluorescence intensity is an indicator of the number of viable cells. The formation of resorufin was monitored using a fluorescence plate reader (Fluoroskan Acent, Thermo Fisher Scientific Inc., Waltham, MA, USA) at an extinction wavelength of 544 nm and an emission wavelength of 590 nm.

The L929 cells were cultured in the related EM (see Section 2.3) or control medium for 24 h (15,000 cells per well) or 48 h (7,500 cells per well), afterwards all medium was removed, 100 μL of fresh DMEM containing 10 % CTB stock solution was added to each well and the cells were incubated for 1 h before fluorescence was measured in a plate reader. Three biological replicates with six technical replicates each were analyzed.

2.5.3 | Microscopic analysis

L929 cells in all culture wells were examined daily during the experiment under a light microscope (Olympus CKX41, Olympus Europa SE & Co. KG, Hamburg, Germany). Microscopic imaging of representative wells was performed using a Cytation 5 Cell Imaging Multi-Mode Reader (BioTek Instruments GmbH, Bad Friedrichshall, Germany). Imaging was performed in brightfield using the intrinsic auto-exposure function of the Gen5 imaging software (Version 3.10.06, BioTek Instruments GmbH, Bad Friedrichshall, Germany) for 4x or 20x objectives.

2.6 | HEK 293E culture conditions and viability assessment

HEK 293E cells (MEXi-293E cells, IBA Lifesciences GmbH, Göttingen, Germany) were routinely cultivated in 125 mL shake flasks (Thermo Fischer Scientific Inc, Waltham, USA) in MEXi-CM (IBA Lifesciences GmbH, Göttingen, Germany) supplemented with 8 mM L-glutamine (Sigma-Aldrich Chemie GmbH, Steinheim, Germany) and 50 mg x L^{-1} Geneticindisulfat (G418)-solution (Carl Roth GmbH, Karlsruhe, Germany) in a 5% CO_2, humidified atmosphere at 37 °C (Heracell vios 160i CO_2 incubator, Thermo Fisher Scientific Inc., Waltham, USA) at a shaking rate of 190 rpm with an orbital diameter of 19 mm. Experiments were performed with cells of passage number up to 15. At the start of an experiment, 50 mL cultivation tubes (Tubespin Bioreaktor 50, Techno Plastic Products AG, Trasadingen, Switzerland) were filled with the related EM (see Section 2.3) or control medium and inoculated with 0.3 x 10^6 cells·mL^{-1}. The starting volume of each culture was 10 mL and the shaking rate was adjusted to 210 rpm. After 24, 48, and 72 hours, a sample of 0.5 mL was taken from each culture, and the viable cell density (VCD) and viability of the culture were analyzed using a trypan blue assay–based Cedex cell counter (Cedex HiRes, Roche Diagnostics GmbH, Mannheim, Germany). Three biological and three technical replicates were analyzed, and mean and standard deviation were calculated for the technical replicates.

2.7 | Saccharomyces cerevisiae culture conditions and growth studies

S. cerevisiae NCYC 1024 cells (National Collection of Yeast Cultures, Norwich, United Kingdom) stored at -80 °C with 15 % glycerol (Carl Roth GmbH, Karlsruhe, Germany) were resuspended in 10 mL yeast extract peptone dextrose (YPD) medium (constituted of 10 g L^{-1} yeast extract, 20 g L^{-1} peptone and 20 g L^{-1} glucose, all Carl Roth GmbH, Karlsruhe, Germany) adjusted to pH 5.8 using 2 M HCl (Carl Roth GmbH, Karlsruhe, Germany) and supplemented with 34 μg mL^{-1} chloramphenicol (Sigma-Aldrich Chemie GmbH, Steinheim, Germany). The cells were incubated overnight (14 h) at 200 rpm and 30 °C in 50 mL cultivation tubes (Greiner Bio-One GmbH, Germany) using a shaking incubator (IKA® KS 4000 ic control, IKA®-Werke GmbH & Co. KG, Germany). Subsequently, this pre-culture was used to inoculate the respective extraction and control medium to an optical density at 600 nm (OD$_{600}$) of ∼ 0.2 in a final volume of 12.5 mL in 125 mL shake flasks (Thermo Fisher Scientific Inc., Waltham, USA). These flasks were again incubated at 30 °C and 200 rpm; samples were collected during an incubation period of 12 h, and OD$_{600}$ measurements were performed using a spectrophotometer (Libra S50, biochrom Ltd, United Kingdom). The experiment was repeated for three different pre-cultures with three technical replicates each for the EM and control medium.

3 | RESULTS AND DISCUSSION

3.1 | L929 cultivation in extraction medium

L929 cells are considered a standard for biocompatibility testing as these cells are recommended by the international organization for standardization and, therefore, are commonly used in laboratories for such purposes [35, 45]. In this work, the potential cytotoxicity of the novel heat-resistant 3D printing material to L929 cells was assessed using the CTB cell viability assay; this test analyzes the metabolic activity of cells as an indicator of their viability. As shown in Figure 2, the CTB assay reveals that ethanol (70%, v/v) as a disinfectant and autoclaving for sterilization of the 3D printing material did not negatively affect the metabolic capacity of L929 cells, emphasizing the biocompatibility of the 3D printing material for this cell type. In fact, the cells cultivated in both EM for 24 h showed slightly higher mean metabolic activities of 113.5 ± 5.4 % (EM 1) and 112.4 ± 2.0 % (EM 2) compared to the control that is defined as 100% viability. Also, after 48 h of cultivation, the cells' mean metabolic activity in both
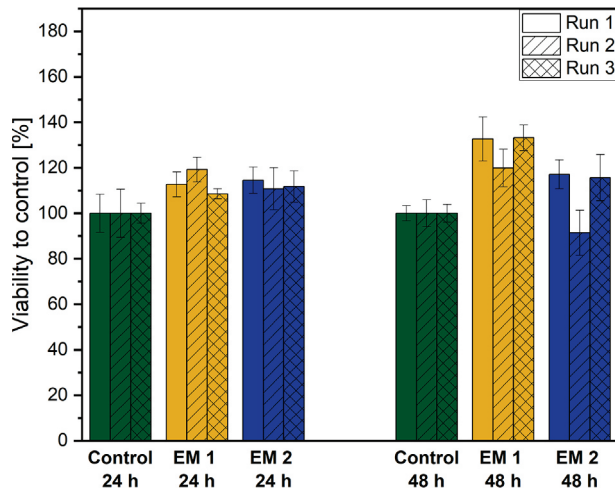
FIGURE 2   Results of CellTiter-Blue® cell viability assay to analyze the metabolic capacity (shown as cell viability in %) of L929 cells during cultivation in extraction medium (EM) compared to regular cell culture medium (control). EM 1: EM obtained by incubation of 3D-printed cubes treated with ethanol (70%, v/v). EM 2: EM obtained by incubation of autoclaved 3D printing material. The experiment was repeated three times, the results of each run are shown as mean ± standard deviation. The cell viability is normalized to the control cultivation that is defined as 100% viability

EM remains higher compared to the control with 128.6 ± 7.5 % for EM 1 and 108.1 ± 14.4 % for EM 2. However, this increase may not be significant and could be further investigated in future studies.

Microscopic analysis of the L929 cells supports our finding that the material shows biocompatibility with this cell type; as demonstrated in Figure 3, the cells show a similar confluence and an unaltered cell morphology in both EM 1 and EM 2. Yet, the microscopic images also reveal the presence of particles in EM 1 and EM 2 but not in the control medium. Thus, we conclude that the particles stem from the 3D printing material; this is emphasized by their angular shape and translucency, which is consistent for all particles. The formation of particles is probably associated with the layer-by-layer fabrication process and the resulting high roughness of the 3D printing material. Despite the presence of the particles, no reduction in cell growth or change in morphology of the directly adjacent cells was observed. Therefore, we envision that L929 cells can also be cultivated inside 3D-printed cell culture systems in direct contact with the material.

The extraction media were analyzed by flow cytometry to assess the size and amount of the observed particles. Each event detected by the instrument corresponds to one particle. As presented in Figure 4, considerably more events were detected in the EM compared to the control with a 2.64-fold and 2.74-fold increase for EM 1 and EM 2, respectively. Moreover, the comparison to a size calibration standard showed that the fraction of particles larger than 4 μm was 4.1 % ± 1.4 % for the control, 13.1 % ± 1.45 % for EM 1, and 7.9 % ± 1.2 % for EM 2. Consequently, most of the particles can not be observed under a standard light microscope. The higher number of particles in the EM in combination with their observed angular shape
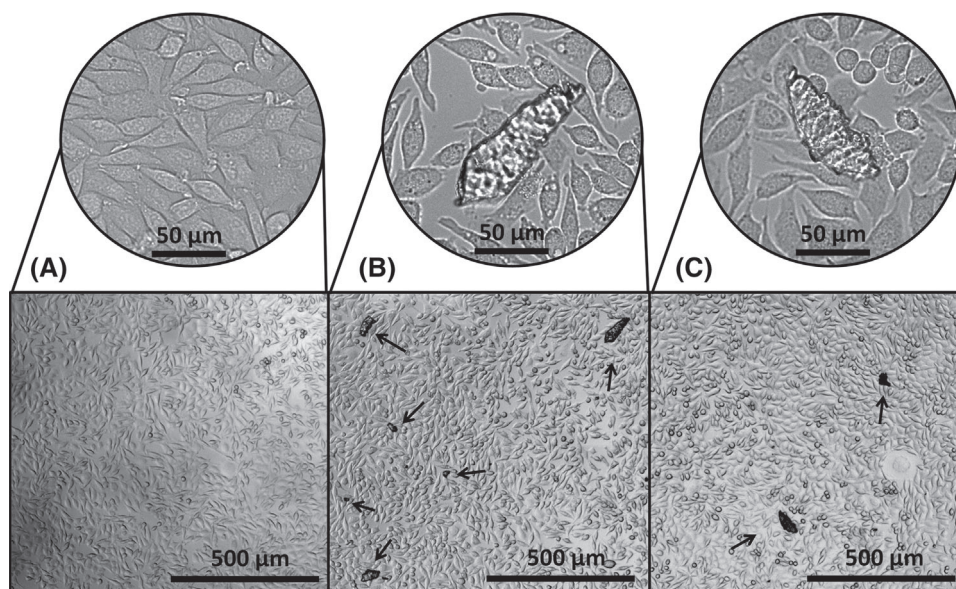
FIGURE 3   Microscopic images of L929 cells after 24 h cultivation in regular cell culture medium (A), EM 1 (B), and EM 2 (C). Black arrows indicate particles observed in the media. The magnifications show a characteristic spot within the same well of a 96-well cell culture plate as the corresponding lower magnified pictures. (EM 1: Extraction medium obtained by incubation of ethanol (70 %, v/v) disinfected 3D-printed cubes; EM 2: Extraction medium obtained by incubation of autoclaved 3D-printed cubes)
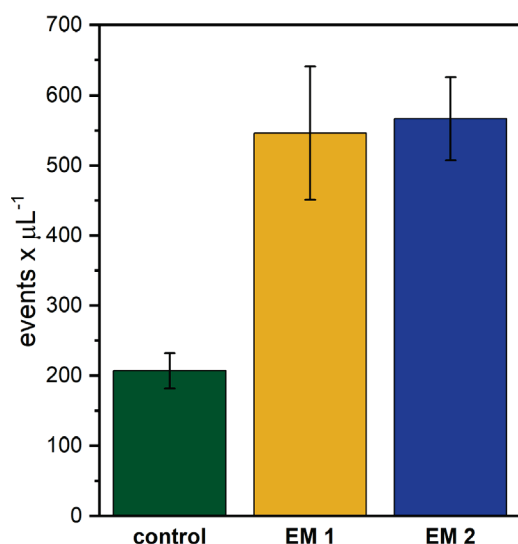
FIGURE 4 Events detected by flow cytometry in the regular cell culture medium (control) and the extraction media (EM). (EM 1: Extraction medium obtained by incubation of ethanol (70 %, v/v) disinfected 3D-printed cubes; EM 2: Extraction medium obtained by incubation of autoclaved 3D-printed cubes). Three technical replicates of three biological replicates of each medium were analyzed; the results are shown as mean ± standard deviation

evidently indicates the detachment of material from the 3D-printed cubes. Since no obvious deformation of the 3D-printed cubes after any post processing step was observed, their surface was further analyzed microscopically. Resulting from the 3D printing process three distinct surfaces can be differentiated (Figure S1). Especially the rough surfaces of the X and Y planes show potential for the detachment of particles. Indeed, the X surfaces of the cubes analyzed after incubation in medium were missing parts of their characteristic surface patterns (Figure S2). These findings further indicate the 3D printing material as the origin of the particles. Our results emphasize that in the design of biocompatibility studies for 3D printing materials, not only the presence of leachables but also particle formation should be considered.
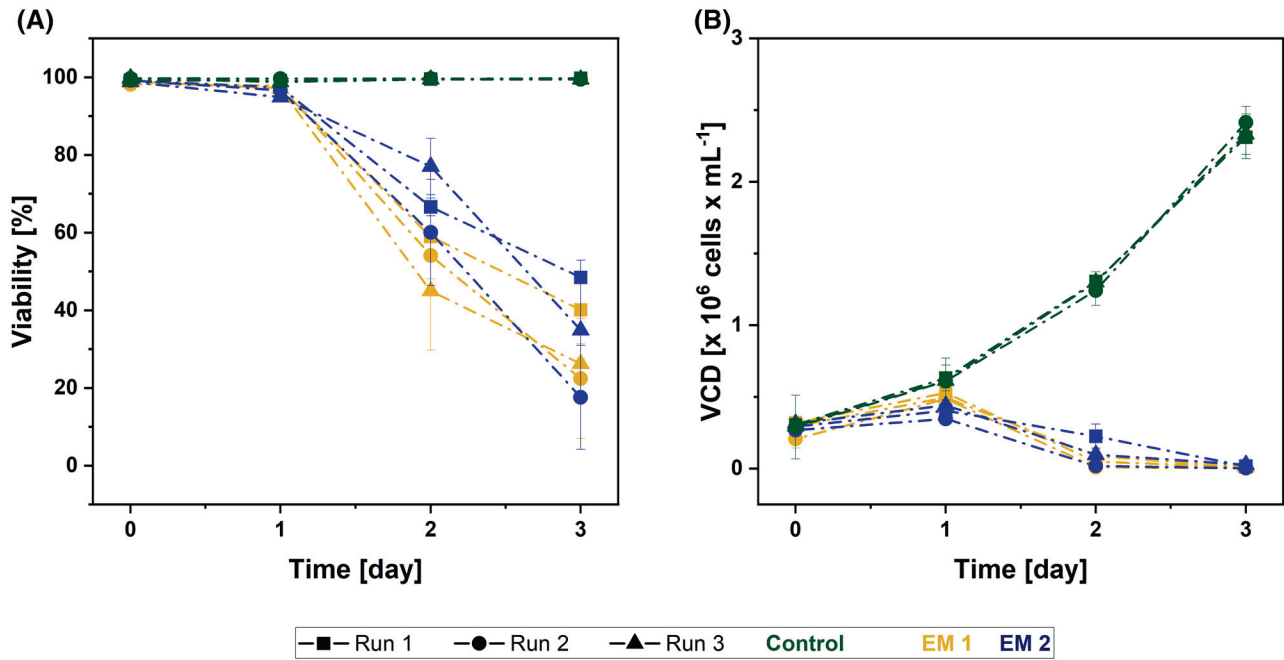
3.2 | HEK 293E cultivation in extraction medium

The mammalian suspension cell line HEK 293 is widely used for academic or pharmaceutical research [46] and, therefore, was chosen as a cell line in our biocompatibility studies. The cell viability and VCD of HEK 293E cells during the cultivation in EM 1, EM 2, and control medium were monitored using a trypan blue assay-based Cedex cell counter over a period of three days and are presented in Figure 5. The cell viability of HEK 293E cells cul-

tivated in the control medium remained above 99% (see Figure 5A) and a VCD slightly above 2.3×10^6 cells mL^{-1} was reached at the end of the experiment (see Figure 5B). In contrast, the cell viability of HEK 293E cells cultivated in both EM decreased considerably from the first day of cultivation. On the second cultivation day, the cell viability decreased below 78 % for all cultures; a trend that proceeded until the end of cultivation. Accordingly, the VCD of these cultures continuously decreased during the experiment and reached values below the inoculation density at the end of the cultivation process. EM obtained from 3D-printed cubes disinfected with ethanol or sterilized by autoclaving showed a similar and markedly negative influence on the viability and VCD of HEK 293E cells. In consequence, under the given conditions, the material is not suitable for cell culture applications with HEK 293E cells.

The negative effect of the EM on viability and growth of HEK 293E cells may be explained by microparticles that had first been observed in the EM used for cultivation of L929 cells (see Section 3.1) and were also detected by flow cytometry in the EM prepared for the HEK 293E cultivation (data not shown). While the particles had no effect on the viability of adherent fibroblasts, they potentially damage suspension cells physically during cultivation. Considering the unimpaired cell viability of L929 cells, toxicity induced by leachables is unlikely. To further investigate a potential mechanical impairment of the viability of suspension cells by the observed particles, removal of these particles before cultivation could be tested in future works.

3.3 | *Saccharomyces cerevisiae* cultivation in extraction medium

The yeast *S. cerevisiae* is one of the most studied eukaryotes that is frequently used in industrial fermentation processes [47]. Possible applications of 3D printing for yeast cell cultivation can include the design of heat-steam sterilizable bioreactors that potentially enable flexible adjustments to shifting experimental requirements (i.e., sensor integration). In this study, we investigated the effect of EM 1 and EM 2 compared to the control medium by tracking the OD_{600}, a simple but commonly applied parameter for yeast cell culture monitoring (see Figure 6). The growth curves show a typical behavior with a lag phase (0-4 h), an exponential phase (4-8 h), a diauxic shift (8-10 h), and the beginning of a second exponential growth phase (10-12 h) reaching an OD_{600} of 11-15 in all cultures after 12 h. For all three individual experiments, the cell growth in both EM remains unaffected; thus, the 3D printing material does not impair yeast cell growth. Furthermore, after

FIGURE 5 Viability and VCD of the HEK 293E cells during the cultivation in extraction medium (EM 1: obtained by incubation of ethanol (70 %, v/v) disinfected 3D-printed cubes; EM 2: obtained by incubation of autoclaved 3D-printed cubes) and regular cell culture medium (control). The experiment was repeated three times, the results of each run are shown as mean ± standard deviation
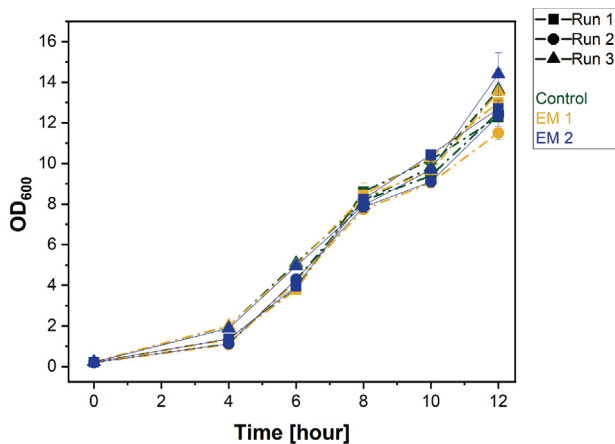
FIGURE 6 Cell density of *S. cerevisiae* during the cultivation in extraction medium (EM 1: obtained by incubation of ethanol (70 %, v/v) disinfected 3D-printed cubes; EM 2: obtained by incubation of autoclaved 3D-printed cubes) and regular cell culture medium (Control) determined by measuring of the optical density at 600 nm. The experiment was repeated three times, the results of each run are shown as mean ± standard deviation

about 8 hours of cultivation, the characteristic diauxic shift can be observed as a flattening of the growth curve. At this point, the metabolism switches from glucose as the main energy source to aerobic utilization of ethanol [48]. In comparison to the controls, this critical change in cell metabolism is unaltered in the cultures containing extrac-

tion media, underlining the biocompatibility of the material for yeast cell cultivation.

4 | CONCLUDING REMARKS

In the medical and biotechnology sectors the biocompatibility and sterilizability of 3D-printed parts is of tremendous importance. In this study, resistance to heat steam sterilization combined with in vitro biocompatibility of a novel heat-resistant polyacrylate material for high-resolution 3D Multijet printing was proven with mouse fibroblasts (L929) and yeast cells (*S. cerevisiae*). However, biocompatibility needs to be re-evaluated for the specific application and cell lines involved—as emphasized by the negative in vitro effect of the material on cell growth and viability of human embryonic kidney cells (HEK 293E) in suspension. This effect may be caused by particles (detached from the 3D printing material) in the extraction media, which may affect the viability and growth of this mammalian suspension cell line. This study therefore highlights the need to consider not only the formation of leachables but also particles in biocompatibility studies, especially for 3D printing materials.

In principle, the investigated 3D printing material shows great potential for rapid prototyping of customized and highly complex cell culture systems due to its resistance to heat steam sterilization, biocompatibility and, capability

for high-resolution 3D printing. This could be of particular interest for the development of new 3D cell culture devices or miniaturized (microfluidic) cell culture platforms.

CONFLICT OF INTEREST

The authors have declared no conflict of interest.

DATA AVAILABILITY STATEMENT

The data that supports the findings of this study is available from the corresponding author upon reasonable request.

ORCID

Katharina V. Meyer https://orcid.org/0000-0003-1198-6664

Christopher Heuer https://orcid.org/0000-0002-3694-0008

References

1. Shahrubudin N, Lee TC, Ramlan R. An overview on 3D printing technology: technological, materials, and applications. Procedia Manuf. 2019;35:1286–1296.
2. Mao M, He J, Li X, Zhang B, et al. The emerging frontiers and applications of high-resolution 3D Printing. Micromachines. 2017;8:113.
3. Chang T-J, Vaut L, Voss M, Ilchenko O, et al. Micro and nanoscale 3D printing using optical pickup unit from a gaming console. Commun Phys. 2021;4:23.
4. Zhang F, Li C, Wang Z, Zhang J, et al. Multimaterial 3D printing for arbitrary distribution with nanoscale resolution. Nanomaterials. 2019;9:1108.
5. Zhou L-Y, Fu J, He Y. A review of 3D printing technologies for soft polymer materials. Adv Funct Mater. 2020;30:2000187.
6. Liravi F, Toyserkani E. Additive manufacturing of silicone structures: a review and prospective. Addit Manuf. 2018;24:232–242.
7. Chen Z, Li Z, Li J, Liu C, et al. 3D printing of ceramics: a review. J Eur Ceram Soc. 2019;39:661–687.
8. Buchanan C, Gardner L. Metal 3D printing in construction: a review of methods, research, applications, opportunities and challenges. Eng Struct. 2019;180:332–348.
9. Li F, Macdonald P, N MG, R C, Breadmore M. Increasing the functionalities of 3D printed microchemical devices by single material, multimaterial, and print-pause-print 3D printing. Lab Chip. 2018;19:35–49.
10. Dawood A, Marti BM, Sauret-Jackson V, Darwood A. 3D printing in dentistry. Br Dent J. 2015;219:521–529.
11. Tack P, Victor J, Gemmel P, Annemans L. 3D-printing techniques in a medical setting: a systematic literature review. Biomed Eng (NY). 2016;15:115.
12. Kumar P, Rajak DK, Abubakar M, Ali SGM, et al. 3D printing technology for biomedical practice: a review. J Mater Eng Perform. 2021;30:5342–5355.
13. Priyadarshini BM, Dikshit V, Zhang Y. 3D-printed bioreactors for in vitro modeling and analysis. Int J Bioprinting. 2020;6:80–95.
14. Alexander F, Eggert S, Wiest J. A novel lab-on-a-chip platform for spheroid metabolism monitoring. Cytotechnology. 2018;70:375–386.
15. Bunge F, Driesche SV, Vellekoop MJ. Microfluidic platform for the long-term on-chip cultivation of mammalian cells for lab-on-a-chip applications. Sensors. 2017;17:1603.
16. Heuer C, Preuß JA, Habib T, Enders A, et al. 3D printing in biotechnology—An insight into miniaturized and microfluidic systems for applications from cell culture to bioanalytics. Eng Life Sci. 2021;1–16.
17. Carvalho V, Gonçalves I, Lage T, Rodrigues RO, et al. 3D printing techniques and their applications to organ-on-a-chip platforms: a systematic review. Sensors. 2021;21:3304.
18. Siller IG, Enders A, Gellermann P, Winkler S, et al. Characterization of a customized 3D-printed cell culture system using clear, translucent acrylate that enables optical online monitoring. Biomed Mater. 2020;15:055007.
19. Lerman MJ, Lembong J, Gillen G, Fisher JP. 3D printing in cell culture systems and medical applications. Appl Phys Rev. 2018;5:041109.
20. Sharma N, Cao S, Msallem B, Kunz C, et al. Effects of steam sterilization on 3D Printed biocompatible resin materials for surgical guides—an accuracy assessment study. J Clin Med. 2020;9:1506.
21. Marei HF, Alshaia A, Alarifi S, Almasoud N, et al. Effect of steam heat sterilization on the accuracy of 3D printed surgical guides. Implant Dent. 2019;28:372–377.
22. Aguado-Maestro I, De Frutos-Serna M, González-Nava A, Merino-De Santos AB, et al. Are the common sterilization methods completely effective for our in-house 3D printed biomodels and surgical guides? Injury. 2021;52:1341–1345.
23. Zhansitov AA, Slonov AL, Shetov RA, Baikaziev AE, et al. Synthesis and Properties of Polyetheretherketones for 3D Printing. Fibre Chem. 2018;49:414–419.
24. Kotz F, Risch P, Helmer D, Rapp BE. High-performance Materials for 3D Printing in Chemical Synthesis Applications. Adv Mater. 2019;31:1805982.
25. Miao J-T, Peng S, Ge M, Li Y, et al. Three-dimensional printing fully biobased heat-resistant photoactive acrylates from aliphatic biomass. ACS Sustain Chem Eng. 2020;8:9415–9424.
26. Romanov V, Samuel R, Chaharlang M, Jafek AR, et al. FDM 3D printing of high-pressure, heat-resistant, transparent microfluidic devices. Anal Chem. 2018;90:10450–10456.
27. Ganin DV, Dudova DS, Shavkuta BS, Korkunova OS, et al. Photocurable polymer composition based on heat-resistant aromatic polyamide for the formation of optical elements by two-photon polymerization. Opt Spectrosc. 2020;128:909–914.
28. Laur V, Kaissar Abboud M, Maalouf A, Palessonga D, et al. Heat-resistant 3D printed microwave devices, in: *Asia-Pacific Microwave Conference Proceedings*, APMC, Institute of Electrical and Electronics Engineers Inc., 2019, pp. 1318–1320.
29. Hu S, Shou T, Guo M, Wang R, et al. Fabrication of New Thermoplastic Polyurethane Elastomers with High Heat Resistance

for 3D Printing Derived from 3,3-Dimethyl-4,4′-diphenyl Diisocyanate. Ind Eng Chem Res. 2020;59:10476–10482.

30. Williams DF. The Language of Biomaterials-Based Technologies. Regen Eng Transl Med. 2019:53–60.

31. Williams DF. There is no such thing as a biocompatible material. Biomaterials. 2014;35:10009–10014.

32. Ratner BD, Hoffman AS, Schoen FJ, Lemons J., Biomaterials Science: An Introduction to Materials in Medicine, 3rd ed, Academic Press: San Diego, CA, USA 2013.

33. Niles AL, Moravec RA, Riss TL. In vitro viability and cytotoxicity testing and same-well multi-parametric combinations for high throughput screening. Curr Chem Genomics. 2009;3:33–41.

34. International Organization for Standardization, ISO 10993-12:2021(E) Biological Evaluation of Medical Devices. ISO copyright office, Venier, Switzerland. 2021.

35. Bernard M, Jubeli E, Pungente MD, Yagoubi N. Biocompatibility of polymer-based biomaterials and medical devices-regulations,: In vitro screening and risk-management. Biomater Sci. 2018;6:2025–2053.

36. Siller IG, Enders A, Steinwedel T, Epping NM, et al. Real-time live-cell imaging technology enables high-throughput screening to verify in vitro biocompatibility of 3D printed materials. Materials (Basel). 2019;12:2125.

37. Meyer KV, Siller IG, Schellenberg J, Gonzalez Salcedo A, et al. Monitoring cell productivity for the production of recombinant proteins by flow cytometry: An effective application using the cold capture assay. Eng Life Sci. 2021;21:288–293.

38. 3D Systems, Multijet Plastic Printers Brochure. Available online: https://www.3dsystems.com/sites/default/files/2020-08/3d-systems-mjp-brochure-usen-2020-07-17-web.pdf (accessed on 30 July 2021).

39. 3D Systems, Safety Data Sheet: VisiJet M2S-HT90. Available online: http://infocenter.3dsystems.com/materials/sites/default/files/sds-files/professional/VisiJet_M2S/HT_90/24245-S12-02-A%2CSDS%20GHS%2CEnglish%2CVisiJet%20M2S-HT90.pdf (accessed on 30 July 2021).

40. 3D Systems, 3D Systems Corporation Regulatory Information Sheet. VisiJet M2S-HT90. Available online: http://infocenter.3dsystems.com/materials/sites/default/files/sds-files/certvi/M2S-HT90%20USP%20Class%20VI%20V1.1.pdf (accessed on 30 July 2021).

41. 3D Systems, Material Selection Guide for ProJet MJP 2500 and 2500 Plus. Available online: https://www.3dsystems.com/sites/default/files/2020-08/3d-systems-visiJet-m2-material-selection-guide-usen-2020-08-20-web.pdf (accessed on 30 July 2021).

42. 3D Systems, Safety Data Sheet: VisiJet M2R-CL. Available online: https://infocenter.3dsystems.com/materials/sites/default/files/sds-files/professional/VisiJet_M2/24224-S12-05-A%2CSDS GHS%2CEnglish%2CVisiJet M2 Sup.pdf (accessed on 30 July 2021).

43. O'Brien J, Wilson I, Orton T, Pognan F. Investigation of the Alamar Blue (resazurin) fluorescent dye for the assessment of mammalian cell cytotoxicity. Eur J Biochem. 2000;267:5421–5426.

44. Gonzalez RJ, Tarloff JB. Evaluation of hepatic subcellular fractions for Alamar blue and MTT reductase activity. Toxicol Vitr. 2001;15:257–259.

45. International Organization for Standardization, ISO 10993-5:2009 Biological evaluation of medical devices — Part 5: Tests for in vitro cytotoxicity. ISO. 2009.

46. Yuan J, Xu WW, Jiang S, Yu H, et al. The scattered twelve tribes of HEK293. Biomed Pharmacol J. 2018;11:621–623.

47. Parapouli M, Vasileiadis A, Afendra A-S, Hatziloukas E. Saccharomyces cerevisiae and its industrial applications. AIMS Microbiol. 2020;6:1–31.

48. Galdieri L, Mehrotra S, Yu S, Vancura A. Transcriptional regulation in yeast during diauxic shift and stationary phase. OMICS. 2010;14:629–638.

SUPPORTING INFORMATION

Additional supporting information may be found in the online version of the article at the publisher's website.

How to cite this article: Winkler S, Meyer KV, Heuer C, Kortmann C, Dehne M, Bahnemann J. *In vitro* biocompatibility evaluation of a heat-resistant 3D printing material for use in customized cell culture devices. Eng Life Sci. 2022;1–10. https://doi.org/10.1002/elsc.202100104

4.2 Automatisierung von Zellkulturassays mittels eines 3D-gedruckten, Servomotor-gesteuerten mikrofluidischen Ventilsystems
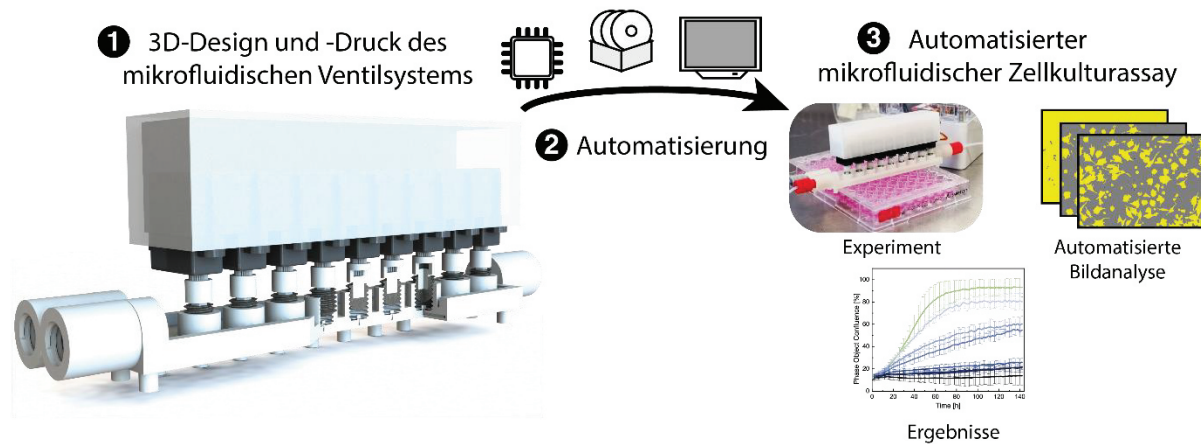
Abbildung 6: *Graphical Abstract* von „*Automation of Cell Culture Assays using a 3D-printed Servomotor-controlled Microfluidic Valve System*". (Eigene Darstellung erstellt mit SOLIDWORKS® 2022, Adobe Illustrator 2019 und OriginPro® 2020)

Durch die höhere physiologische Relevanz gewinnen fortgeschrittene mikrofluidische Zellkultursysteme wie beispielsweise den *organ-on-a-chip* Systemen zunehmend an Popularität. Um diese Systeme zu automatisieren und komplexe Assays zu ermöglichen, können mikrofluidische Ventilsysteme zur konzentrations- und zeitaufgelösten Steuerung von Medien und Reagenzien genutzt werden. Allerdings sind diese Systeme Biowissenschaftler:innen aufgrund der komplizierten Fertigung und Steuerung nur schwer zugänglich. Im Gegensatz dazu können 3D-gedruckte mikrofluidische Ventilsysteme als leicht anpassbare und leicht zu fertigende Alternative dienen.

Entsprechend wurde in diesem Teil der Arbeit ein vollautomatisiertes, 3D-gedrucktes mikrofluidisches Ventilsystem entwickelt. Dazu wurde das zuvor auf Biokompatibilität getestete und autoklavierbare 3D-Druck Material VisiJet M2S-HT90 der Firma 3D Systems Inc. (s. Kapitel 4.1) zur Fertigung der mikrofluidischen Komponenten verwendet. Diese setzen sich aus einem einzigen 3D-gedruckten Teil zusammen und bestehen aus Anschlüssen für Medium und Zusätze, einem Mikromischer, neun *plunger* Mikroventilen (dt.: Kolbenventil) sowie einem Kanalausgang je Ventil. Die Ventile besitzen eine 100 μm dünne Membran, welche zur Öffnung bzw. Schließung des Ventils ausgelenkt wird. Einzigartig daran ist, dass die Membran nicht nachträglich integriert werden muss, sondern zusammen mit den restlichen Komponenten bereits während des Druckprozesses entsteht. Somit wird im Gegensatz zu nachträglich angebrachten Magnetventilen eine zusätzliche Sterilgrenze vermieden und das Kontaminationsrisiko minimiert. Die 3D-gedruckten Mikroventile werden durch miniaturisierte, aufgesetzte Servomotoren gesteuert. Dies stellt eine beispiellose Kombination aus Fertigungs- und Aktuationsprinzip von Mikroventilen dar. Sie stellt im Vergleich zu klassisch gefertigten, pneumatischen Systemen eine kostengünstigere, leichter anzupassende und bedienungs-

tomatisierung der Servomotoren erfolgt durch einen portablen Raspberry Pi Computer sowie eigens geschriebener Python Skripte. Das fertige System wurde bezüglich seiner Mischgenauigkeit sowie der Robustheit der Ventile in verschiedenen Experimenten charakterisiert.

Nach Heißdampfsterilisation der mit Zellkulturmedium in Kontakt stehenden 3D-gedruckten Komponenten, wurde das System zur Automatisierung eines Zytotoxizitätsassays als Machbarkeitsstudie verwendet. Hierbei wurde mithilfe des Ventilsystems zunächst eine Konzentrationsreihe des für die Krebstherapie verwendeten Zytotoxins Camptothecin (CPT) erzeugt. Dabei werden mit CPT versetztes Zellkulturmedium und CPT-freies Zellkulturmedium über zwei Spritzenpumpen in das mikrofluidische System geleitet. Durch die Variation der Flussraten der beiden Pumpen können somit verschiedene CPT Konzentrationen erzeugt werden. Nach Durchmischung durch einen integrierten Mikromischer wird durch die gezielte Öffnung der Ventile ein definiertes Volumen jeder Konzentration direkt in die davor vorgesehene *wells* (dt.: Vertiefung) einer 96-*well* Gewebekulturplatte abgegeben. Das Ventilsystem besitzt dazu acht Ausgänge für die Erstellung der Konzentrationsreihe sowie einen Ausgang für zwischenzeitliches Spülen der Kanäle. Als Kontrolle dienten per Hand pipettierte Konzentrationsreihen. Für beide Konzentrationsreihen wurde die Auswirkung des Toxins auf das Zellwachstum von Mausfibroblasten (L929) beobachtet. Die Analyse erfolgte durch *live-cell-imaging* sowie anschließender automatisierter Bildanalyse der Konfluenz. Final wurden die IC50 Werte (Wirkstoffkonzentration bei 50 % Inhibition) bestimmt und miteinander verglichen.

Das 3D-gedruckte, mikrofluidische Ventilsystem zeigte dabei ein minimales Spülvolumen von $\sim$ 200 µL und bis zu Verdünnungen mit dem Faktor $\sim$ 40 eine gute Mischgenauigkeit. Zudem haben die Ventile – inklusive der 3D-gedruckten Membran – in einem Robustheitstest mehrere tausend Aktuationen ohne Defekt überstanden. Die mikrofluidischen und pipettierten Zytotoxizitätsassays zeigen ein von der CPT-Konzentration anhängiges Zellwachstum und die IC50-Werte sind nach 60-80 h Kultivierung nahezu identisch.

Das 3D-gedruckte und sterilisierbare, mikrofluidische Ventilsystem erlaubt somit die verlässliche Automatisierung von Zellkulturassays und demonstriert eindrucksvoll den Nutzen des 3D-Drucks für die schnelle Entwicklung neuartiger LOC-Systeme – vom 3D-Computermodell bis zur Anwendung. Dabei ist das System im Gegensatz zu Pipettierrobotern nicht nur auf klassische Zellkulturassays beschränkt. Durch seinen mikrofluidischen Charakter kann es prinzipiell auch zur Perfusion fortgeschrittener OOC Systeme oder vaskularisierten 3D Zellkulturen verwendet werden. Durch die additive Fertigung können die Ausgänge jederzeit modifiziert und mit bereits entwickelten mikrofluidischen Zellkultursystemen verbunden werden. Die Veröffentlichung der Computermodelle sowie der Skripte zur Automatisierung erlaubt den Nachbau bzw. die einfache Anpassung des Systems, sodass es ebenso von Wissenschaftler:innen anderer Labore als Automatisierungsplattform für weitere biologische Anwendungen verwendet werden kann.

Im nachfolgenden Artikel „*Automation of Cell Culture Assays using a 3D-printed Servomotor-controlled Microfluidic Valve System*" veröffentlicht in der Fachzeitschrift „*Lab on a Chip*" werden die Ergebnisse ausführlich beschrieben und diskutiert.

Automation of Cell Culture Assays using a 3D-printed Servomotor-controlled Microfluidic Valve System

Journal:	*Lab on a Chip*
Manuscript ID	LC-ART-07-2022-000629.R1
Article Type:	Paper
Date Submitted by the Author:	27-Aug-2022
Complete List of Authors:	Winkler, Steffen; Leibniz Universitat Hannover, Institute of Technical Chemistry Menke, Jannik; Leibniz Universitat Hannover, Institute of Technical Chemistry Meyer, Katharina; Leibniz Universitat Hannover, Institute of Technical Chemistry Kortmann, Carlotta; Leibniz Universitat Hannover, Institute of Technical Chemistry Bahnemann, Janina; University of Augsburg Faculty of Mathematics and Natural Sciences, Insititute of Physics

SCHOLARONE™
Manuscripts

ARTICLE

Automation of Cell Culture Assays using a 3D-printed Servomotor-controlled Microfluidic Valve System

Steffen Winkler[a], Jannik Menke[a], Katharina V. Meyer[a], Carlotta Kortmann[a], Janina Bahnemann[b],*

Microfluidic valve systems show great potential to automate mixing, dilution, and time-resolved reagent supply within biochemical assays and novel on-chip cell culture systems. However, most of these systems require a complex and cost-intensive fabrication in clean room facilities, and the valve control element itself also requires vacuum or pressure sources (including external valves, tubing, ports and pneumatic control channels). Addressing these bottlenecks, the herein presented biocompatible and heat steam sterilizable microfluidic valve system was fabricated via high-resolution 3D printing in a one-step process – including inlets, micromixer, microvalves, and outlets. The 3D-printed valve membrane is deflected via miniature on-chip servomotors that are controlled using a Raspberry Pi and a customized Python script (resulting in a device that is comparatively low-cost, portable, and fully automated). While a high mixing accuracy and long-term robustness is established, as described herein the system is further applied in a proof-of-concept assay for automated IC_{50} determination of camptothecin with mouse fibroblasts (L929) monitored by a live-cell-imaging system. Measurements of cell growth and IC_{50} values revealed no difference in performance between the microfluidic valve system and traditional pipetting. This novel design and the accompanying automatization scripts provide the scientific community with direct access to customizable full-time reagent control of 2D cell culture, or even novel organ-on-a-chip systems.

1. Introduction

Acting on the micro- to nanometer scale, microfluidic systems have enabled researchers to precisely study or manipulate cells, viruses, and/or proteins by using microbioreactors[1], microfluidic cell separators[2], micromixers[3], integrated biosensors[4], and/or novel organoid/organ-on-a-chip systems[5,6]. Unfortunately, relatively low accessibility and the considerable costs of clean room facilities (which are required for standard lithographic fabrication of microfluidic chips) have heretofore prevented this technology from being imported to industrial application on a large scale[7,8]. 3D printing of microfluidics has started to rise in popularity – since that approach results in drastically reduced chip prototyping times and decreased acquisition costs – and printing resolution has advanced to the point where printing on the micrometer or even nanometer scale is now feasible[9,10,11]. The tantalizing promise of rapid prototyping, considerably higher complexity in the third dimension, customizability, and the ability to use and incorporate several different materials (including biocompatible[12,13], cell adherable[14] or heat-resistant polymers[13]) have all piqued the interest of researchers.

Automated liquid control for multiplexing and assaying within microfluidic systems is often accomplished by using microvalves that are directly integrated during the fabrication process to create microfluidic valve systems. Such systems have demonstrated to be capable of effectively managing assay operations in high-throughput by using microvalve arrays[15]. However, compared to established pipetting robots and high-throughput screening in the pharmaceutical industry, microfluidic valve systems are typically not superior in throughput, but in performing complex protocols with programmed queues of reactants. For instance, such systems have been used to automate and parallelize on-chip cell seeding and facilitate the cultivation of human umbilical vein endothelial cells (HUVECs) in a modular plug-and-play microfluidic valve system[16]. While pipetting systems are usually fixed to a certain plate design, microfluidic valve systems are more versatile and can be plugged to other microfluidic systems that have complex architectures at the micro-scale. For instance, one microfluidic platform was used to immobilize tumor organoids inside microgrooves and was in turn combined with a second microfluidic system for combinatorial and dynamic drug screening[17].

On the other hand, there are high-end pipetting systems available that have been combined with live-cell-imaging systems via robotics and automated incubators to fully automate cell culture handling and monitoring[18,19]. However, apart from the high cost, these systems are severely limited to standard well-plates and perfusion of sophisticated 3D cell culture systems is not possible. In contrast, microfluidic valve systems are highly customizable and can be interfaced with

a. Institute of Technical Chemistry, Leibniz University Hannover, Hannover, Germany
b. Institute of Physics, University of Augsburg, Augsburg, Germany
*Correspondence: Prof. Dr. Janina Bahnemann (janina.bahnemann@uni-a.de), Institute of Physics, University of Augsburg, Universitätsstraße 1, 86159 Augsburg, Germany.

microfluidically controlled 3D cell culture systems, such as organ-on-a-chip systems and vascularized (3D-printed) hydrogels, which have the potential to become important research platforms for drug discovery and tissue engineering in the near future[6,20,21,22].

The type and operation principles of the microvalves utilized are essential, since they pre-define many features of the microfluidic valve system (e.g., footprint, manufacturability, fabrication costs, operating hardware, complexity in set-up and control, etc.). Typically, they include a flexible membrane – such as Quake-style[23], doormat[24] or plunger[25] valves – that is deformed for channel closure or opening[26]. While microvalves can be actuated in many different ways (e.g., mechanically, magnetically, electrostatically, acoustically, thermally or piezoelectrically, etc.), pneumatic actuation is most commonly used for microfluidic automatization[27]. In that approach, pressure or the creation of a vacuum for membrane deformation is distributed to the valves via a microfabricated control channel layer on top of the flow channel layer. In the simplest case, one control channel operates a single flow channel. More advanced systems for increased throughput use microfluidic multiplexing, where the number of total valves is increased to reduce the number of total control channels to 2 $\log_2$ of n flow channels[28]. However, aside from the fact that most pneumatically driven microfluidic valve systems are difficult to fabricate, further major drawbacks include a more complicated set-up and control. While the microfluidic chip relies on additional pneumatic control channels and pressure/vacuum inlet ports, the whole system requires extra tubing, external solenoid valves, and at least one pressure/vacuum source – all of which combine to substantially increase complexity, cost, system footprint, and the overall statistical risk of failure. Accordingly, the actual use of these systems is still generally limited to a small fraction of micro-engineers.

In an attempt to address these limitations, a 3D-printed microfluidic valve system for spatiotemporal reagent control that is operated by miniature servomotors has been developed. This compact on-chip microvalve control mechanism is connected to a Raspberry Pi computer, which enables automatization and allows the system to function as a portable, remotely controllable, and low-cost device. As a novelty, inlets, outlets, micromixer, microvalves and even valve membranes were entirely fabricated in a single part via 3D printing using a biocompatible and autoclavable material. All of these elements were easily plugged to the servomotors, thereby eliminating the need for the sort of complex fabrication and/or set-up procedures typically required by conventional microfluidic valve systems. While a sufficient mixing accuracy and valve robustness is shown, its applicability for programmable assaying in cell culture is demonstrated as a proof-of-concept. Ultimately, in view of the rapid customization abilities already well known through published 3D models, we envision this device as a dynamic reagent control system suitable for use with more complex microfluidic cell culture systems, like organ-on-a-chip devices.

2. Materials and Methods

2.1 Fabrication, Post-Processing and Sterilization of 3D-printed Parts

All 3D-printed parts were designed using SolidWorks 2020 (Dassault Systems Deutschland GmbH, Stuttgart, Germany) and are published as .sldprt computer-aided design (CAD) files with this work. The microfluidic chip and printed adapters were fabricated using a high-resolution MultiJet 3D printer (ProJet® MJP 2500 Plus, 3D Systems, Rock Hill, SC, USA). The 3D printing material VisiJet® M2S-HT90 and the VisiJet® M2 Sup were used as build material and support material, respectively. The detailed chemical composition of the build material is not provided by the manufacturer. However, from the safety data sheet it can be concluded that the raw material contains several hazardous chemicals, while the printed polymerized build material is specified as polyacrylate[29]. The material is suitable for cell culture applications as it is heat resistant for sterilization and biocompatible with L929 cells according to the manufacturer's USP class VI and a recent study in accordance with the international standard ISO 10993-12:2021(E)[13,30]. For removal of the support material, parts printed using the ProJet® MJP 2500 Plus were post-processed in accordance with the protocols identified and described in recent publications[13]. However, the protocols were slightly modified here by flushing each microchannel in the beginning of each post-processing step. For cell culture applications, the chip was connected to the fittings and tubes as described in chapter 0, and then heat-steam sterilized.

2.2 Platform Assembly

The 3D-printed system was controlled via a custom Python script using the open-source software Python 3.5.3 (Python Software Foundation, Delaware, USA) and Thonny 3.1.0 (Institute of Computer Science of University Tartu, Tartu, Estonia), which was run on a Raspberry Pi 3 Model B V1.2 (Raspberry Pi Foundation, Cambridge, UK) with a Raspbian GNU/Linux 9 operating system (Raspberry Pi Foundation, Cambridge, UK). A pulse-width modulation (PWM) controller (SparkFun Servo pHAT for Raspberry Pi; SparkFun Electronics Inc., Niwot, USA) was mounted directly on the Raspberry Pi and connected to four 17 x 6.2 x 16 mm Goteck GS-D1083 Micro Servos (Dong Yang Model Technology Co., Ltd., Huizhou, China). Furthermore, a HLS8L-DV3V-S-C relay (Ningbo Helishun Electron Co., Ltd., Ningbo, China) was interposed between the servos and the board in order to enable a shutdown of the servos. Aladdin AL1000 syringe pumps (Word Precision Instruments LLC, Sarasota, USA) were connected to the Raspberry Pi via USB, and to the chip via standard chromatography PTFE tubing (Ø 0.5 mm) and fittings. Prior to running experiments, the 3D-printed microfluidic valve chip was prepared by inserting M5x6 setscrews into the threads above each valve, which were very gently hand-tightened to insure a snug fit. Each of these contained a 3D-printed adapter as the connection of the servomotors to the M5 setscrews. In turn, servos were connected to a 3D-printed housing using standard M1 screws, and were set to the starting position at servo

position = 60 ° and mounted on the adapters. Closure of the valve occurred at the servo position = 90 ° and opening of the value occurred at -15 °, respectively. The servos were switched off when not being operated in order to avoid a permanent load on the servo during the closed state of the valve.

2.3 Long-term Robustness

For the long-term stability determinations, the valves were successively and repeatedly opened and closed by the servos as a stress test over a total time period of 4-5 days. For each opening event, one valve was opened while the rest of the valves remained closed, and the valve was then rinsed off for 10 s at 500 µL/min with ddH$_2$O using an Ismatec IPC peristaltic pump (Cole-Parmer GmbH, Wertheim, Germany). Including the time taken to open/close the valve, the time from the opening of the first valve to the opening of the second valve was estimated by the script to be 10.12 s. Failure of the valve or servo was determined by observing leakage from the valve diaphragm or insufficient closing/opening of the valve, resulting in discharge at an incorrect outlet. The entire experiment was permanently recorded by camera and the number of actuations until failure was determined as a quotient of the elapsed time until failure and the time between two opening events. Experiments were performed with four distinct valves/servos (n = 4) each for a normally post-processed chip, an additionally heat-steam sterilized chip (121 °C, 30 min), and a heat-steam sterilized and incubated chip (ddH$_2$O, 37 °C, 4 weeks). The script and the Ismatec pump commands – including the automatization script and variables that were used – can be found as .py files in the Supporting Information.

2.4 Rinsing Volume Determinations

At first, one channel was filled with an Allura Red AC (Merck KGaA, Darmstadt, Germany) food dye stock solution in ddH$_2$O with an absorbance of 20 a.u. at 494 nm after opening a single valve. Then, this solution was constantly removed by ddH$_2$O using an Aladdin AL-1000 syringe pump (Waukesha-Pearce Industries, South Main, USA) at a flow rate of 500 µL/min, and each drop with an average volume of 26.2 ± 0.3 µL was individually collected at the outlet in standard 0.2 mL PCR tubes. If necessary, the droplets were diluted to the proven linear absorbance range at ≤ 2 a.u. and absorbance of each solution was determined in a NanoDrop 1000 spectrophotometer (Thermo Fisher Scientific Inc., Waltham, USA). The droplet containing 100 % food dye solution was measured three times and used for normalization. The whole experiment was performed three times (n = 3), with three distinct channels and valves.

2.5 Mixing Accuracy

At first, all channels were filled with ddH$_2$O. Then, after opening a single valve, one channel was filled with mixtures of ddH$_2$O and Allura Red AC food dye stock solution by variation of the flow rates of two distinct Aladdin AL-1000 syringe pumps. For the experiments using mixtures ranging from 20 % to 100 % dye, a stock solution with absorbance = 2 a.u. at 494 nm was used. For experiments at higher dilutions (from 1.25 % - 20 % dye), a

stock solution with absorbance of 20 a.u. at 494 nm was used instead, in order to keep the absorbance above the detection limit of the spectrophotometer. The mixtures were pumped at a total flow rate of 500 µL/min with varying rinsing volumes. The absorbance of the dye containing mixtures was determined in a NanoDrop 1000 spectrophotometer. The whole experiment was performed three times (n = 3), with three distinct channels and valves.

2.6 Cell Culture Conditions

L929 cells (DSMZ-German Collection of Microorganisms and Cell Cultures GmbH, Braunschweig, Germany, No. ACC2) were routinely cultivated in 75 cm^2 cell culture flasks (Corning, CellBind Surface, Corning, NY, USA) in Dulbecco's Modified Eagle's Medium (DMEM; Sigma-Aldrich Chemie GmbH, Steinheim, Germany), supplemented with 10 % fetal calf serum (Sigma-Aldrich Chemie GmbH, Steinheim, Germany) and 1 % Penicillin/Streptomycin (Sigma-Aldrich Chemie GmbH, Steinheim, Germany) in a 5 % CO$_2$, humidified atmosphere at 37 °C (Heracell 240 incubator, Thermo Fisher Scientific Inc., Waltham, USA). For passaging, cells were harvested at 70-85 % confluence using a Trypsin/EDTA solution (Biochrom GmbH, Berlin, Germany).

2.7 IC$_{50}$ Determinations of Camptothecin

The cytotoxic effect of the anti-cancer drug camptothecin (CPT) was used to induce a concentration-dependent growth rate and to thereby compare the resulting IC$_{50}$ values of assays created either using the valve system, on one hand, or by manual pipetting, on the other. CPT acts as DNA topoisomerase I inhibitor by preventing DNA replication during S phase, and its toxic effect primarily stems from lethal collision of the DNA cleavage complex with replication forks[31].

Prior to an assay, cells were seeded in 96-well plates (Sarstedt AG and Co. KG, Nürnbrecht, Germany) at a density of 3,500 cells per well in a 100 µL cell culture medium. To ensure a uniform distribution of these cells, the plate was maintained at room temperature for 20 min before transfer to the incubator. After 24 ± 2 h, assays were performed both via manual pipetting and also by using the microfluidic valve system on the same cell culture plate.

For the manually pipetted assay, a 1 mM stock solution of CPT (Merck KGaA, Darmstadt, Germany) in ≥ 99.7 % pure DMSO (Carl Roth GmbH, Karlsruhe, Germany) was prepared. The stock solution was used for creating pre-dilutions in DMSO from which each 1 µL was transferred to the respective wells. Finally, 100 µL of cell culture medium was added to each well, resulting in a total volume of 200 µL and a 0.5 % DMSO concentration (including the control without CPT).

In turn, the pre-sterilized and assembled microfluidic valve system was placed on top of the same cell culture plate, with the outlets pointing to their respective wells. Two 10 mL syringes with 0.5 % DMSO, containing cell culture medium both with and without 10 µM CPT, were then connected to the chip. The automated microfluidic assay was started, and 100 µL of a respective mixture was added to each well. Rinsing volumes in between each step, as well as other parameters related to these

experiments, are summarized in Table S.3 and contained in the .py and .xlsx files of the Supporting Information. All CPT concentrations were performed with three technical replicates for each of these methods.

The plate was transferred to an IncuCyte S3 (Sartorius AG, Göttingen, Germany) live-cell-imaging system that was operated in a 5% CO_2, humidified atmosphere at 37 °C, and thereafter it was monitored automatically by the system using phase contrast with a 20 x objective creating four pictures per well every two hours. All microscopic images were analyzed automatically using the corresponding software IncuCyte 2021C (Sartorius AG, Göttingen, Germany). For determination of confluence, an image mask was created on three respective images using the parameters in Table S.1. The data of the mean confluence of each well was exported and normalized to the control, and then IC_{50} values for each time point were determined using logarithmic CPT concentrations in OriginPro 2019b (OriginLab Corporation, Northampton, USA) via non-linear fits using the intrinsic dose response function with

weights and the top asymptote fixed to 100 %. Finally, the mean IC_{50} values and standard deviations were calculated from three distinct experiments (n = 3).

3. Results and Discussion

3.1 Design and Operation Principle of the 3D-printed, Servomotor-controlled Microfluidic Valve System

The design of the microfluidic valve system itself is presented in Figure 1, while the assembly and operation are explained in the videos in the Supporting Information. The 3D-printed chip contains two inlets, a HC-shaped micromixer, nine plunger microvalves, and nine outlets including the waste outlet. A more detailed illustration of the chip design can be found in a technical drawing in Figure S.1 of the Supporting Information. The inlets allow waterproof connection to standard chromatography fittings and tubing, and are connected to the channel system with 500 x 500 µm channels.
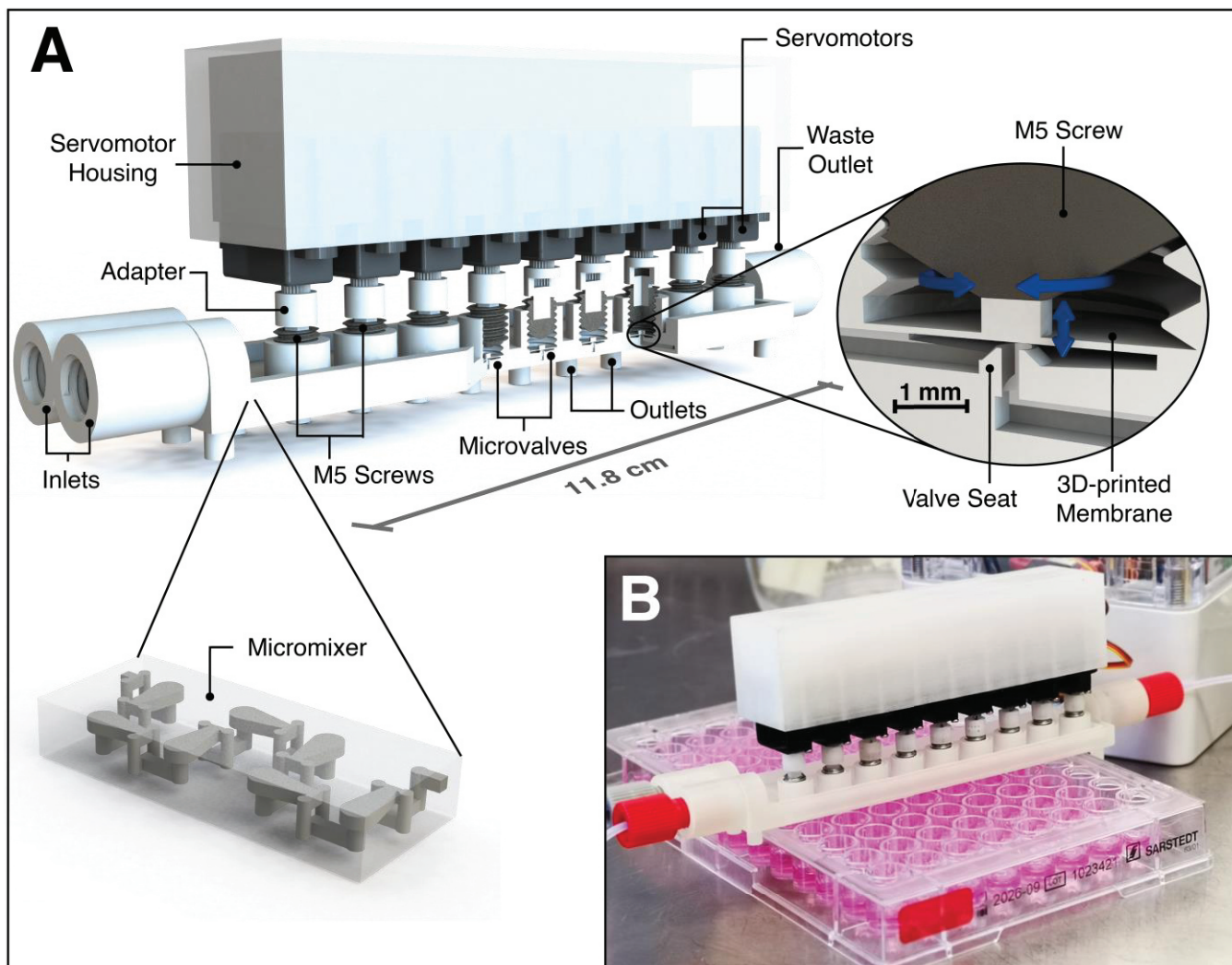
Figure 1: A) CAD illustration of the fully assembled microfluidic valve system. The 3D-printed microfluidic chip includes two inlets compatible to standard HPLC fittings, a micromixer, nine microvalves, eight outlets for mixture distribution, and a waste outlet. The complex 3D structures of the 3D-printed HC-shaped micromixer (published by Enders et al.[3]) ensure rapid mixing. The valves are operated by 6.2 mm wide servomotors, each of which is connected via a 3D-printed adapter to a M5 setscrew. The membrane is pressed into the valve seat by servo-driven setscrew rotation, resulting in the closure of the valve. All motors are integrated into a servomotor housing to enable quick attachment to the 3D-printed microfluidic chip. B) Picture of the 3D-printed and fully assembled microfluidic valve system during assay operation under the safety cabinet.

The HC-shaped micromixer – based on the design by Enders et al.[3] – ensures rapid mixing of the prevailing laminar flow. Therefore, the mixer creates a chaotic flow in combination with the principle of "split-and-recombine" by using complex 3D structures — that can only be produced at great expense with other fabrication techniques. The valve design is a slightly down-scaled redesign of a normally-open plunger valve reported in Au et al.[32], and it consists of both inlet and outlet channels, a valve seat, and a 100 μm thin 3D-printed membrane with a 4 mm Ø circular area. While most microfluidic systems depend on pneumatically controlled valve actuation (which includes additional control channels, control channel connectors, tubing and fittings, external valves, and at least one pressure source), the valve closure of this 3D-printed valve system is managed on chip solely by low-cost miniature servomotors. The motors are connected to M5 setscrews using a 3D-printed adapter, and membrane deflection is realized via rotation of the setscrews inside 3D-printed threads. Finally, all motors are attached to a 3D-printed housing which allows for quick plugging into and/or release from the (pre-sterilized) microfluidic chip (see Figure S.2 for technical drawings). The cost for a single servomotor is $3-10, depending on the supplier, whereas the cost of the 3D printing material is $10 per chip. While the presented microfluidic chip is designed to automate

a specific proof-of-concept assay (as described in chapter 0), it can readily be rearranged and/or extended with additional inlets, mixers, valves, or even new functional units.

To facilitate the operation of complex assays, this system was automated as schematically illustrated in Figure 2. The chip is designed to fit onto a standard 96-well plate, with eight of the outlets pointing into respective wells of one column. Modulation of the pump ratio of two syringe pumps at the chip inlets is used to create different mixtures, while control of the servomotors ensures the correct distribution to designated outlets. A waste outlet allows for rinsing of the main flow channel with a new mixture prior to the delivery to its desired outlet. While the valves are closed via setscrew rotation, membrane deflection during valve opening is achieved only via flow pressure. Since the membranes do not equally deflect during opening – resulting in distinct flow resistances and rates – the valve system is actually operated with a single valve opened at a time. Furthermore, all servos are switched off between two operations in order to prevent a permanent load on the servomotor and potentially induce its early failure. In terms of automatization, the servomotors and the pumps are connected to a compact Raspberry Pi single-board computer and are thereby controlled using a customized Python script. The Python script includes variables for various alternating
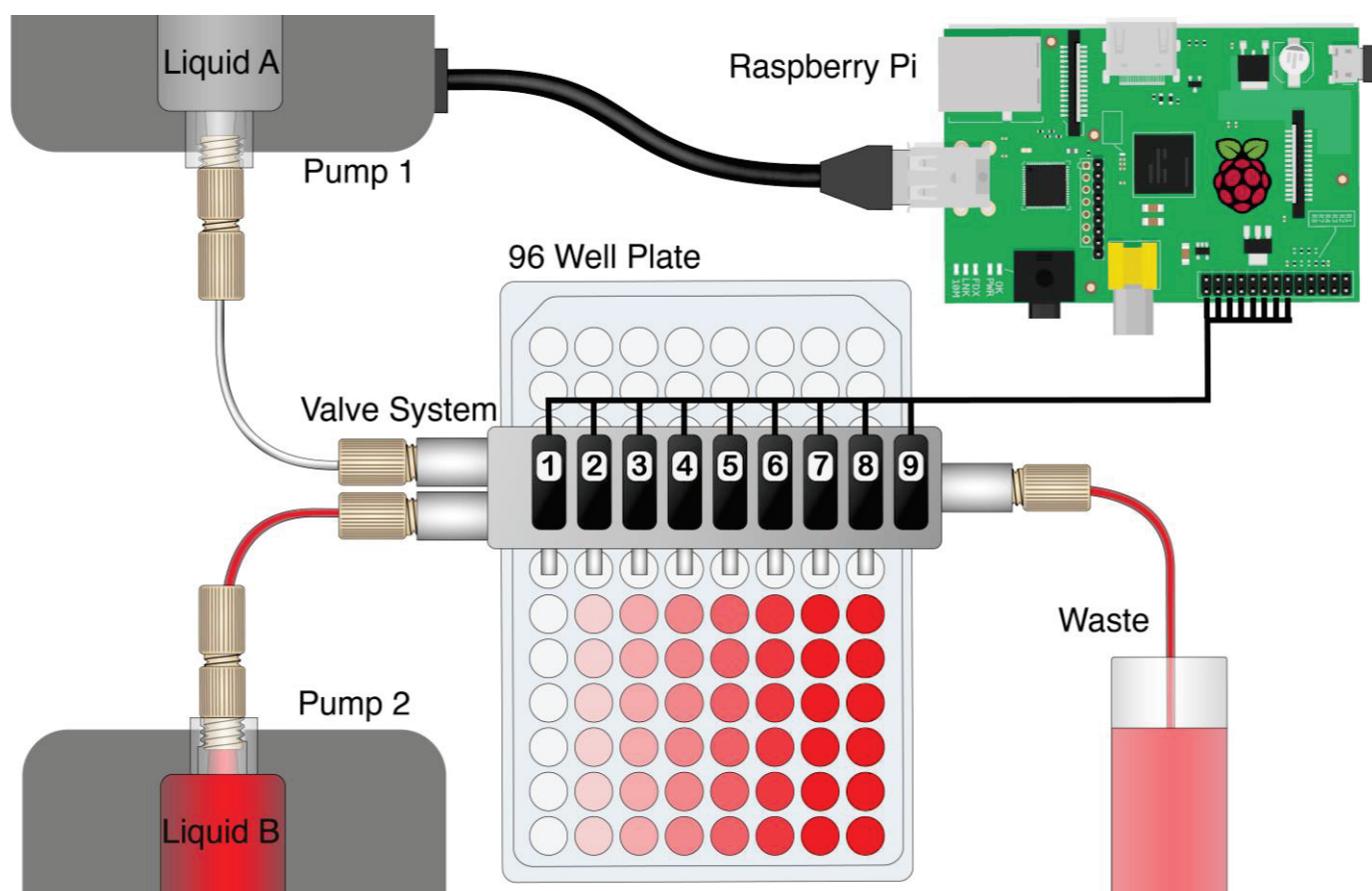
Figure 2: Automatization set-up and operation principle of the microfluidic valve system. Alternation in flow rates of two syringe pumps allows variation of mixtures of two selected liquids that are delivered to the valve system and distributed into the respective wells of a 96-well plate via a servomotor-controlled valve opening. One outlet of the chip is connected to a waste reservoir allowing rinsing steps. The servomotors and the pumps are connected to a Raspberry Pi computer and controlled through the use of a customized Python script.

parameters – including starting times, pump channels, pump rates, valve numbers, and incubation times. All of these parameters can be very quickly adapted for matching new assay protocols or modified chip designs.

3.2 Characterization of the Microfluidic Valve System

3.2.1 Long-term Robustness

Since the 3D-printed valve system contains delicate elements (such as thin valve membranes, small thread profiles, and miniature servos), the long-term stability of the system was thoroughly investigated. To be suitable for use in cell culture, the chip – including the valve membranes – also needs to withstand heat-steam sterilization. Although not required for subsequent proof-of-concept cell culture assay, the system must withstand several weeks of humid conditions in an incubator to be applicable to customized cell culture systems, such as organ-on-a-chip devices. Heat may cause deformation of the valve membrane, while moisture may be absorbed and cause the material to swell – which could affect its overall stability. Therefore, three chips (without electronic components) were pre-treated under different conditions: A normally post-processed chip, a heat-steam sterilized chip, and a chip that was both heat-steam sterilized and also incubated for four weeks (ddH$_2$O, 37 °C). Experiments were performed with four distinct valves/servos (n = 4).

After inducing continuous and repetitive actuation of the valves over the course of 4-5 days as a stress test, with at least 5806 opening and closing events occurring per valve, no failure of either the valve membrane or the threads was observed in any of the tested chips. Accordingly, it is concluded that this system is well-suited for extended use in humid and warm conditions enabling cell culture assay automatization for several weeks. Furthermore, the stability of the polymer membrane might actually be increased at these conditions, since the deformability of the membrane is expected to improve at moderate to high temperatures. Nor was any distribution of the liquid to an unintended outlet ever observed during these tests – leading to the conclusion that sufficient force of the servos and stability of the 3D-printed threads has also been established. Surprisingly, the servos of the system were actually identified as the relative weak spot, since 8 out of the 12 servos malfunctioned after approximately 1500 - 4200 opening and closing events (as summarized in Table S.2). This weakness may be shored up by using higher quality servos or motors, instead of the lowest priced servos that were used in our experiments. Nonetheless, the stability of all parts is deemed to be generally sufficient for both short-term and long-term use, and we conclude that this valve system enables the automatization of simple chemical or biochemical assays or even – due to its compatibility with heat steam sterilization – full-time reagent control for mammalian cell cultures directly inside an incubator.

3.2.2 Rinsing Volume Determinations

A significant rate of replacement of a present solution by another is crucial to avoid unwanted effects of residual substances at later steps of an assay. Since laminar flow is present, rinsing with an amount of the internal dead volume of

the chip of 32-50 µL (inlets to outlets) was deemed to be insufficient. Due to friction on the channel walls, the fluid layers at the edges of a channel are forced out of the channel much more slowly than in the centre, resulting in axial mixing of old
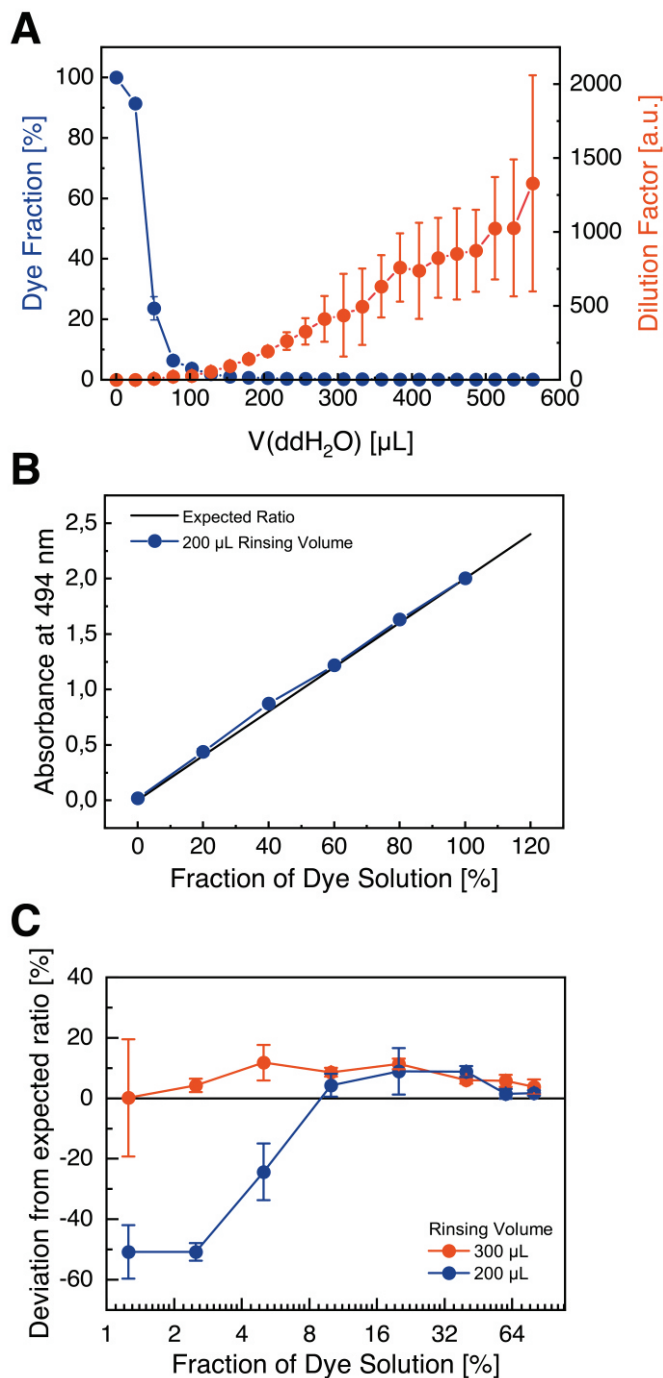
Figure 3: A) Dye fraction spectroscopically determined at the outlets after rinsing with ddH$_2$O. 99.0 %, 99.8 %, and 99.9 % of the dye was removed after about 150 µL, 300 µL, and 500 µL rinsing volumes, respectively. B+C) Mixing accuracy of the microfluidic valve system measured at the chip outlets, illustrating: B) Absorbance of the dye contained in mixtures generated with the valve system compared to the expected ratio; and C) Deviation from the ideal ratio of the measured dye absorbance in dependence of two distinct rinsing volumes passing through the system prior to the measurement, showing high inaccuracies for too low rinsing volumes. All experiments were performed three times (n = 3), with three distinct channels and valves.

and new solution. As a result, the rinsing volumes needed for complete removal of a present solution are higher than initially assumed and must be determined experimentally. Thus, the dependence of ddH$_2$O rinsing volume to the fraction of a present red dye solution at the outlets of the chip was investigated and is summarized in Figure 3A. The dye serves as a spectroscopically detectable substitute for substances used in cell culture assays. As expected, the percentage of the dye decreases significantly during the first 100 µL and approaches asymptotically to zero. Furthermore, removal of 99 % (1:100), 99.8 % (1:500) and 99.9 % (1:1000) of the dye is achieved by around 150 µL, 300 µL, and 500 µL rinsing volumes, respectively. In conclusion, the exchange of a present mixture by another one using 300 µL rinsing volume is likely to be sufficient for most applications – but if necessary, the rinsing volume may be increased for assays using highly active substances or large concentration ranges.

3.2.3 Mixing Accuracy

The mixing accuracy determines the systems resolution and operable concentration range for potential applications. Especially for dose-response assays, such as the assay presented in Section 3.3, high dilution factors may be required. Regarding the microfluidic valve system, increasing dilution

factors lead to a larger difference between the two pump rates at the chip inlets and thus to higher errors.

As presented in Figure 3B, mixtures of red dye solution and ddH$_2$O show an expected linear dependency with mean deviations of maximum 10 % from the ideal ratios measured at the chip outlet after pumped volumes of 200 µL. This accuracy is assumed to be sufficient for many present assays in research. However, at low ratios (such as 1.25 %, 2.5 %, or 5 %), mixtures contain a significantly decreased amount of dye with about 50 % deviation from the ideal ratios (Figure 3C). Nonetheless, this deviation decreases for higher rinsing volumes (such as 300 µL), indicating that at low flow rates of the dye stock solution the dye is not adequately delivered to the system. This may be explained by the high-pressure differential that exists between the two pumps. As a consequence, for assays with a higher concentration range, an increased rinsing volume for low fractions of a substance is recommended.

3.3 Proof-of-Concept Cell Culture Cytotoxicity Assay

To evaluate the systems performance in a real-world application, IC$_{50}$ determination of the cytotoxin camptothecin (CPT) with mouse fibroblasts (L929) was performed as a proof-of-concept (POC) and the results were compared to results obtained via traditional manually pipetting. L929 fibroblasts were used as they are a cell line recommended by standard
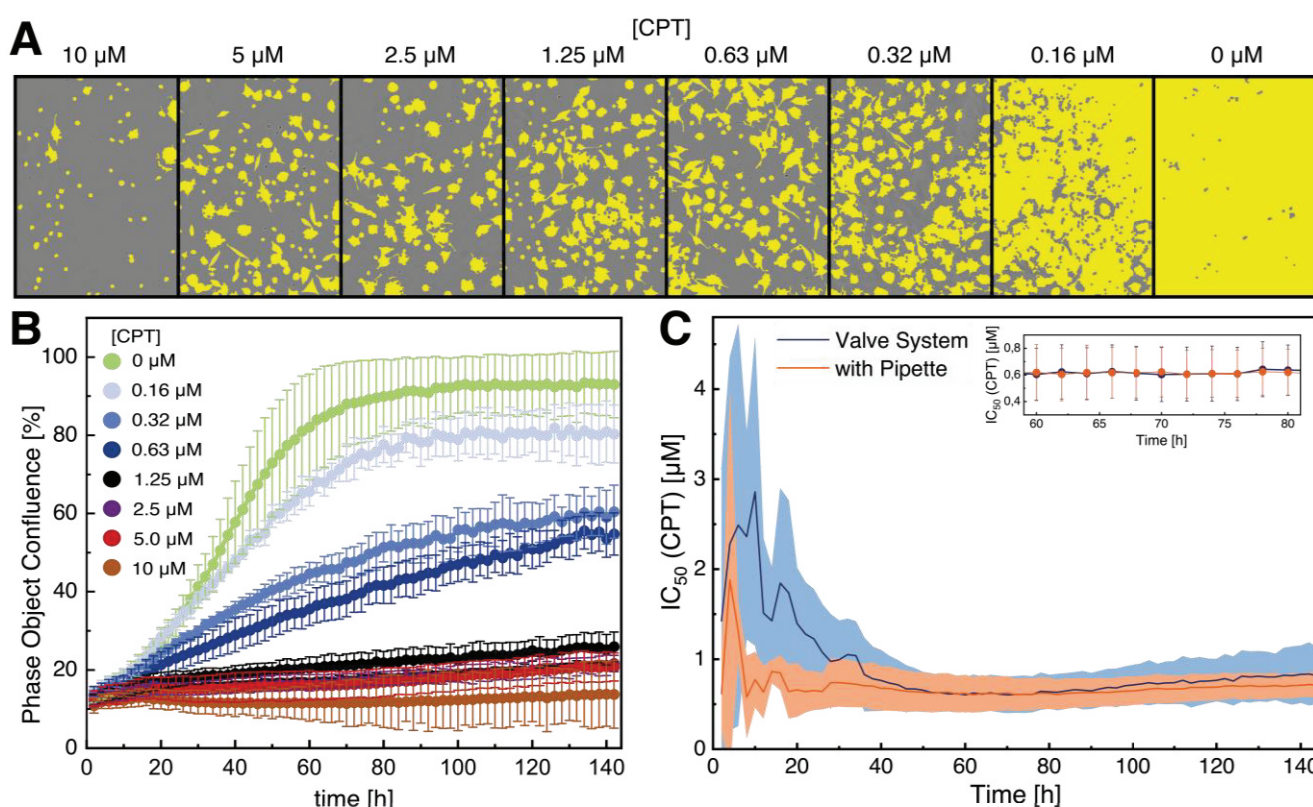
Figure 4: Results of the proof-of-concept assay for IC$_{50}$ determination of the cytotoxin camptothecin (CPT) with L929 cells. Illustrated are: A) Representative microscopic images (200 x magnification) and analyzed cell confluence (yellow) of L929 cells after assaying with the 3D-printed microfluidic valve system and three days of cultivation in the presence of varying CPT concentrations, monitored and analyzed by an IncuCyte S3 live-cell-imaging system; B) Cell growth curves of L929 cells at different CPT concentrations for 6 d after assaying with the 3D-printed microfluidic valve system, showing a clear concentration-dependent growth inhibition and a typical sigmoidal progression of the cell growth in absence of CPT; and C) Mean time-resolved IC$_{50}$ values of three distinct experiments (n=3) (errors indicated by area) of assays performed with the microfluidic valve system and manually by pipetting. Initial IC$_{50}$ values become constant after 50 h with similar average IC$_{50}$ values of 0.62 ± 0.19 µM and 0.62 ± 0.20 µM for the valve system and pipetting, respectively.

organizations such as the International Standard Organization (ISO) or the United States Pharmacopeia (USP)[33,34] for cytotoxicity and biocompatibility assays, while CPT is a well-known anti-cancer drug and serves as a widely used positive control for cytotoxicity and apoptosis[35].

The results of the proof-of-concept assay are presented in Figure 4, as a function of the cell growth that was monitored and analyzed by live-cell-imaging. After three days of cultivation, a clear concentration-dependent increase in confluence was observed (Figure 4A). As expected, the growth curve of cell in the control wells lacking CPT show a lag ($\sim$ 0-20 h), an exponential ($\sim$ 20-60 h) and a saturation phase ($\sim$ 80-140 h) (Figure 4B), while cells in wells containing high CPT concentrations show no growth at all. For comparison of the valve system and the standard pipetting technique, the IC_{50} was used as reference value. Since the imaging system allows the time-resolved quantification of the confluence, IC_{50} values were calculated for each time point (illustrated in Figure 4C). The IC_{50} values – including the corresponding standard deviations – decreased over time and became constant after about 50 h. This result is neither unusual nor unexpected, since cells require a certain amount of time to grow and establish a concentration-dependent difference in confluence. At very long cultivation times, IC_{50} values increase due to the control reaching 100 % confluence, and thus become unreliable. Importantly, at constant IC_{50} values between 60-80 h – where the toxic effect has been established and the control does not reach 100 % confluence – the average IC_{50} values observed in this time period were highly similar, with 0.62 ± 0.19 µM and 0.62 ± 0.20 µM for the pipetted assay and for the assay automated by the microfluidic valve system, respectively. Thus, we conclude that the valve system does ensure a sufficient accuracy for cellular dose-response experiments, and that the deviations in mixing accuracy of the systems do not significantly affect the results. The key result was confirmation that the presented system affords researchers a real opportunity for cell culture assay automatization within the safety cabinet or even directly inside the incubator, using a portable point-of-use device that can be rapidly adapted for the intended use.

Conclusions

In contrast to pipetting robots (which represent the current "gold standard" in liquid handling), microfluidic valve systems facilitate far greater spatiotemporally-controlled multiplexing at a compact design. Due to the on-chip valve control by servomotors in the herein presented system, features of pneumatically controlled actuation – such as control channels, connection ports, tubing, external valves, and a vacuum/pressure supply – have been essentially rendered obsolete. The presented 3D-printed microfluidic valve system demonstrated a sufficient accuracy and long-term robustness to allow for its realistic real-world application in a majority of assays. Since a similar performance of the microfluidic valve system and manual pipetting in a proof-of-concept IC_{50} cell culture assay was observed, this proof-of-concept demonstrates that this system is appropriate and feasible for

use in cell culture automatization. Importantly, the effort required to reconfigure this system is negligible compared with other manufacturing techniques, which renders direct integration of microfluidic cell culture chambers (or even organ-on-chip systems) realizable – thereby effectively enabling 24/7 operation even within unsterile environments. Finally, the integration of the microfluidic valve systems into live-cell-imaging systems illustrates a highly promising fusing of liquid handling and cell microscopy, and, in combination with machine-learning and online AI-based image processing, potentially opens the door for fully automated process optimization of adherent cell cultivation in the future.

Author Contributions

Conceptualization, J. B., S. W.; methodology, S. W., J. M., K. V. M. and C. K.C.; investigation, S. W. and J. M.; data curation, S. W. and J. M.; writing-original draft preparation, S. W.; writing-review and editing, S. W., K. M. and J. B.; visualization, S. W.; supervision, J. B.; project administration, J. B.; funding acquisition, J. B

Conflicts of interest

There are no conflicts to declare.

Acknowledgements

References

1   1   S. M. Bjork and H. N. Joensson, *Current opinion in biotechnology*, 2019, **55**, 95–102.
2   2   A. Enders, J.-A. Preuss and J. Bahnemann, *Micromachines*, 2021, **12,** https://pubmed.ncbi.nlm.nih.gov/34577708/.
3   3   A. Enders, I. G. Siller, K. Urmann, M. R. Hoffmann and J. Bahnemann, *Small*, 2019, **15**, e1804326.
4   4   J.-A. Preuß, P. Reich, N. Bahner and J. Bahnemann, *Advances in biochemical engineering/biotechnology*, 2020, **174**, 43–91, https://pubmed.ncbi.nlm.nih.gov/32313965/.
5   5   F. Yu, W. Hunziker and D. Choudhury, *Micromachines*, 2019, **10**.
6   6   Q. Wu, J. Liu, X. Wang, L. Feng, J. Wu, X. Zhu, W. Wen and X. Gong, *BioMed Eng OnLine*, 2020, **19**, 9, https://link.springer.com/article/10.1186/s12938-020-0752-0.
7   7   S. Winkler, A. Grünberger and J. Bahnemann, *Advances in biochemical engineering/biotechnology*, 2021, https://pubmed.ncbi.nlm.nih.gov/33495924/.
8   8   H. Andersson and A. van den Berg, *Lab on a chip*, 2006, **6**, 467–470, https://pubmed.ncbi.nlm.nih.gov/16572207/.
9   9   C. M. B. Ho, S. H. Ng, K. H. H. Li and Y.-J. Yoon, *Lab on a chip*, 2015, **15**, 3627–3637, https://pubs.rsc.org/en/content/articlehtml/2015/lc/c5lc00685f?casa_token=9FJcAVRcU9AAAAAA:lKIAGIOiWTjdLcxOYVEnZZLp-

wmacOKxmkTqYWOlc1ILeGL3OkN2LNBCjwl_B5HVYG8KiYL1g orG.

10 10 A. V. Nielsen, M. J. Beauchamp, G. P. Nordin and A. T. Woolley, *Annual review of analytical chemistry (Palo Alto, Calif.)*, 2020, **13**, 45–65.

11 11 K.-S. Lee, D.-Y. Yang, S. H. Park and R. H. Kim, *Polym. Adv. Technol.*, 2006, **17**, 72–82.

12 12 I. G. Siller, A. Enders, T. Steinwedel, N.-M. Epping, M. Kirsch, A. Lavrentieva, T. Scheper and J. Bahnemann, *Materials*, 2019, **12**, 2125, https://www.researchgate.net/publication/334180960_Real-Time_Live-Cell_Imaging_Technology_Enables_High-Throughput_Screening_to_Verify_in_Vitro_Biocompatibility_of_3D_Printed_Materials.

13 13 S. Winkler, K. V. Meyer, C. Heuer, C. Kortmann, M. Dehne and J. Bahnemann, *Engineering in Life Sciences*, 2022, https://www.researchgate.net/publication/359636650_In_vitro_biocompatibility_evaluation_of_a_heat-resistant_3D_printing_material_for_use_in_customized_cell_culture_devices.

14 14 I. G. Siller, A. Enders, P. Gellermann, S. Winkler, A. Lavrentieva, T. Scheper and J. Bahnemann, *Biomedical Materials*, 2020, **15**, 55007, https://www.researchgate.net/publication/341034633_Characterization_of_a_customized_3D-printed_cell_culture_system_using_clear_translucent_acrylate_that_enables_optical_online_monitoring.

15 15 T. A. Thorsen, *BioTechniques*, 2004, **36**, 197–199.

16 16 A. R. Vollertsen, D. de Boer, S. Dekker, B. A. M. Wesselink, R. Haverkate, H. S. Rho, R. J. Boom, M. Skolimowski, M. Blom, R. Passier, A. van den Berg, A. D. van der Meer and M. Odijk, *Microsyst Nanoeng*, 2020, **6**, 107, https://www.nature.com/articles/s41378-020-00216-z.

17 17 B. Schuster, M. Junkin, S. S. Kashaf, I. Romero-Calvo, K. Kirby, J. Matthews, C. R. Weber, A. Rzhetsky, K. P. White and S. Tay, *Nat Commun*, 2020, **11**, 5271, https://www.nature.com/articles/s41467-020-19058-4.

18 18 G. Pegoraro and T. Misteli, *Trends in genetics : TIG*, 2017, **33**, 604–615.

19 19 B. Larson, L. Hussain and J. Schroeder, in *Immuno-Oncology. Cellular and Translational Approaches*, ed. S.-L. Tan, Springer US; Imprint Humana, New York, NY, 1st edn., 2020, pp. 103–115.

20 20 R. Kodzius, F. Schulze, X. Gao and M. R. Schneider, *Genes*, 2017, **8**.

21 21 U. Blache and M. Ehrbar, *Advances in wound care*, 2018, **7**, 232–246.

22 22 R. Xie, W. Zheng, L. Guan, Y. Ai and Q. Liang, *Small*, 2020, **16**, e1902838.

23 23 M. A. Unger, H. P. Chou, T. Thorsen, A. Scherer and S. R. Quake, *Science (New York, N.Y.)*, 2000, **288**, 113–116.

24 24 K. Hosokawa and R. Maeda, *J. Micromech. Microeng.*, 2000, **10**, 415–420, https://iopscience.iop.org/article/10.1088/0960-1317/10/3/317/meta?casa_token=F4Ps4OEkkd0AAAAA:kRtujr-NOvlACvDGOZgxNaBEoTLWgGEo4fBNYf2P1Z13SDDGgCoHqzYV-dXPf_9AuE6_aQ9i.

25 25 J. Y. Baek, J. Y. Park, J. I. Ju, T. S. Lee and S. H. Lee, *J. Micromech. Microeng.*, 2005, **15**, 1015–1020, https://iopscience.iop.org/article/10.1088/0960-1317/15/5/017/meta?casa_token=ejX2YH_4cf8AAAAA:FdJnb4BJJivc-5z1e4ZeShVDX8VY5EbM10EOsscnAeMHVAS5fmlqbryTkILQ-dfAbUDvfabF.

26 26 A. K. Au, H. Lai, B. R. Utela and A. Folch, *Micromachines*, 2011, **2**, 179–220, https://www.mdpi.com/2072-666X/2/2/179/htm#b39-micromachines-02-00179.

27 27 J.-Y. Qian, C.-W. Hou, X.-J. Li and Z.-J. Jin, *Micromachines*, 2020, **11**.

28 28 T. Thorsen, S. J. Maerkl and S. R. Quake, *Science (New York, N.Y.)*, 2002, **298**, 580–584.

29 29 3D Systems, *Safety Data Sheet: VisiJet M2S-HT90. Available online: http://infocenter.3dsystems.com/materials/sites/default/files/sds-files/professional/VisiJet_M2S/HT_90/24245-S12-02-A%2CSDS%20GHS%2CEnglish%2CVisiJet%20M2S-HT90.pdf (accessed on 16 August 2021).*

30 30 3D Systems.

31 31 L. F. Liu, S. D. Desai, T. K. Li, Y. Mao, M. Sun and S. P. Sim, *Annals of the New York Academy of Sciences*, 2000, **922**, 1–10.

32 32 A. K. Au, N. Bhattacharjee, L. F. Horowitz, T. C. Chang and A. Folch, *Lab Chip*, 2015, **15**, 1934–1941, https://pubs.rsc.org/en/content/articlelanding/2015/lc/c5lc00126a.

33 33 International Organization for Standardization, *ISO 10993-12:2021 Biological Evaluation of Medical Devices. ISO copyright office, Venier, Switzerland.*, 2021.

34 34 The United States Pharmacopeial Convention, *United States Pharmacopoeia 44 - NF 39 - <87> Biological Reactivity Tests, In Vitro.*, 2022.

35 35 C. D. Willey, E. S.-H. Yang and J. A. Bonner, in *Clinical radiation oncology*, ed. J. E. Tepper, J. A. Bogart and L. L. Gunderson, Elsevier, Philadelphia, PA, 2016, 63-79.e4.

5 Zusammenfassung und Ausblick

In der vorliegenden Dissertation wurden das Potential und die Herausforderungen der additiven Fertigung für biotechnologische Anwendungen mit einem besonderen Fokus auf die Automatisierung von Zellkultursystemen untersucht. Ziel dieser Arbeit war es, die Sterilisierbarkeit und Biokompatibilität eines hitzestabilen 3D-Druckmaterials zu evaluieren und dessen Einsatz für die Automatisierung in der Zellkultur in Form automatisierter, 3D-gedruckter mikrofluidischer Systeme zu ermöglichen.

Da der 3D-Druck Entwicklungszeiten stark reduziert, die Designfreiheit erhöht und den Zugang zur Fertigung individualisierter Systeme ermöglicht, findet er zunehmend Anwendung in den Lebenswissenschaften. Für viele Produkte aus der Medizin oder Biotechnologie, die im direkten Kontakt zu lebenden Organismen stehen, ist die Biokompatibilität und Sterilisierbarkeit der verwendeten Materialien eine zwingende Notwendigkeit. Als Richtlinien für die Biokompatibilitätsbestimmung dienen verschiedene Normen, wie die ISO 10993 sowie die USP-Klassifizierung. Mithilfe dieser Normen zertifizieren auch 3D-Druckhersteller die Biokompatibilität ihrer Materialien. Allerdings werden dabei die Materialien i.d.R. nur für wenige Organismen unter bestimmten Testbedingungen geprüft. Dies erschwert es Wissenschaftler:innen, die geeignete Kombination aus Material, Drucker und Organismus für ihre Anwendung zu finden. Insbesondere bei höheren Anschaffungskosten professioneller 3D-Drucker sollte die eingehende Prüfung der Biokompatibilität angebotener Materialien vor dem Erwerb der Drucker erfolgen. Ansonsten könnten sich die verfügbaren Materialien womöglich hinterher als inkompatibel herausstellen und nicht mehr wie vorgesehen verwendet werden. Dies gilt ganz besonders, wenn nur wenige, ausschließlich vom Druckerhersteller angebotene 3D-Druckmaterialien verwendet werden können, wie es beim *multi-jet printing* der Fall ist.

In dem ersten experimentellen Teil dieser Arbeit (s. Kapitel 4.1) konnte die Biokompatibilität des 3D-Druckmaterials VisiJet M2S-HT90 der Firma 3D Systems Inc. gegenüber Mausfibroblasten (L929) und Hefen (*S. cerevisiae*) gezeigt werden. Das 3D-Druckmaterial ist ein neu auf dem Markt erschienenes Polyacrylat zur Fertigung hochaufgelöster 3D-Druck-Teile und zeichnet sich ganz besonders durch eine hohe Hitzebeständigkeit aus. Die verwendeten Zelltypen werden vielfach für die adhärente Zellkultur bzw. in der Bioprozessentwicklung in Forschung sowie Industrie genutzt, sodass vielseitige Anwendungsmöglichkeiten für das 3D-Druckmaterial entstehen. Im Gegensatz dazu zeigt das durch das Material deutlich gehemmte Wachstum von HEK 293E-Suspensionszellen, dass die Biokompatibilität stark von dem eingesetzten Organismus abhängt. Folglich sollte die Biokompatibilität eines Materials stets für den jeweils verwendeten Organismus ermittelt werden, da diese nicht ohne weiteres auf andere Organismen übertragen werden kann. Außerdem konnte gezeigt werden, dass die Sterilisation des Materials mittels Heißdampf die Biokompatibilität des Materials nicht beeinflusst. Somit können mit diesem Material 3D-gedruckte Zellkultursysteme besonders leicht sterilisiert und als *ready-to-use* (dt.: sofort nutzbar) Systeme eingesetzt werden. Der Nachweis der Biokompatibilität zusammen mit der hohen Druckauflösung des MJP-Verfahrens

ermöglicht in Zukunft auch die Verwendung des 3D-Druckmaterials zur Fertigung neuartiger mikrofluidscher Zellkultursysteme wie den *organ-on-a-chip* Systemen.

Neben der Biokompatibilitätsbestimmung eines 3D-Druckmaterials ist das zweite Ziel dieser Arbeit, die Automatisierung mikrofluidischer Zellkultursysteme durch 3D-gedruckte mikrofluidische Systeme zu ermöglichen. Um den potentiellen Nutzen und die Limitierungen mikrofluidischer Ventilsysteme einschätzen zu können, sollte zunächst ein Vergleich zu Pipettierrobotern als derzeitiger Goldstandard gezogen werden. Pipettierroboter werden hauptsächlich zur Automatisierung von 2D-Zellkulturen verwendet, welche in standardisierten Gewebekulturplatten kultiviert und somit leicht gehandhabt werden können. Für 2D-Zellassays im Hochdurchsatzverfahren sind Pipettierrobotersysteme, wie sie z.B. im Wirkstoffscreening verwendet werden, nicht wegzudenken und mikrofluidische Systeme können hier nicht mithalten. Allerdings können mikrofluidische Systeme deutlich kompakter gefertigt werden, sodass sie z.B. leichter innerhalb von Sicherheitsbänken und Inkubatoren betrieben werden können. Der größte Vorteil mikrofluidischer Automatisierung besteht jedoch darin, komplexere Zellkulturplattformen betreiben zu können. Diese können beispielsweise semi-permeable Membranen, mechanische Bauteile, Sensorik oder 3D-Zellkulturen enthalten. Auf diese Weise können komplexere physiologische Prozesse nachgeahmt und intensiver untersucht werden. Zum Beispiel können durch die Automatisierung von *organ-on-a-chip* Systemen durch mikrofluidische Ventilsysteme Wirkstoffscreenings durchgeführt werden, mit denen im Gegensatz zu 2D-Kulturen auch der Einfluss von Wirkstoffkandidaten auf einzelne Organfunktionen untersucht werden kann.

Im zweiten experimentellen Teil dieser Doktorarbeit (s. Kapitel 4.2) konnte ein 3D-gedrucktes, mikrofluidisches Ventilsystem für die Automatisierung eines Zellkulturassays als Machbarkeitsstudie entwickelt werden und das zweite wichtige Ziel der Arbeit erreicht werden. Die Fertigung aller mikrofluidischer Komponenten wie Anschlüsse, Mikrokanäle, Mikromischer und Mikroventile als einzelnes Teil in nur einem einzigen Schritt ist durch klassische Herstellungsverfahren ausgeschlossen. Das in dieser Arbeit entwickelte enorm leicht zu fertigende System ermöglicht von nun an auch Biowissenschaftler:innen die schnelle Herstellung und Automatisierung eigener mikrofluidischer Systeme. Einzigartig dabei ist zudem die Aktuation 3D-gedruckter Mikroventile mittels miniaturisierter Elektromotoren. Diese Kombination bietet eine kostengünstigere, schneller zu fertigende und leichter zu etablierende Alternative zu den am häufigsten verwendeten, pneumatisch automatisierten Mikroventilen. Somit wird ein weiteres Ziel dieser Arbeit, der erleichterte Zugang zu mikrofluidischen Systemen, erfüllt. Durch eine hohe Performance sowie hohe Robustheit der Mikroventile kann das System unmittelbar zur Automatisierung mikrofluidischer Zellkulturassays verwendet werden. Die Ergebnisse eines Zytotoxizitätsassays als Machbarkeitsstudie haben bewiesen, dass das System händischem Pipettieren in nichts nachsteht.

Im Gegensatz zu Pipettiertechniken kann das entwickelte mikrofluidische Ventilsystem zukünftig auch zur Automatisierung mikrofluidischer Zellkultursysteme verwendet werden. Dazu können beispielsweise die

Anschlüsse an den Ventilausgängen an bestehende Zellkultursysteme angepasst oder auch Zellkulturkammern direkt hinter den Ventilen in das System integriert werden. In Zukunft soll das System die Zugabe von Medium und Mediumzusätzen über einen längeren Kultivierungsprozess von Wochen oder Monaten ermöglichen. Dabei können zugegebene Stoffe (wie z.B. Wirkstoffe, Wachstumsfaktoren oder Farbstoffe) vollständig wieder ausspült werden, sodass zeitaufgelöste Konzentrationsprofile erzeugt werden können. Werden die mikrofluidischen Ventilsysteme gemeinsam mit mikrofluidischen Zellkulturplattformen zusätzlich in *live-cell-imaging* Systeme integriert, kann auch die Echtzeitanalyse von Fluoreszenz- und Phasenkontrastbildern durch automatisierte Bildanalyse ermöglicht werden. Somit wäre auch die Regelung des mikrofluidischen Systems durch das *live-cell-imaging* System anhand der Zellmorphologie denkbar. Insbesondere komplexe Zelldifferenzierungsprotokolle, die zur korrekten Durchführung erfahrene, hochqualifizierte Forscher:innen benötigen, könnten auf diese Weise automatisiert und optimiert werden. Noch bestehen jedoch große Herausforderungen, wie z.B. der technische Einbau mikrofluidischer Systeme in *live-cell-imaging* Systeme.

Die additive Fertigung mikrofluidischer Systeme für die adhärente Zellkultur ist aufgrund der erforderlichen Biokompatibilität und Sterilisierbarkeit keineswegs leicht zu realisieren. Kann jedoch ein geeignetes Material gefunden werden, so bietet der 3D-Druck die Möglichkeit, komplexe Systeme zu fertigen und sie exakt auf bestimmte Anwendungen zuzuschneiden. Diese gewonnenen Freiheiten können insbesondere auch durch Biowissenschaftler:innen zur Entwicklung eigener Zellkultursysteme genutzt werden. Dabei können entwickelte Elemente, wie Anschlüsse, Mikromischer und Mikroventile, als separate funktionelle Module im CAD-Modell frei mitaneinander kombiniert werden. Durch diese Modularität muss ein neues System nicht von Grund auf neu entwickelt werden, es lässt sich aber für neue Anwendungen weiterhin anpassen. Angesichts des ständigen Fortschritts des 3D-Drucks hinsichtlich Materialvielfalt, Auflösung und Anschaffungskosten ist auch eine wachsende Popularität der additiven Fertigung in den Lebenswissenschaften zu erwarten. Damit jedoch neue Ideen auf bereits entwickelten Systemen aufbauen können, braucht es neben einem 3D-Drucker und biokompatibler Materialien auch offen zugängliche 3D-Modelle. Mit dieser Arbeit werden die Einsatzmöglichkeiten des 3D-Drucks in der Mikrofluidik vergrößert, indem das neu entwickelte, 3D-gedruckte mikrofluidische System durch alle Wissenschaftler:innen frei verfügbar zur Automatisierung adhärenter Zellkultursysteme genutzt werden kann. Nun ist es an der Zeit, den Austausch von 3D-Modellen zu fördern, neue Anwendungsfelder für 3D-gedruckte mikrofluidische Zellkultursysteme zu entdecken und „die kommende 3D-Druck-Revolution der Mikrofluidik" [7] einzuleiten.

Literaturverzeichnis

[1]   Sachdeva, S., Davis, R. W., Saha, A. K., Microfluidic Point-of-Care Testing: Commercial Landscape and Future Directions. *Frontiers in bioengineering and biotechnology* 2020, *8*, 602659.

[2]   Ladner, T., Grünberger, A., Probst, C., Kohlheyer, D. et al., 15 – Application of Mini- and Micro-Bioreactors for Microbial Bioprocesses, in: Larroche, C., Sanromán, M. Á., Du, G., Pandey, A. (Eds.), *Current developments in biotechnology and bioengineering: Bioprocesses, bioreactors and controls*, Elsevier, Amsterdam, Boston, Heidelberg, London, New York, Oxford, Paris, San Diego, San Francisco, Singapore, Sydney, Tokyo 2016, pp. 433–461.

[3]   Wu, Q., Liu, J., Wang, X., Feng, L. et al., Organ-on-a-chip: recent breakthroughs and future prospects. *BioMed Eng OnLine* 2020, *19*, 9.

[4]   Iyer, V., Yang, Z., Ko, J., Weissleder, R. et al., Advancing microfluidic diagnostic chips into clinical use: a review of current challenges and opportunities. *Lab Chip* 2022.

[5]   Mohammed, M. I., Haswell, S., Gibson, I., Lab-on-a-chip or Chip-in-a-lab: Challenges of Commercialization Lost in Translation. *Procedia Technology* 2015, *20*, 54–59.

[6]   Andersson, H., van den Berg, A., Where are the biologists? *Lab on a chip* 2006, *6*, 467–470.

[7]   Bhattacharjee, N., Urrios, A., Kang, S., Folch, A., The upcoming 3D-printing revolution in microfluidics. *Lab on a chip* 2016, *16*, 1720–1742.

[8]   Terry, S. C., Jerman, J. H., Angell, J. B., A gas chromatographic air analyzer fabricated on a silicon wafer. *IEEE Trans. Electron Devices* 1979, *26*, 1880–1886.

[9]   Manz, A., Graber, N., Widmer, H. M., Miniaturized total chemical analysis systems: A novel concept for chemical sensing. *Sensors and Actuators B: Chemical* 1990, *1*, 244–248.

[10]   Bahnemann, J., Grünberger, A., Microfluidics in Biotechnology: Overview and Status Quo, in:, *Microfluidics in Biotechnology*, Springer, Cham, 2022, pp. 1–16.

[11]   Scott, S. M., Ali, Z., Fabrication Methods for Microfluidic Devices: An Overview. *Micromachines* 2021, *12*.

[12]   Duffy, D. C., McDonald, J. C., Schueller, O. J., Whitesides, G. M., Rapid Prototyping of Microfluidic Systems in Poly(dimethylsiloxane). *Analytical chemistry* 1998, *70*, 4974–4984.

[13]   Niculescu, A.-G., Chircov, C., Bîrcă, A. C., Grumezescu, A. M., Fabrication and Applications of Microfluidic Devices: A Review. *International journal of molecular sciences* 2021, *22*.

[14]   Siekmann, H. E., Thamsen, P. U., *Strömungslehre: Grundlagen. Springer-Lehrbuch*, 2nd Ed., Springer Berlin Heidelberg, Berlin, Heidelberg 2008.

[15]   Enders, A., Siller, I. G., Urmann, K., Hoffmann, M. R. et al., 3D Printed Microfluidic Mixers–A Comparative Study on Mixing Unit Performances. *Small (Weinheim an der Bergstrasse, Germany)* 2019, *15*, e1804326.

[16]   Enders, A., Preuss, J.-A., Bahnemann, J., 3D Printed Microfluidic Spiral Separation Device for Continuous, Pulsation-Free and Controllable CHO Cell Retention. *Micromachines* 2021, *12*.

[17]   Chen, C. H., Lu, Y., Sin, M. L. Y., Mach, K. E. et al., Antimicrobial susceptibility testing using high surface-to-volume ratio microchannels. *Analytical chemistry* 2010, *82*, 1012–1019.

[18]   Leclerc, E., Sakai, Y., Fujii, T., Microfluidic PDMS (polydimethylsiloxane) bioreactor for large-scale culture of hepatocytes. *Biotechnology progress* 2004, *20*, 750–755.

[19]   Arshavsky-Graham, S., Segal, E., Lab-on-a-Chip Devices for Point-of-Care Medical Diagnostics. *Advances in biochemical engineering/biotechnology* 2022, *179*, 247–265.

[20]   Zhang, B., Korolj, A., Lai, B. F. L., Radisic, M., Advances in organ-on-a-chip engineering. *Nat Rev Mater* 2018, *3*, 257–278.

[21]   Dekker, S., Isgor, P. K., Feijten, T., Segerink, L. I. et al., From chip-in-a-lab to lab-on-a-chip: a portable Coulter counter using a modular platform. *Microsyst Nanoeng* 2018, *4*, 34.

[22]   O'Neill, P. F., Ben Azouz, A., Vázquez, M., Liu, J. et al., Advances in three-dimensional rapid prototyping of microfluidic devices for biological applications. *Biomicrofluidics* 2014, *8*, 52112.

[23]   Chen, C., Mehl, B. T., Munshi, A. S., Townsend, A. D. et al., 3D-printed Microfluidic Devices: Fabrication, Advantages and Limitations-a Mini Review. *Analytical methods : advancing methods and applications* 2016, *8*, 6005–6012.

[24]   Kotz, F., Helmer, D., Rapp, B. E., Emerging Technologies and Materials for High-Resolution 3D Printing of Microfluidic Chips. *Advances in biochemical engineering/biotechnology* 2022, *179*, 37–66.

[25]   Childs, E. H., Latchman, A. V., Lamont, A. C., Hubbard, J. D. et al., Additive Assembly for PolyJet-Based Multi-Material 3D Printed Microfluidics. *J. Microelectromech. Syst.* 2020, *29*, 1094–1096.

[26]   Gyimah, N., Scheler, O., Rang, T., Pardy, T., Can 3D Printing Bring Droplet Microfluidics to Every Lab?-A Systematic Review. *Micromachines* 2021, *12*.

[27]   He, Y., Wu, Y., Fu, J., Gao, Q. et al., Developments of 3D Printing Microfluidics and Applications in Chemistry and Biology: a Review. *Electroanalysis* 2016, *28*, 1658–1678.

[28]   Au, A. K., Bhattacharjee, N., Horowitz, L. F., Chang, T. C. et al., 3D-printed microfluidic automation. *Lab Chip* 2015, *15*, 1934–1941.

[29]   Lee, K. G., Park, K. J., Seok, S., Shin, S. et al., 3D printed modules for integrated microfluidic devices. *RSC Adv.* 2014, *4*, 32876–32880.

[30]   Siller, I. G., Preuss, J.-A., Urmann, K., Hoffmann, M. R. et al., 3D-Printed Flow Cells for Aptamer-Based Impedimetric Detection of E. coli Crooks Strain. *Sensors (Basel, Switzerland)* 2020, *20*.

[31]   Yuen, P. K., Embedding objects during 3D printing to add new functionalities. *Biomicrofluidics* 2016, *10*, 44104.

[32]   Romanov, V., Samuel, R., Chaharlang, M., Jafek, A. R. et al., FDM 3D Printing of High-Pressure, Heat-Resistant, Transparent Microfluidic Devices. *Analytical chemistry* 2018, *90*, 10450–10456.

[33]   Siller, I. G., Enders, A., Gellermann, P., Winkler, S. et al., Characterization of a customized 3D-printed cell culture system using clear, translucent acrylate that enables optical online monitoring. *Biomedical materials (Bristol, England)* 2020, *15*, 55007.

[34]   Ford, M. J., Loeb, C. K., Pérez, L. X. P., Gammon, S. et al., 3D Printing of Transparent Silicone Elastomers. *Adv Materials Technologies* 2022, *7*, 2100974.

[35]   Krujatz, F., Lode, A., Seidel, J., Bley, T. et al., Additive Biotech-Chances, challenges, and recent applications of additive manufacturing technologies in biotechnology. *New biotechnology* 2017, *39*, 222–231.

[36]   Zhou, L.-Y., Fu, J., He, Y., A Review of 3D Printing Technologies for Soft Polymer Materials. *Adv. Funct. Mater.* 2020, *30*, 2000187.

[37]   Guttridge, C., Shannon, A., O'Sullivan, A., O'Sullivan, K. J. et al., Biocompatible 3D printing resins for medical applications: A review of marketed intended use, biocompatibility certification, and post-processing guidance. *Annals of 3D Printed Medicine* 2022, *5*, 100044.

[38]   Muita, K., Westerlund, M., Rajala, R., The Evolution of Rapid Production: How to Adopt Novel Manufacturing Technology. *IFAC-PapersOnLine* 2015, *48*, 32–37.

[39]   Shahrubudin, N., Lee, T. C., Ramlan, R., An Overview on 3D Printing Technology: Technological, Materials, and Applications. *Procedia Manufacturing* 2019, *35*, 1286–1296.

[40]   Kristiawan, R. B., Imaduddin, F., Ariawan, D., Ubaidillah et al., A review on the fused deposition modeling (FDM) 3D printing: Filament processing, materials, and printing parameters. *Open Engineering* 2021, *11*, 639–649.

[41]   Nielsen, A. V., Beauchamp, M. J., Nordin, G. P., Woolley, A. T., 3D Printed Microfluidics. *Annual review of analytical chemistry (Palo Alto, Calif.)* 2020, *13*, 45–65.

[42]   Au, A. K., Huynh, W., Horowitz, L. F., Folch, A., 3D-Printed Microfluidics. *Angewandte Chemie International Edition* 2016, *55*, 3862–3881.

[43]   Amin, R., Knowlton, S., Hart, A., Yenilmez, B. et al., 3D-printed microfluidic devices. *Biofabrication* 2016, *8*, 22001.

[44]   Macdonald, N. P., Cabot, J. M., Smejkal, P., Guijt, R. M. et al., Comparing Microfluidic Performance of Three-Dimensional (3D) Printing Platforms. *Analytical chemistry* 2017, *89*, 3858–3866.

[45]   Waldbaur, A., Rapp, H., Länge, K., Rapp, B. E., Let there be chip—towards rapid prototyping of microfluidic devices: one-step manufacturing processes. *Anal. Methods* 2011, *3*, 2681.

[46]   Ge, Q., Li, Z., Wang, Z., Kowsari, K. et al., Projection micro stereolithography based 3D printing and its applications. *Int. J. Extrem. Manuf.* 2020, *2*, 22004.

[47]   Sochol, R. D., Sweet, E., Glick, C. C., Wu, S.-Y. et al., 3D printed microfluidics and microelectronics. *Microelectronic Engineering* 2018, *189*, 52–68.

[48]   Habib, T., Brämer, C., Heuer, C., Ebbecke, J. et al., 3D-Printed microfluidic device for protein purification in batch chromatography. *Lab on a chip* 2022, *22*, 986–993.

[49]   Rafiee, M., Farahani, R. D., Therriault, D., Multi-Material 3D and 4D Printing: A Survey. *Advanced Science* 2020, *7*, 1902307.

[50]   Capel, A. J., Edmondson, S., Christie, S. D. R., Goodridge, R. D. et al., Design and additive manufacture for flow chemistry. *Lab Chip* 2013, *13*, 4583–4590.

[51]   Mahmood, M. A., Popescu, A. C., 3D Printing at Micro-Level: Laser-Induced Forward Transfer and Two-Photon Polymerization. *Polymers* 2021, *13*.

[52]   Lao, Z., Xia, N., Wang, S., Xu, T. et al., Tethered and Untethered 3D Microactuators Fabricated by Two-Photon Polymerization: A Review. *Micromachines* 2021, *12*.

[53]   Raimondi, M. T., Eaton, S. M., Nava, M. M., Laganà, M. et al., Two-photon laser polymerization: from fundamentals to biomedical application in tissue engineering and regenerative medicine. *Journal of applied biomaterials & functional materials* 2012, *10*, 55–65.

[54]   Sakellari, I., Kabouraki, E., Gray, D., Purlys, V. et al., Diffusion-assisted high-resolution direct femtosecond laser writing. *ACS nano* 2012, *6*, 2302–2311.

[55]   Guillaume, O., Kopinski-Grünwald, O., Weisgrab, G., Baumgartner, T. et al., Hybrid spheroid microscaffolds as modular tissue units to build macro-tissue assemblies for tissue engineering. *Acta Biomaterialia* 2022.

[56]   Williams, D. F., On the mechanisms of biocompatibility. *Biomaterials* 2008, *29*, 2941–2953.

[57]   Piironen, K., Haapala, M., Talman, V., Järvinen, P. et al., Cell adhesion and proliferation on common 3D printing materials used in stereolithography of microfluidic devices. *Lab Chip* 2020, *20*, 2372–2382.

[58]   S. Alsoufi, M., W. Alhazmi, M., K. Suker, D., A. Alghamdi, T. et al., Experimental Characterization of the Influence of Nozzle Temperature in FDM 3D Printed Pure PLA and Advanced PLA+. *AJME* 2019, *7*, 45–60.

[59]   Asvany, O., Yamada, K. M. T., Brünken, S., Potapov, A. et al., Vibrational dynamics. Experimental ground-state combination differences of CH_5^+. *Science (New York, N.Y.)* 2015, *347*, 1346–1349.

[60]   Karakurt, I., Lin, L., 3D printing technologies: techniques, materials, and post-processing. *Current Opinion in Chemical Engineering* 2020, *28*, 134–143.

[61]   González, G., Baruffaldi, D., Martinengo, C., Angelini, A. et al., Materials Testing for the Development of Biocompatible Devices through Vat-Polymerization 3D Printing. *Nanomaterials (Basel, Switzerland)* 2020, *10*.

[62]   Grigaleviciute, G., Baltriukiene, D., Bukelskiene, V., Malinauskas, M., Biocompatibility Evaluation and Enhancement of Elastomeric Coatings Made Using Table-Top Optical 3D Printer. *Coatings* 2020, *10*, 254.

[63]   An, Y. H., Alvi, F. I., Kang, Q., Laberge, M. et al., Effects of sterilization on implant mechanical property and biocompatibility. *The International journal of artificial organs* 2005, *28*, 1126–1137.

[64]   Khanna, I., Drug discovery in pharmaceutical industry: productivity challenges and trends. *Drug Discovery Today* 2012, *17*, 1088–1102.

[65]   International Organization for Standardization, ISO 10993-5:2021 Biological Evaluation of Medical Devices. ISO copyright office, Venier, Switzerland. 2021.

[66]   International Organization for Standardization, ISO 10993-12:2021(E) Biological Evaluation of Medical Devices. ISO copyright office, Venier, Switzerland. 2021.

[67]   Lücking, T. H., Sambale, F., Schnaars, B., Bulnes-Abundis, D. et al., 3D-printed individual labware in biosciences by rapid prototyping: In vitro biocompatibility and applications for eukaryotic cell cultures. *Eng. Life Sci.* 2015, *15*, 57–64.

[68]   Pintor, A. V. B., Queiroz, L. D., Barcelos, R., Primo, L. S. G. et al., MTT versus other cell viability assays to evaluate the biocompatibility of root canal filling materials: a systematic review. *International endodontic journal* 2020, *53*, 1348–1373.

[69]   Bigl, K., Schmitt, A., Meiners, I., Münch, G. et al., Comparison of results of the CellTiter Blue, the tetrazolium (3-4,5-dimethylthioazol-2-yl-2,5-diphenyl tetrazolium bromide), and the lactate dehydrogenase assay applied in brain cells after exposure to advanced glycation endproducts. *Toxicology in Vitro* 2007, *21*, 962–971.

[70]   Piao, M. J., Kang, K. A., Lee, I. K., Kim, H. S. et al., Silver nanoparticles induce oxidative cell damage in human liver cells through inhibition of reduced glutathione and induction of mitochondria-involved apoptosis. *Toxicology letters* 2011, *201*, 92–100.

[71]   Li, W., Zhou, J., Xu, Y., Study of the in vitro cytotoxicity testing of medical devices. *Biomedical reports* 2015, *3*, 617–620.

[72]   Riss, T., Niles, A., Moravec, R., Karassina, N. et al. (Eds.), *Assay Guidance Manual [Internet]*, Eli Lilly & Company and the National Center for Advancing Translational Sciences, 2019.

[73]   Siller, I. G., Enders, A., Steinwedel, T., Epping, N.-M. et al., Real-Time Live-Cell Imaging Technology Enables High-Throughput Screening to Verify in Vitro Biocompatibility of 3D Printed Materials. *Materials (Basel, Switzerland)* 2019, *12*.

[74]   Vlata, Z., Porichis, F., Tzanakakis, G., Tsatsakis, A. et al., A study of zearalenone cytotoxicity on human peripheral blood mononuclear cells. *Toxicology letters* 2006, *165*, 274–281.

[75]   Kamp, H. G., Eisenbrand, G., Schlatter, J., Würth, K. et al., Ochratoxin A: induction of (oxidative) DNA damage, cytotoxicity and apoptosis in mammalian cell lines and primary cells. *Toxicology* 2005, *206*, 413–425.

[76]   The United States Pharmacopeial Convention, United States Pharmacopoeia 44 – NF 39 – <88> Biological Reactivity Tests, In Vivo 2021.

[77]   The United States Pharmacopeial Convention, United States Pharmacopoeia 44 – NF 39 – <87> Biological Reactivity Tests, In Vitro 2021.

[78]   OECD, *Test No. 251: Rapid Androgen Disruption Activity Reporter (RADAR) assay. OECD Guidelines for the Testing of Chemicals, Section 2*, OECD Publishing, Paris 2022.

[79]   Alifui-Segbaya, F., Varma, S., Lieschke, G. J., George, R., Biocompatibility of Photopolymers in 3D Printing. *3D Printing and Additive Manufacturing* 2017, *4*, 185–191.

[80]   Ma, C., Peng, Y., Li, H., Chen, W., Organ-on-a-Chip: A New Paradigm for Drug Development. *Trends in pharmacological sciences* 2021, *42*, 119–133.

[81]   Herrmann, K. (Ed.), *Animal Experimentation: Working Towards a Paradigm Change*, Koninklijke Brill NV incorporates the imprints Brill Brill Hes & De Graaf Brill Nijhoff Brill Rodopi Brill Sense and Hotei Publishing, Erscheinungsort nicht ermittelbar 2019.

[82]   Mejía-Salazar, J. R., Rodrigues Cruz, K., Materón Vásques, E. M., Novais de Oliveira, O., Microfluidic Point-of-Care Devices: New Trends and Future Prospects for eHealth Diagnostics. *Sensors (Basel, Switzerland)* 2020, *20*.

[83]   Zhang, F.-Q., Jiang, J.-L, Zhang, J.-T., Niu, H. et al., Current status and future prospects of stem cell therapy in Alzheimer's disease. *Neural regeneration research* 2020, *15*, 242–250.

[84]   Shin, A., Kim, S., The History, Current Status, Benefits, and Challenges of 3D Printed Organs, 2022.

[85]   Nies, C., Rubner, T., Lorig, H., Colditz, V. et al., A Microcavity Array-Based 4D Cell Culture Platform. *Bioengineering (Basel, Switzerland)* 2019, *6*.

[86]   Osaki, T., Sivathanu, V., Kamm, R. D., Engineered 3D vascular and neuronal networks in a microfluidic platform. *Sci Rep* 2018, *8*, 5168.

[87]   Fendler, C., Denker, C., Harberts, J., Bayat, P. et al., Microscaffolds by Direct Laser Writing for Neurite Guidance Leading to Tailor-Made Neuronal Networks. *Advanced biosystems* 2019, *3*, e1800329.

[88]   Chen, Y.-A., King, A. D., Shih, H.-C., Peng, C.-C. et al., Generation of oxygen gradients in microfluidic devices for cell culture using spatially confined chemical reactions. *Lab Chip* 2011, *11*, 3626–3633.

[89]   Lavrentieva, A., Spencer-Fry, J., Hydrogels for 3D Cell Culture, in:, *Basic Concepts on 3D Cell Culture*, Springer, Cham, 2021, pp. 105–123.

[90]   Tang, S. Q., Li, K. H. H., Lee, S. J., Zeng, J. J. et al., Novel multi-way microvalve with ease of fabrication and integration for microfluidics application. *Sensors and Actuators B: Chemical* 2019, *286*, 289–300.

[91]   Au, A. K., Lai, H., Utela, B. R., Folch, A., Microvalves and Micropumps for BioMEMS. *Micromachines* 2011, *2*, 179–220.

[92]   McDonald, J. C., Whitesides, G. M., Poly(dimethylsiloxane) as a material for fabricating microfluidic devices. *Accounts of chemical research* 2002, *35*, 491–499.

[93]   Hosokawa, K., Maeda, R., A normally closed PDMS (polydimethylsiloxane) microvalve. *IEEJ Trans. SM* 2000, *120*, 177–178.

[94]   Baek, J. Y., Park, J. Y., Ju, J. I., Lee, T. S. et al., A pneumatically controllable flexible and polymeric microfluidic valve fabricated via in situ development. *J. Micromech. Microeng.* 2005, *15*, 1015–1020.

[95]   Sundararajan, N., Kim, D., Berlin, A. A., Microfluidic operations using deformable polymer membranes fabricated by single layer soft lithography. *Lab on a chip* 2005, *5*, 350–354.

[96]   Qian, J.-Y., Hou, C.-W., Li, X.-J., Jin, Z.-J., Actuation Mechanism of Microvalves: A Review. *Micromachines* 2020, *11*, 172.

[97]   Kim, J., Stockton, A. M., Jensen, E. C., Mathies, R. A., Pneumatically actuated microvalve circuits for programmable automation of chemical and biochemical analysis. *Lab Chip* 2016, *16*, 812–819.

[98]   Mohd Ghazali, F. A., Hasan, M. N., Rehman, T., Nafea, M. et al., MEMS actuators for biomedical applications: a review. *J. Micromech. Microeng.* 2020, *30*, 73001.

[99]   Yunas, J., Mulyanti, B., Hamidah, I., Mohd Said, M. et al., Polymer-Based MEMS Electromagnetic Actuator for Biomedical Application: A Review. *Polymers* 2020, *12*.

[100]   Liu, B., Yang, J., Yang, J., Li, D. et al., A thermally actuated microvalve using paraffin composite by induction heating. *Microsyst Technol* 2019, *25*, 3969–3975.

[101]   Weibel, D. B., Kruithof, M., Potenta, S., Sia, S. K. et al., Torque-actuated valves for microfluidics. *Analytical chemistry* 2005, *77*, 4726–4733.

[102]   Allan T Evans, Jong M Park, Ryan P Taylor, Tyler R Brosten et al., *A low power, micromachined, proportional valve for drug delivery*, 2016.

[103]   Gunda, A., Özkayar, G., Tichem, M., Ghatkesar, A. M. K., Proportional Microvalve Using a Unimorph Piezoelectric Microactuator. *Micromachines* 2020, *11*, 130.

[104]   Nguyen, N.-T., Truong, T.-Q., Wong, K.-K., Ho, S.-S. et al., Micro check valves for integration into polymeric microfluidic devices. *J. Micromech. Microeng.* 2004, *14*, 69–75.

[105]   Ball, C. S., Renzi, R. F., Priye, A., Meagher, R. J., A simple check valve for microfluidic point of care diagnostics. *Lab Chip* 2016, *16*, 4436–4444.

[106]   Bauer, M., Ataei, M., Caicedo, M., Jackson, K. et al., Burst valves for commercial microfluidics: a critical analysis. *Microfluid Nanofluid* 2019, *23*, 1–12.

[107]   Gómez-Sjöberg, R., Leyrat, A. A., Pirone, D. M., Chen, C. S. et al., Versatile, fully automated, microfluidic cell culture system. *Analytical chemistry* 2007, *79*, 8557–8563.

[108]   Schuster, B., Junkin, M., Kashaf, S. S., Romero-Calvo, I. et al., Automated microfluidic platform for dynamic and combinatorial drug screening of tumor organoids. *Nature Communications* 2020, *11*, 5271.

Anhang

Weitere Projekte, die während der Promotion bearbeitet wurden:

A.1: Entwicklung eines 3D-gedruckten *Desease-on-a-Chip* zur axonalen Infektion durch neuroinvasive Viren

Durch den anterograden Transport in den Axonen von Hinterwurzelganglien können neuroinvasive Viren wie die Herpes-Simplex-Viren (HSV) und Varizella-Zoster-Viren (VZV) das zentrale Nervensystem befallen und schwerwiegende Erkrankungen auslösen. Um diesen Prozess *in vitro* studieren zu können, müssen die Axonenden vom Soma separiert werden, um die Lyse nach direkter Infektion des Somas zu verhindern. In diesem Projekt wurden in Kooperation mit der Arbeitsgruppe von Prof. Dr. Abel Viejo-Borbolla von der Medizinischen Hochschule Hannover 3D-gedruckte Systeme entwickelt, um mittels einer Kollagenbarriere Axon und Soma voneinander zu trennen. Dabei wurden Systeme für das horizontale wie vertikale Wachstum der Axone entwickelt. Die Systeme erlaubten dabei die Parallelisierung mehrerer Zellkulturen innerhalb eines Chips. Es konnte bereits eine Biokompatibilität zu Vero-Zellen als Testzelllinie gezeigt werden. Das Wachstum der Axone dorsaler Hinterwurzelganglien durch die Kollagenbarriere und eine anschließende Infektion durch neuroinvasive konnte aber nicht abschließend untersucht werden. Dieses Projekt war zudem die Grundlage der betreuten Masterarbeit von Daniel Hennig.

A.2: Entwicklung einer mikrofluidischen Sensorplattform zur automatisierten online-Messung von OUR, CER und pH in Bioreaktoren

Die Sauerstoffaufnahmerate (engl.: *oxygen uptake rate*, OUR), die Kohlenstoffdioxidemissionsrate (engl.: *carbondioxide emission rate*, CER) sowie der pH in Bioreaktoren enthalten wertvolle Information über den Zustand von Zellen während der Kultivierung und können zur Bioprozessoptimierung genutzt werden. In Zusammenarbeit mit Katharina Dahlmann, Dr. Dörte Solle und Prof. Dr. Janina Bahnemann wurde eine mikrofluidische Sensorplattform zur online-Messung dieser Größen entwickelt. Die Plattform besitzt integrierte *Sensorplugs* (PreSens Precision GmbH) zur Sauerstoff-, Kohlendioxid- und pH-Messung. Als *at-line* System konnten OUR, CER und pH sowohl an Schüttelkolben als auch an dem automatisierten Reaktorsystem Ambr 250 (Sartorius Stedim Biotech) gemessen werden. Durch das Stoppen der Pumpe, welche die Plattform mit Zellsuspension perfundiert, konnte die durch Ovarien des chinesischen Hamsters (CHO) bewirkte Abnahme der Sauerstoff- bzw. Zunahme der Kohlenstoffdioxidkonzentration innerhalb der Sensorplattform detektiert werden. Nach Vergleich mit der offline Analytik von Metaboliten wie Glutamin und Glutamat konnte die Glutamin Depletion und die damit verbundene Umstellung des Zellstoffwechsels in den Signalen von OUR wie CER detektiert werden.

A.3: 3D-gedruckte, mikrofluidische Perfusionssysteme zur parallelen Kultivierung von 3D Zellkulturen

Um den steigenden Ansprüchen der Zellkulturforschung an Systeme mit physiologerischen Bedingungen gerecht zu werden, werden mikrofluidische Systeme zur Integration dreidimensionaler Zellkulturen entwickelt. In diesem Projekt wurde ein 3D-gedrucktes mikrofluidisches Perfusionssystem entwickelt, in das in Hydrogel eingebettete Zellen als 3D Zellkultur integriert werden können. Der Chip besteht dabei aus zwei 3D gedruckten Teilen, zwischen die eine Membran integriert wird. Die Membran trennt dabei eine mit Medium durchströmte Perfusionskammer von einer Kammer zur Integration des Hydrogels. Nach Sterilisation können bis zu vier verschiedene 3D Zellkulturen in den Chip integriert und mikroskopiert werden. Die Plattform erlaubt anschließend die Variation von Mediumzusätzen, der Hydrogelzusammensetzung oder auch verschiedener Zelllinien.

Betreute Abschlussarbeiten

Bachelorarbeiten

Jannik Menke – *„Optimization and Characterization of a 3D-printed, Servo controlled microfluidic Valve System"*, 2021

Masterarbeiten

Phil-Oliver Thiel – *"Ultraschallbasierte Durchmischung von Zellsuspensionen in Mikrobioreaktoren"*, 2021

Daniel Hennig – *„Novel 3D-Printed Disease-on-a-Chip for Axonal Infection by Neuroinvasive Viruses"*, 2021

Veröffentlichungen und Konferenzbeiträge

Veröffentlichungen (antichronologisch)

Winkler S, Menke J, Kortmann C, Meyer KV, Bahnemann J (2022): Automation of Cell Culture Assays using a 3D-printed Servomotor-controlled Microfluidic Valve System, *Lab on a Chip*

Winkler S, Meyer KV, Heuer C, Kortmann C , Dehne M, Bahnemann J (2022): In vitro biocompatibility evaluation of a heat-resistant 3D printing material for use in customized cell culture devices

Bousis S, Winkler S, Haupenthal J, Fulco F, Diamanti E, Hirsch AKH (2022): An Efficient Way to Screen Inhibitors of Energy-Coupling Factor (ECF) Transporters in a Bacterial Uptake Assay, *International Journal of molecular sciences*

Bahnemann J, Enders A, Winkler S (2021): Microfluidic Systems and Organ (Human) on a Chip, *Learning Materials in Biosciences*

Winkler S, Grünberger A, Bahnemann J. (2021): Microfluidics in Biotechnology: Quo Vadis, *Advances in biochemical engineering/biotechnology*

Siller IG, Enders A, Gellermann P, Winkler S, Lavrentieva A, Scheper T, Bahnemann J. (2020): Characterization of a customized 3D-printed cell culture system using clear, translucent acrylate that enables optical online monitoring, *Biomedical Materials*

Kremser M, Winkler S, Eitner F, Bénardeau A, Kraehling JR (2019): Comparison of different measurement methods of cGMP, *Journal of translational medicine*

Konferenzen und Fortbildungen (antichronologisch)

Vorträge

<u>Winkler S</u>, Nowak S, Kropp K, Viejo-Borbolla A, Bahnemann J (2020): Novel 3D-printed Disease-on-a-Chip for Axonal Infection by Neuroinvasive Viruses, Annual EUROoCs Conference 2020, Uppsala, Schweden

<u>Preuss J</u>, **Winkler S**, Bahnemann J (2022): 3D Printing: An Accelerator for Customized Microfluidic Applications, BioCHIP Berlin 2022, Berlin, Deutschland

Posterbeiträge

<u>Winkler S</u> (2019): 3D cell cultivation in 3D-printed, biocompatible microfluidic chips, 2nd International EUROMBR 2019, Braunschweig, Deutschland

Workshops und Fortbildungen

Promotion plus+ qualifiziert, Hannover, Deutschland

GMP Kurs der Thomas Beer und Tobias Halfpap GbR, Hannover, Deutschland, 2020

GMP/GLP Kurs durch Dr. Robert Faurie, Hannover, Deutschland, 2020

Workshop „Marketing-Grundlagen" von Prof. Dr. Oscar-Werner Reif, Hannover, Deutschland, 2020

2nd International EUROMBR, Braunschweig, Deutschland, 2019

Lebenslauf

Persönliche Angaben

Name: Steffen Nils Winkler

Geburtsdatum und –ort: 21.01.1994, Hamburg

Ausbildung

2019 - 2022   Promotionsstudium im Fach Chemie an der Leibniz Universität Hannover

2016 - 2019   Masterstudium Biochemie an der Medizinischen Hochschule Hannover

2013 - 2016   Bachelorstudium Biochemie an der Leibniz Universität Hannover

2004 - 2013   Allgemeine Hochschulreife am Gymnasium Stormarnschule Ahrensburg

Beruflicher Werdegang

2022 – lfd.   Wissenschaftlicher Mitarbeiter an der Universität Augsburg

2019 - 2022   Wissenschaftlicher Mitarbeiter am Institut für Technische Chemie der Leibniz Universität Hannover

2018   Dreimonatiges Forschungspraktikum im Forschungszentrum Wuppertal der Bayer AG

2018   Masterarbeit am Helmholtzzentrum für Pharmazeutische Forschung Saarland (HIPS)

2017   Wissenschaftlicher Hilfskraft an der Medizinischen Hochschule Hannover

2017   Forschungspraktikum in der Biophysikalischen Chemie der Medizinischen Hochschule Hannover

2015   Wissenschaftliche Hilfskraft in der Physikalischen Chemie der Leibniz Universität Hannover

Danksagung

Ein besonderer Dank gilt Herrn Prof. Dr. Thomas Scheper für die Möglichkeit unter seiner Institutsleitung im Institut für Technische Chemie promovieren zu können. Du hast über lange Zeit ein großartiges Institut aufgebaut und die familiäre Atmosphäre des großen TCI verdanken wir maßgeblich dir.

Meine große Anerkennung und Dank gilt Frau Prof. Dr. Janina Bahnemann, die mich in meiner Zeit am TCI als meine Doktormutter stets unterstützt und gefördert hat. Durch deinen modernen Führungsstil gibst du der für die Bearbeitung komplexer Fragestellungen notwendigen Kreativität großen Freiraum. Man ist bei dir immer auf ein offenes Ohr gestoßen und deine enthusiastische Art hat einen stets motiviert! Ich freue mich darauf, in Augsburg weiter mit dir die Zukunft zu gestalten!

Ich bedanke mich auch bei meinem Prüfer Prof. Dr. Sascha Beutel und meiner Prüferin Prof. Dr. Marie Weinhart. Danke dafür, dass ihr mich geprüft habt!

Ich möchte meinen Dank auch an Frau Prof. Dr. Antonina Lavrentieva aussprechen, welche mich insbesondere zu den Arbeiten in der Tierzellkultur unterstützt hat. Ich bedanke mich herzlich bei Dr. Christian Ude, welcher mich mit seinem enormen Erfahrungsschatz und wissenschaftlichen Disput immer wieder inspirieren konnte.

Ein großer Dank gilt den Mitarbeitern der Werkstätten, mit Thorleif Hentrop und Kai Patzer, die mich besonders bei software- und elektrotechnischen Fragestellungen unterstützt haben, sowie Thorsten Strempel und Friedbert Gellermann, welche für die Fertigung mechanischer Bauteile stets zur Stelle waren. Ich bedanke mich auch bei Marina Weiß, Martin Pähler, Dr. Ivo Havlik, Dr. Michael Dors, Christiane Hellwig und Ulrike Dreschel bei der Unterstützung technischer und verwaltungstechnischer Angelegenheiten im Alltag.

Ich bedanke mich ganz herzlich bei meinem gesamten Arbeitskreis für eure Unterstützung! Eure vielen Talente machen den AK zu etwas Besonderem. Ich möchte dir Katharina besonders danken für die tolle Zusammenarbeit mit dir an unseren gemeinsamen Projekten. Danke ebenso an die 3D-Druck Experten Anton, John und Taieb für eure Unterstützung, Erfahrung und Kreativität.

Bei meinem Bachelor- und Masterranden Jannik Menke, Daniel Hennig und Phil-Oliver Thiel sowie den Wissenschaftlichen Hilfskräften unseres AKs möchte ich mich an dieser Stelle auch bedanken. Danke euch allen für eure Unterstützung!

Zudem möchte ich mich bei allen Doktoranden des großen TCI bedanken. Danke für die tolle Zeit mit euch! Es waren (trotz Pandemie!) so viele entspannte, spaßige, aufregende und gemeinsame Momente dabei, die meine Promotionszeit wirklich unvergesslich gemacht haben. Ich wünsche euch allen nur das Beste!

Ich möchte mich in diesem Zusammenhang bei meinem alten wie neuen Büro bedanken. Danke liebes Büro 165 für eure Unterstützung, die besonders in der Anfangszeit meiner Promotion Gold wert waren. Büro162: Danke, mit euch gab es nie Langeweile! Ich freue mich, euch als meine Freunde gewonnen zu haben.

Ganz zum Schluss möchte ich mich bei meiner Familie, meiner Frau Dimyana und meinen Freunden bedanken. Meiner Familie verdanke ich, dass ich jetzt dort bin wo ich stehe. Durch ihre ständige Unterstützung habe ich erst meinen Weg in die Naturwissenschaften finden können, was überaus glücklich gemacht hat. Danke dir Dimy, dass du da warst und mir immer zur Seite stehst. In den schwierigen Zeiten hast du mir halt gegeben. Ich bedanke mich auch bei meinen Freunden und allen anderen, die mich unterstützt haben.

Durch euch alle zusammen stehe ich nun dort, wo ich jetzt bin. Danke!